HU ISSN 1785-6892

DESIGN OF MACHINES AND STRUCTURES

A Publication of the University of Miskolc

VOLUME 2, NUMBER 1 (2012)

MISKOLC UNIVERSITY PRESS

CONTENTS

Design of Machines and Structures, Vol. 2, No. 1 (2012), pp. 5–14.

HEATING BEHAVIOUR OF SMALL PLASTIC GEARS

JÁNOS BIHARI
University of Miskolc, Department of Machine and Product Design
3515 Miskolc-Egyetemváros
machbj@uni-miskolc.hu

Plastic gears are used in many areas of life. Designing and installing these types of gears often needs physical post-control due to the deficiency of the relevant standards and work-helps. In order to have real results by the control, we must use a kind of testing equipment, which is able to simulate exactly the stress as well as the typical problems. To be able to compile the right tests we must learn the types of these problems. Some of problems will be introduced in this paper.

1. Introduction

Heating of plastic gears is an important problem because the strength parameters deterioration of most base materials to be concerned is faster than that of steel gears. In classical design the main reason of heating is the friction between the teeth surfaces. In some design method the heating coming from the internal material friction is also taken into consideration but they cannot be used or only in a limited matter for small size plastic gears. In case of plastic gears it is especially important due to the material deformation induced by the friction caused heating. In this paper some characteristic problems are shown, which should be expediently taken into regard of design and control of such kind of gears.

Definitions:

- Small gears:
  Module < 1 mm (precision engineering, DIN 58405)
  Characteristic external dimension < 50 mm
- Micro gears:
  Module < 0,2 mm (VDI micro gears)
  Characteristic external dimension < 20 mm

2. Limitations of design methods

Overviewed the often used design methods for small size plastic gears and the problems of those methods (*Figure 1–5*.) [1.], it can be seen that from the four basic cases in three, the acceptable accurate determination of the heat process is not possible as a part of the design according to either the complexity and cost demand or there are no methods or enough data for doing the calculation. In use of classical design methods the standards and offers to be concerned can be applied in larger size ranges however, in case of smaller sizes, especially for micro driven-gear there are no documents. So, it is generally true, that in case of small size and micro driven-gear equipped drives the heating should be controlled by experiments.

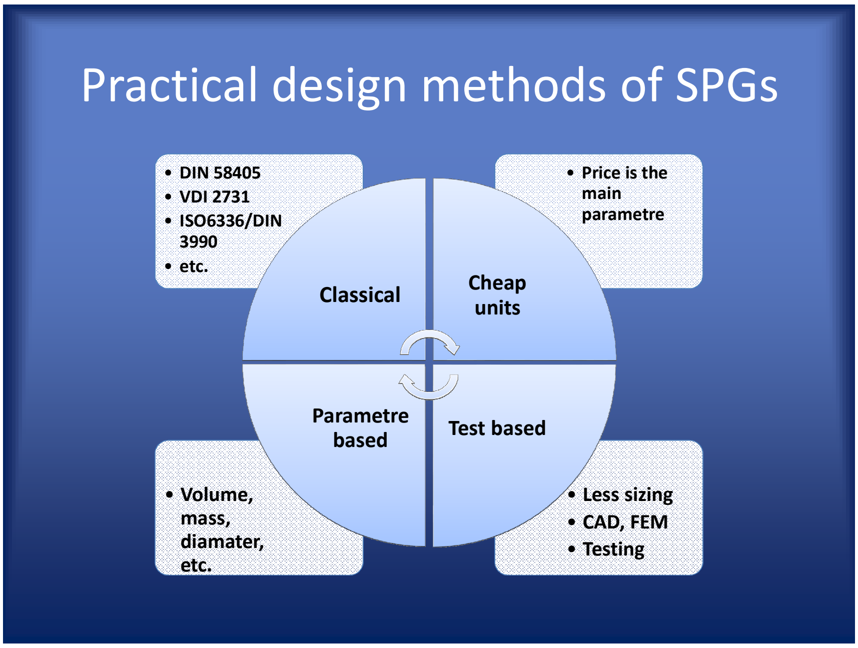

Figure 1.

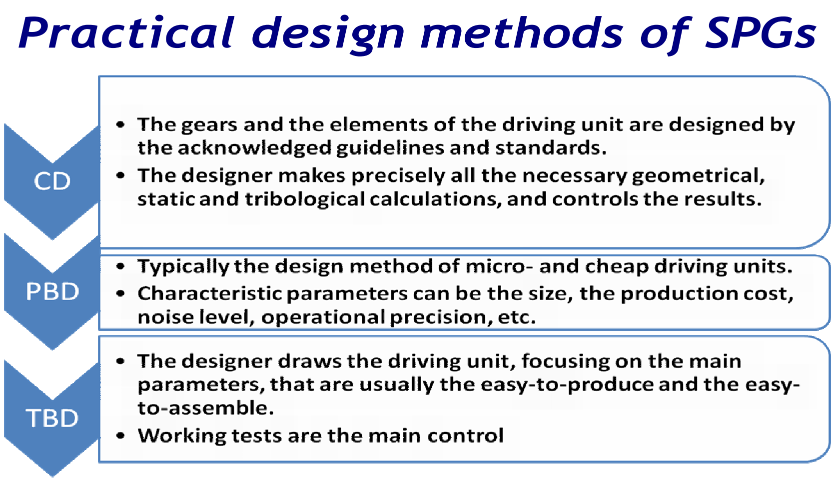

Figure 2.

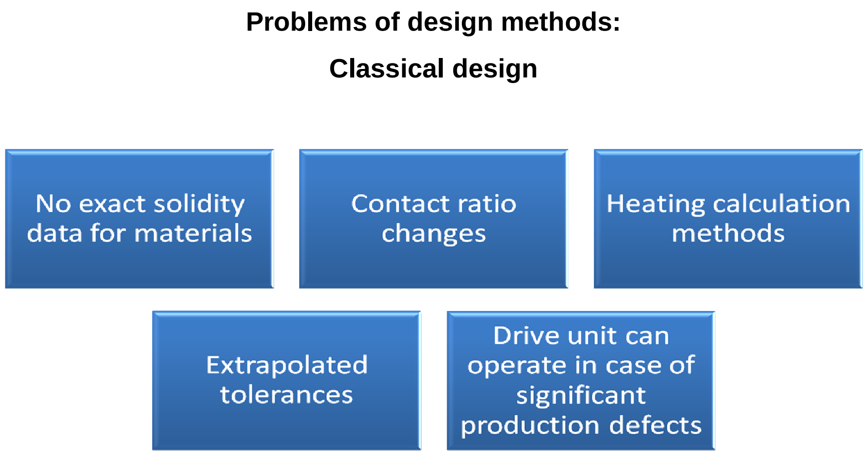

Figure 3.

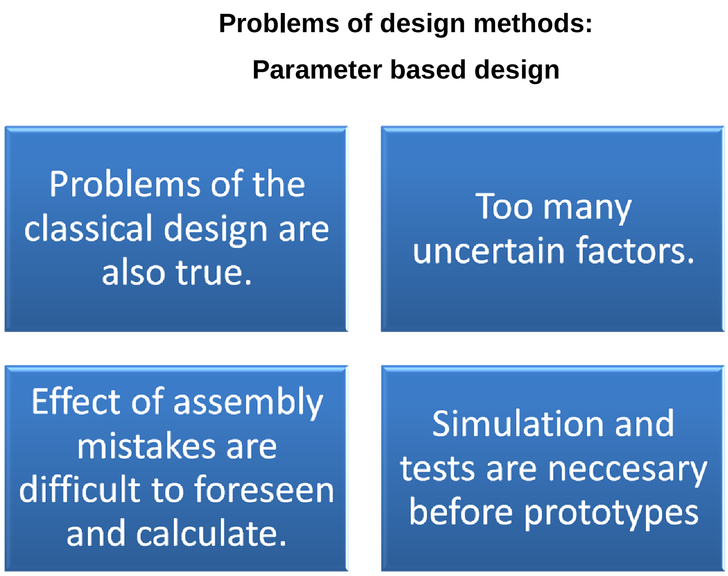

Figure 4.

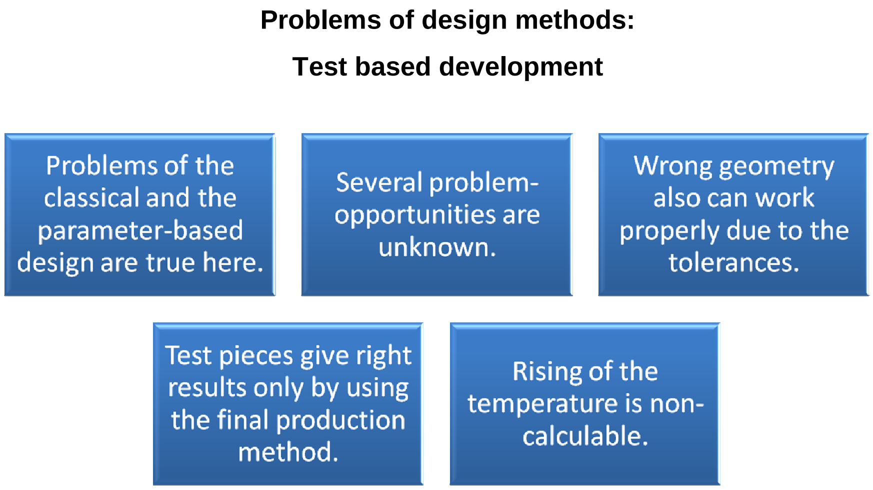

Figure 5.

In heating of plastic gears the deformation due to loading and the re-deformation due to unloading have an important role. This elastic deformation is always accompanied by internal friction. This kind of heating can be almost totally eliminated by determination of the strength requirements however, the system elements do not satisfy all the time the strength requirements in case of parameter based design, test-based development or design of cheap units. In such kind of situation only on base of element tests or knowledge of previous test results can be judged whether the strength of the gears is suitable or not.

3. Critical design positions from point of heating

The gear deformation can be induced more factors along the non-suitable strength property. For instance over-loading, non-optimal linkage of teeth and abnormal contact of surfaces, which have not been designed for that. The heating can be reduced in these cases as well by well selected lubrication. However, it should be taken into regard, that in the size range under investigation the characteristic procedure is the lifespan lubrication and the reinforced cooling of the lubricant never can be proceeded in practice.

3.1. The over-loading

The small size units involving driving gears often should be built in together with the electronic engine, which assures the propulsion. The designing possibilities are reduced due to the generally limited assortment of small engines and the power assortment scale is increased as much as by 50% steps. In micrometres the scaling is more robust. It can be easily happened, that only significantly higher power engine is at service, so the protective system for the drive cannot be designed neither at the power in way nor the counter-driven gear sides. So the increase of loading on the driven out-side it overloads the drive. In small measure the pollution of the moved structure on the driven out-side might be enough. This is an unambiguous situation. The problem can be occurred if not the true conclusions are formulated in case of the damaged drive under investigation.

3.2. Geometrical faults of the gear-drive house and mounting errors

The cheap drives are generally built into the die casted houses. For reduction of costs the houses are generally made from more pieces and for the fastening of the house pieces to each other a few screw bonding is applied. Generally snap pits are used. The bearing axles and often the axles themselves are manufactured by using the same materials. Additional problem, that the assembly timing of such units is generally short. If the tools at service are not suitable then the probability of errors is higher.

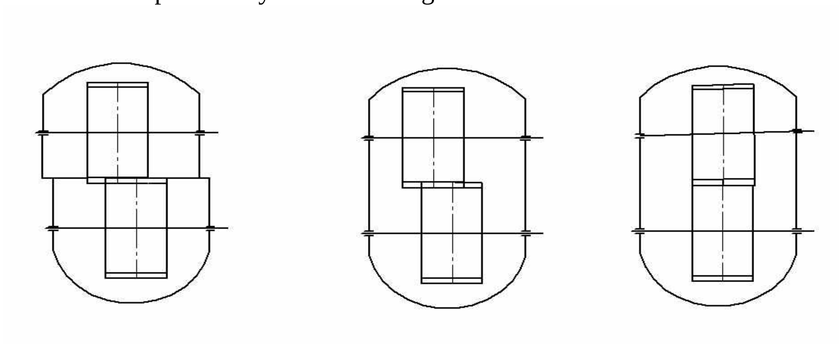

Figure 6. Bad drives

In *Figure 6.* there are examples for three typical problems. According to constructional reason not rare cross-spaced houses are used. The problem shown in the left side can be reason of either a mounting or manufacturing fault. The fault can be seen in the middle is an often experienced situation, namely the gear has no axial direction shoulder, they are mounted by extrusion to the steel axle and so the force transmission is assured by closed fitting. In this case the gear has been slipped on the axle due to assembly failure. On the right side the bearings are made with the house by one piece. If the tolerance ranges are prescribed badly then the distances of the bearings support can be relevantly different. In all of the three cases the loading is transferred on a smaller surface from one gear to the other then it would be necessary.

3.3. Incorrect tolerance determination of axle distances

In the small and micro ranges there are no standard tolerances [6], [7]. The tolerances can be prescribed by extrapolation of the ones valid in the larger ranges. Problems, connected with inconvenient selection of tolerances can be seen in *Figure 7*.

In situation of drafts 1 and 3 the axle distances are too big. In this case the bending on the tooth root is bigger than the allowable, and teeth jumping over might be occurred. In the draft 2 the axle distance is too short; one of the addendum circles reaches down into the dedendum circle of the other one, following deformation of teeth and gear.

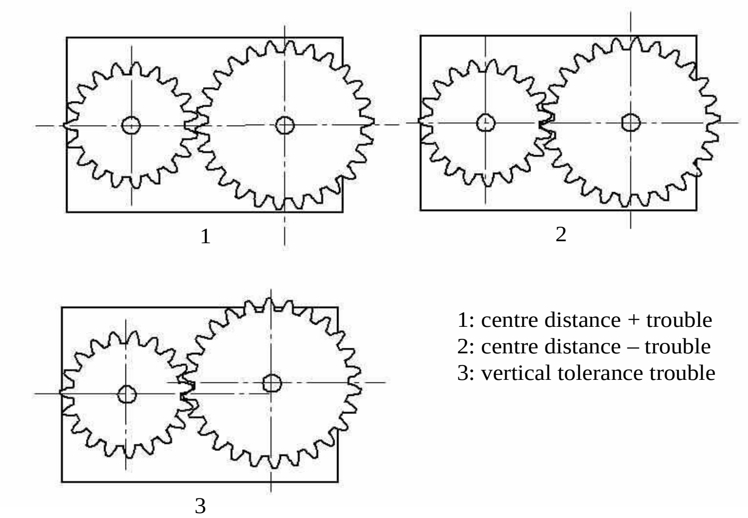

Figure 7. Centre distance troubles

4. Special design cases

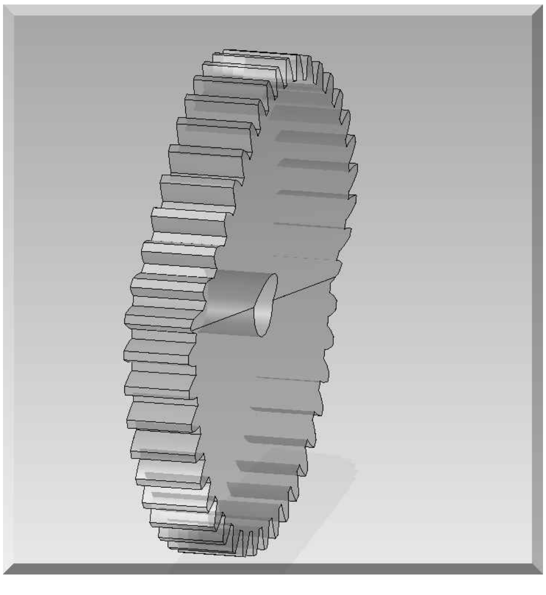

Figure 8. Narrow wheel body deformation at parameter based design

If the space is limited, so the wideness of the gear is small there might be deformation of the wheel body due to over-loading and axle distance failure. In this case the total wheel body is over-heated (*Figure 8.; Figure 9.*).

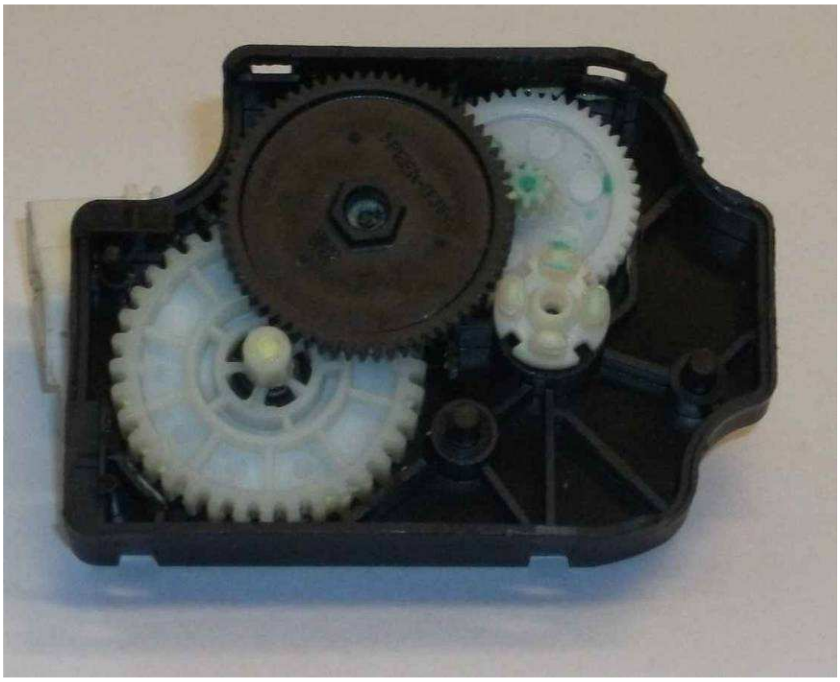

Figure 9. Thin wheel in a drive unit, with fibre-reinforcement reducing the deformation

In case of parameter based design due to geometrical limitations the small diameter gears body will be thin (*Figure 10.*). This kind of gears is generally fixed to the axle by cementation but the use of sintered joins is also not rare [5]. If the axle distance is too big, then not the tooth root deforms but the ribbon like gear body that is the teeth are diverged. If the axle distance is too small, then the head ribbon pushes the small gear teeth interval spaces so it is again the gear body that will be deformed. In this case the deformation can be occurred due to the over loading too.

Special loading state can be occurred in small tool machines and purpose oriented facilities. In *Figure 11.* a screw nail is wreathed by machine into chipboard. The hardness of the different structures is also different, so during the wreath the loading is also varying. For the loading variation an example is given by the diagram. The time of over-loading is very short and just only one-two teeth are involved.

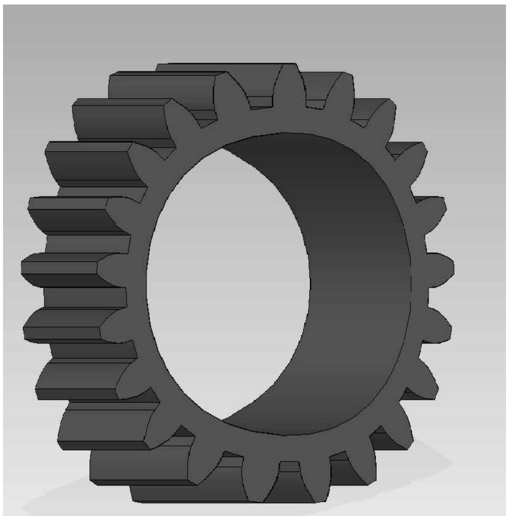

Figure 10. Deformation of narrow gear body

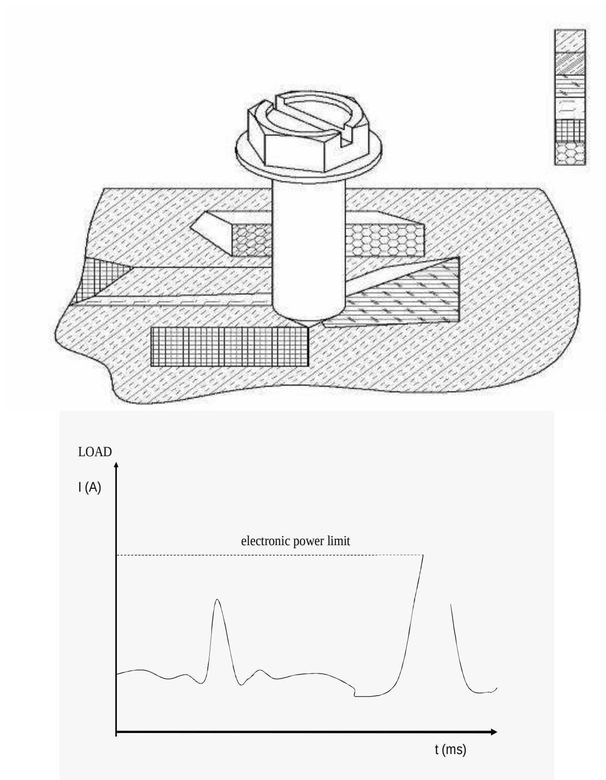

Figure 10. Momentary over-loading in case of chipboard screwing

According to the process can be seen in the diagram the drive is protected from the over-loading electronically (*Figure 10.*). Opposite, at over-loading some teeth can be deformed strongly, following local heating. Going round in case of badly determined tolerance these teeth can be reached down into the dedendum circle of the other gear or due to shrinkage they are not fitted between two teeth of the large gear. (*Figure 11.*)

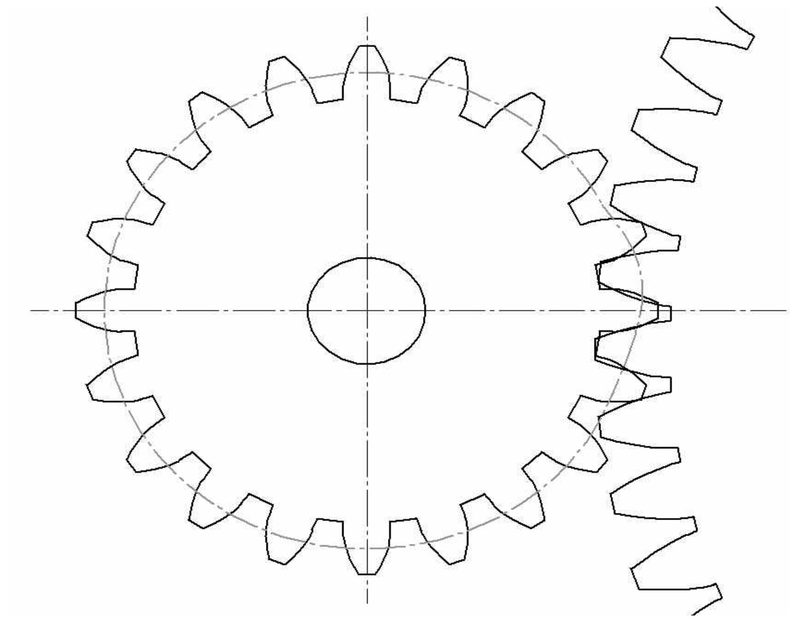

Figure 11. Effect of local heating

The same can be happened if a drive in standing position is taken out for a continual loading, then being started. This is a frequent situation at air technical equipment for baffle moving units. In these facilities the air stream tries to move continuously the baffle, which is kept many times in the right position only the propulsion. In this situation the force effect coming from the air stream loads only the linking teeth.

5. Summary

In determination of the small size plastic gears heating the effect coming from the teeth surface contact friction can be exceeded by that of the internal friction. Finding the failures is difficult because the small size plastic gears equipped by propulsions might have operating capability opposite to critical design, manufacturing and mounting errors. Additional problem is that the plastics have good vibration absorber property, so the noise of the propulsions does not deviate from the normal case. In consequence, in this size range the proceeding of the material and application specific test are absolutely necessary.

Acknowledgement

"This research was carried out as part of the TAMOP-4.2.1.B-10/2/KONV-2010-0001 project with support by the European Union, co-financed by the European Social Fund."

REFERENCES

[1] J. Bihari–L. Kamondi: *Design grounds of a machine for testing small plastic gears*. Advanced engineering 5/1. (2011), 15–25., 2011. p.
[2] L. Bottenbruch–R. Binsack: *Technische Thermoplaste 4.* Polyamide. Hanser Verlag, Wien, 1998.
[3] G. Pahl–W. Beitz: *Konstruktionslehre-Handbuch für Studium und Praxis.* Springer Verlag, Berlin, 1981.
[4] L. Starke–B. R. Meyer: *Toleranzen*. Passungen und Oberflächengüte in der Kunststofftechnik, *Hanser Verlag, Wien*, 2004.
[5] Thüringen C.: *Zahnradgetriebe für Mikromotoren*. VDI Verlag, Düsseldorf, 2000.
[6] VDI 2225 Blatt 3: Konstruktionsmethodik – Technisch-wirtschaftliches Konstruieren – Technisch-wirtschaftliche Bewertung, 1998.
[7] VDI 2731 Blatt 1: Mikrogetriebe Grundlagen, 2009.
[8] D. Züfle: *Getrieneanalyse und Qualitätssimulation*. TAE-Seminar Praxis der Zahnradferigung, Friedrichshafen, 2004.

Design of Machines and Structures, Vol. 2, No. 1 (2012), pp. 15–24.

DETERMINATION OF IDEAL CURVE HAVING CONSTANT WEDGE ANGLE FOR ROLLER FREEWHEELS

ZOLTÁN BIHARI–JÓZSEF SZENTE
Department of Machine and Product Design, University of Miskolc
H-3515 Miskolc-Egyetemváros
machbz@uni-miskolc.hu; machszj@uni-miskolc.hu

Abstract. The task of the starter motors is to rotate the combustion engines to the necessary rotational speed. An element of the mechanism is a free running clutch. It has two functions. The first one is the torque transmission from the driving member to the driven shaft, and to speed up the combustion engine. The9 other function is to disconnect the elements, when the combustion engine has been already turned over, and the driven shaft rotates faster than the driver.

In this paper the pressure angle as the most important parameter of operation is investigated. A new curve is developed for inner profile of housing, which operates to constant wedge angle.

Keywords: free running clutch, roller freewheel, logarithmic spiral

1. Introduction

The task of the starter motors is to rotate the combustion engines to the necessary rotational speed. An element of the mechanism is a free running clutch. It has two functions. The first one is the torque transmission from the driving member to the driven shaft and to speed up the combustion engine. The other function is to disconnect the elements, when the combustion engine has already turned over, and the driven shaft rotates faster than the driver.

In a previous paper we have discussed the operation and geometry of the roller freewheels, and the effect of load, deformation and wear on the operation of clutches has been analysed [4]. In paper [5] we have defined the geometry, which occurs constant wedge angle. In this paper the fundamental knowledge is presented and a new method, which helps us to determine the inner profile curve at the housing of clutch. This method gives a chance to reconstruct roller freewheels having unknown geometry.

2. Elements and operation of roller freewheels

Figure 1 shows a sketch from a roller freewheel having a so called outer star-wheel. It has four components: the housing, the hub, the rollers and the springs.

Figure 2 shows a detail of a roller freewheel, where the roller connects with the housing and the hub. The figure contains the necessary dimensions. The shape of the rollers and the hub is cylinder, and the housing has a curved surface usually based on logarithmic spiral.

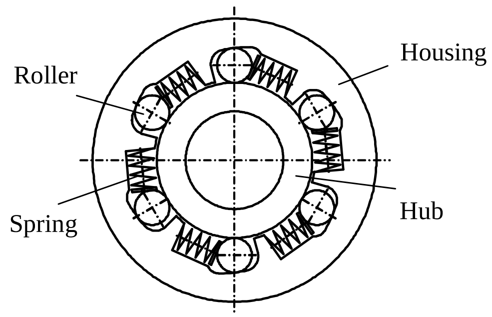

Figure 1. Roller freewheel assembl

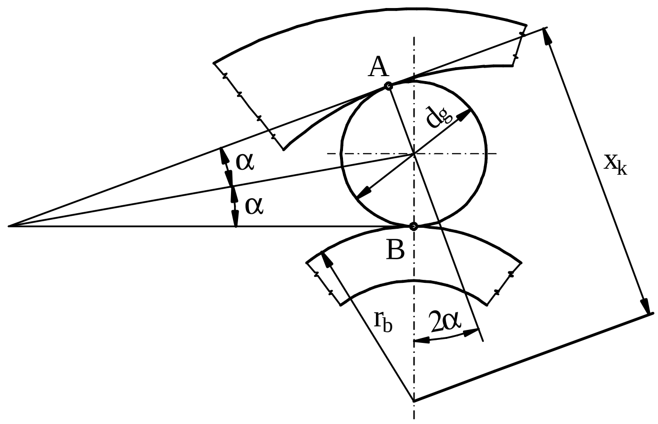

Figure 2. The geometry of the contact

For the operating of the roller freewheel it is very important requirement, that the profile of the housing and the hub should produce a taper gap. The tangent lines at the contact points determine the angle 2α, which defines the dimension of the gap. 2α is called as wedge angle. r_b is the radius of the hub, and d_g is the diameter of the roller in *Figure 2*. The operating of the roller freewheels is shown in *Figure 3*.

During the connection, the driving element is the housing, which is rotated by torque M_1 into the shown direction. To generate the equilibrium, the torque M_t on the hub equals M_1, but the directions of the torques are opposite. M_1 means the torque on one roller. When uniform load distribution is assumed between rollers, then

$$M_1 = \frac{M}{z}, \tag{2.1}$$

where torque M is the total load on the clutch and z is the number of rollers. The calculated tangential force F_t from the torque at the contact point of the roller and the hub is

$$F_t = \frac{M_1}{r_b}. \tag{2.2}$$

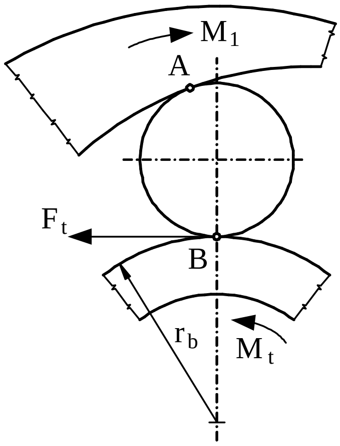

Figure 3. The operating principle of the roller freewheels

The tangential force presses the roller into the taper gap, as long as this tangential force is smaller than the friction resistance, that is $F_t < F_s$. The operating condition of the clutches is the self-locking. If the inequality is not realized, there is no self-locking and the hub slides on the roller. In this case the clutch cannot work. The equilibrium of forces is represented in *Figure 4*. From vector triangle we can write the following expression:

$$F_t = F_n \cdot tan\,\alpha \,. \tag{2.3}$$

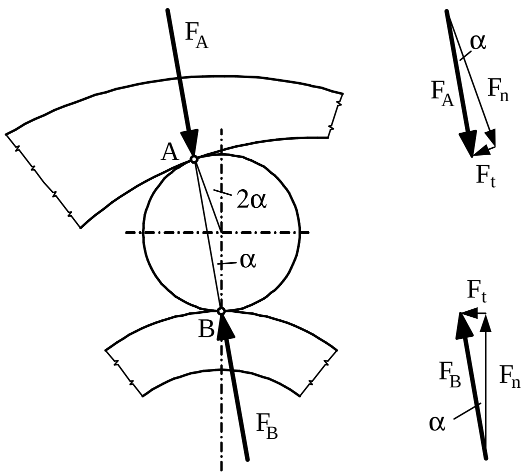

Figure 4. The equilibrium of forces acting to the roller

The working condition is obtained by simplification from the above relation:

$$tan\,\alpha < \mu \;\text{ and }\; \alpha < arctan\,\mu \,. \tag{2.4}$$

It is found, that the operation of the roller freewheels is defined by the relation between the wedge angle and the friction coefficient, and it does not depend on the magnitude of the load. The clutch will slip in that case only, if the inequality (2.4) is unrealized.

3. Profile of housing in accordance with the literature

Roller freewheels with outer star wheel are generally used by automotive industry. They have logarithmic spiral profile according to the literature. The logarithmic spiral has a special property: there is a constant angle β between the radius and the tangent line in any point of the curve. Using this curve as a profile of star wheel the wedge angle 2α has slight changes at different contact points. It becomes almost constant.
The task is to find a new curve, which has constant wedge angle 2α in any arbitrary contact point. This is granted when the centre point of the roller having variable radius r_g moves on a logarithmic spiral path.

4. The equation of the profile having constant wedge angle

During determination of profile the radius of the inner ring (r_b), and the wedge angle (2α) are considered as constant. In this case we can fit rollers with different radius (r_g) on any points of the inner ring and the profile of outer star wheel. Therefore, r_g can be interpreted as a function of θ in the following form:

$$r_g = r_g(\theta). \tag{4.1}$$

An illustration from the structure and the used notations are shown in *Figure. 5*.

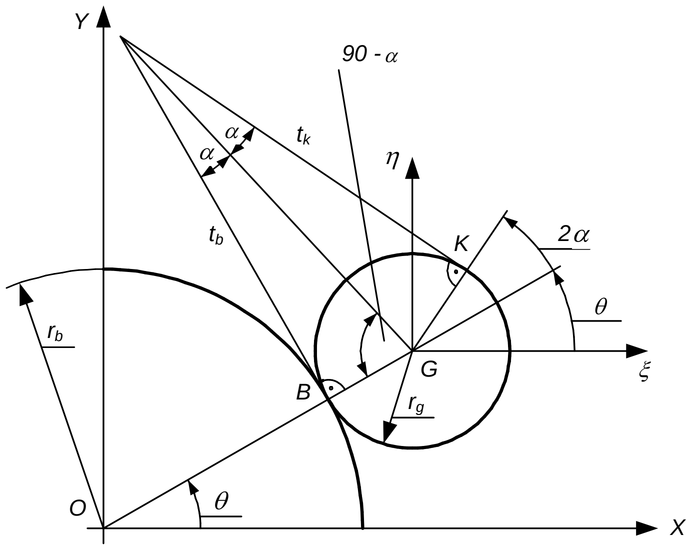

Figure 5. Layout draft of the roller freewheel

The coordinates *x* and *y* of the point „K” on the curve can be written using auxiliary co-ordinate system ξ - η as follows:

$$x = x_G + \xi_K \ , \tag{4.2}$$

$$y = y_G + \eta_K \ . \tag{4.3}$$

All the parameters of the above equations are the function of angle θ:

$$x_G = (r_b + r_g) \cdot \cos\theta \ , \tag{4.4}$$

$$y_G = (r_b + r_g) \cdot \sin\theta \ , \tag{4.5}$$

$$\xi_K = r_g \cdot \cos(\theta + 2\alpha) \ , \tag{4.6}$$

$$\eta_K = r_g \cdot \sin(\theta + 2\alpha) \ . \tag{4.7}$$

Substituting expressions from (4.4) to (4.7) into (4.2) and (4.3) contexts, coordinates *x* and *y* of the point „K” are obtained as a function of angle θ:

$$x = (r_b + r_g) \cdot \cos\theta + r_g \cdot \cos(\theta + 2\alpha) \ , \tag{4.8}$$

$$y = (r_b + r_g) \cdot \sin\theta + r_g \cdot \sin(\theta + 2\alpha) \ . \tag{4.9}$$

Derive the coordinates *x* and *y* according to θ to determine the slope of the tangent line:

$$x' = \frac{dx}{d\theta} = -(r_b + r_g) \cdot \sin\theta + r_g' \cdot \cos\theta - r_g \cdot \sin(\theta + 2\alpha) + r_g' \cdot \cos(\theta + 2\alpha) \ , \tag{4.10}$$

$$y' = \frac{dy}{d\theta} = (r_b + r_g) \cdot \cos\theta + r_g' \cdot \sin\theta + r_g \cdot \cos(\theta + 2\alpha) + r_g' \cdot \sin(\theta + 2\alpha) \ . \tag{4.11}$$

The slope of the tangent line (t_k) at the point „K” is:

$$\frac{dy}{dx} = \frac{r_g' \cdot [\sin\theta + \sin(\theta + 2\alpha)] + r_g \cdot [\cos\theta + \cos(\theta + 2\alpha)] + r_b \cdot \cos\theta}{r_g' \cdot [\cos\theta + \cos(\theta + 2\alpha)] - r_g \cdot [\sin\theta + \sin(\theta + 2\alpha)] - r_b \cdot \sin\theta} \ . \tag{4.12}$$

which can be written as follows (see *Figure 5.*)

$$tg(\frac{\pi}{2} + \theta + 2\alpha) = \frac{\sin(\frac{\pi}{2} + \theta + 2\alpha)}{\cos(\frac{\pi}{2} + \theta + 2\alpha)} \ . \tag{4.13}$$

After further modifications based on the trigonometric relationships we have

$$\frac{\sin(\frac{\pi}{2}+(\theta+2\alpha))}{\cos(\frac{\pi}{2}+(\theta+2\alpha))}=\frac{\sin\frac{\pi}{2}\cdot\cos(\theta+2\alpha)+\cos\frac{\pi}{2}\cdot\sin(\theta+2\alpha)}{\cos\frac{\pi}{2}\cdot\cos(\theta+2\alpha)-\sin\frac{\pi}{2}\cdot\sin(\theta+2\alpha)}=\frac{\cos(\theta+2\alpha)}{-\sin(\theta+2\alpha)}. \quad (4.14)$$

The slope of the tangent line using equations (4.12) and (4.14) is described by the following relation:

$$\frac{r_g'\cdot[\sin\theta+\sin(\theta+2\alpha)]+r_g\cdot[\cos\theta+\cos(\theta+2\alpha)]+r_b\cdot\cos\theta}{r_g'\cdot[\cos\theta+\cos(\theta+2\alpha)]-r_g\cdot[\sin\theta+\sin(\theta+2\alpha)]-r_b\cdot\sin\theta}=\frac{\cos(\theta+2\alpha)}{-\sin(\theta+2\alpha)}\ . \quad (4.15)$$

Multiplying both sides of the equation with the members of denominator we get the following formula:

$$\begin{aligned}&-r_g'\cdot\sin\theta\cdot\sin(\theta+2\alpha)-r_g'\cdot\sin^2(\theta+2\alpha)-r_g\cdot\cos\theta\cdot\sin(\theta+2\alpha)+\\&-r_g\cdot\cos(\theta+2\alpha)\cdot\sin(\theta+2\alpha)-r_b\cdot\cos\theta\cdot\sin(\theta+2\alpha)=\\&=r_g'\cdot\cos\theta\cdot\cos(\theta+2\alpha)+r_g'\cdot\cos^2(\theta+2\alpha)-r_g\cdot\sin\theta\cdot\cos(\theta+2\alpha)+\\&-r_g\cdot\sin(\theta+2\alpha)\cdot\cos(\theta+2\alpha)-r_b\cdot\sin\theta\cdot\cos(\theta+2\alpha)\end{aligned} \quad (4.16)$$

Sorting each member of the equation according to the coefficients we obtain the following form:

$$\begin{gathered}r_g'\cdot[+\sin\theta\cdot\sin(\theta+2\alpha)+\cos\theta\cdot\cos(\theta+2\alpha)]+\\r_g'\cdot[+\sin^2(\theta+2\alpha)+\cos^2(\theta+2\alpha)]+\\r_g\cdot[+\cos\theta\cdot\sin(\theta+2\alpha)-\sin\theta\cdot\cos(\theta+2\alpha)]+\\r_b\cdot[+\cos\theta\cdot\sin(\theta+2\alpha)-\sin\theta\cdot\cos(\theta+2\alpha)]=0\ .\end{gathered} \quad (4.17)$$

We can recognize trigonometric identities so the equation would be as follows:

$$\begin{gathered}r_g'\cdot\cos[\theta-(\theta+2\alpha)]+\\r_g'\cdot 1+\\r_g\cdot\sin[(\theta+2\alpha)-\theta]+\\r_b\cdot\sin[(\theta+2\alpha)-\theta]=0\ .\end{gathered} \quad (4.18)$$

After simplifying:

$$r_g'\cdot\cos(-2\alpha)+r_g'+r_g\cdot\sin(2\alpha)+r_b\cdot\sin(2\alpha)=0\ . \quad (4.19)$$

Because of the cosine function is symmetrical ($\cos(x) = \cos(-x)$) therefore

$$r_g' \cdot \cos(2\alpha) + r_g' + r_g \cdot \sin(2\alpha) + r_b \cdot \sin(2\alpha) = 0 \tag{4.20}$$

can be prescribed. Expressing r_g' from the above equation:

$$r_g' = -\frac{(r_g + r_b) \cdot \sin 2\alpha}{1+\cos 2\alpha} = -\frac{\sin 2\alpha}{1+\cos 2\alpha} \cdot (r_g + r_b)\ . \tag{4.21}$$

Examining the constant coefficient (before the bracket) of the above equation, we have a simple formula:

$$-\frac{\sin 2\alpha}{1+\cos 2\alpha} = -\frac{2 \cdot \sin\alpha \cdot \cos\alpha}{1+\cos^2\alpha - \sin^2\alpha} = -\frac{2 \cdot \sin\alpha \cdot \cos\alpha}{2 \cdot \cos^2\alpha} = -tg\,\alpha = A = const. \tag{4.22}$$

The result is a first-order, variable-separable differential equation:

$$r_g' = A \cdot (r_g + r_b)\,, \tag{4.23}$$

namely

$$\frac{dr_g}{d\theta} = A \cdot (r_g + r_b)\ . \tag{4.24}$$

After rearranging the equation, it has to be integrated, then both sides have to be involved with "e":

$$\frac{dr_g}{r_g + r_b} = A \cdot d\theta \qquad / \int \tag{4.25}$$

$$\ln \cdot (r_g + r_b) = A \cdot \theta + C \qquad /^e\ . \tag{4.26}$$

Organizing the result and introducing a simplification $e^C = K$, we obtain the general solution of the first-order, variable-separable differential equation (4.29)

$$r_g + r_b = e^{(A \cdot \theta + C)} = e^{A \cdot \theta} \cdot e^C, \tag{4.27}$$

$$r_g + r_b = K \cdot e^{A \cdot \theta}\,, \tag{4.28}$$

$$r_g = K \cdot e^{A \cdot \theta} - r_b = K \cdot e^{-\theta \cdot tg\,\alpha} - r_b\ . \tag{4.29}$$

If we suppose that r_b = constant and we demand the value of $r_g = r_{g0}$ on the place of $\theta = \theta_0$, we can calculate the value of „K” as particular solution of the differential equation.

$$K = \frac{r_g + r_b}{e^{-\theta \cdot tg\,\alpha}} = (r_g + r_b) \cdot e^{\theta \cdot tg\,\alpha} \Rightarrow K_0 = (r_{g0} + r_b) \cdot e^{\theta_0 \cdot tg\,\alpha} \quad . \tag{4.30}$$

For the sake of verification we have to replace the result into the original differential equation:

$$r_g{}' = A \cdot (r_g + r_b)$$

$$A \cdot K \cdot e^{A \cdot \theta} = A \cdot [(K \cdot e^{A \cdot \theta} - r_b) + r_b] = A \cdot K \cdot e^{A \cdot \theta} - A \cdot r_b + A \cdot r_b \tag{4.31}$$

Because of the equality existing between the two sides of equation, the result is acceptable. Formula (4.29) is an equation of the curve, at which the angle α (and the wedge angle 2α) does not change at any possible contact point.

5. The proof of the permanence of the wedge angle 2α

Although the calculation presented above clearly shows that the wedge angle 2α is constant in any contact point, let's consider an other approach. This hypothesis proves clearly that the wedge angle 2α is permanent using another condition. A result of the method is also the parametrical equation of the ideal curve.

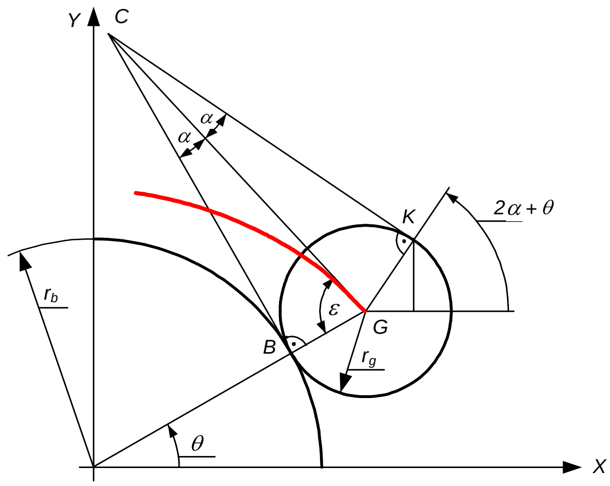

Figure 6. Moving of the roller central point

Let's consider the situation shown in *Figure 6*. If the red curve is a logarithmic spiral, than the parameter of the equation is ε. In this case of logarithmic spiral angle ε is constant. Therefore the angle α at apex "C" from right-angled triangle BGC must be also constant.

So in this case of the curve when constant wedge angle is produced the centre of the roller must be run along a logarithmic spiral. The current position of the point G(θ) is described as:

$$G = R_0 \cdot e^{-\theta \cdot ctg\,\varepsilon}, \tag{5.1}$$

where

$$\varepsilon = \frac{\pi}{2} - \alpha \,. \tag{5.2}$$

The value of the inner ring radius (r_g) at the place $\theta = 0$ be r_{g0} and the angle α is a design parameter of the freewheel, which can be determined using the friction relationships. The coordinates of an arbitrary point on the ideal curve can be described using the following formula (see *Figure 6*.):

$$x_K = x_G + r_g \cdot \cos(2\alpha + \theta),$$
$$y_K = y_G + r_g \cdot \sin(2\alpha + \theta), \tag{5.3}$$

namely

$$x_K = R_0 \cdot e^{-\theta \cdot ctg\,\varepsilon} \cdot \cos\theta + r_g \cdot \cos(2\alpha + \theta),$$
$$y_K = R_0 \cdot e^{-\theta \cdot ctg\,\varepsilon} \cdot \sin\theta + r_g \cdot \sin(2\alpha + \theta)\,. \tag{5.4}$$

Compared to equations (4.8) and (4.9) we find the following

$$R_0 \cdot e^{-\theta \cdot ctg\,\varepsilon} = r_b + r_g \,. \tag{5.5}$$

Using this equation we can calculate the roller radius r_g:

$$r_g = R_0 \cdot e^{-\theta \cdot ctg\,\varepsilon} - r_b \,. \tag{5.6}$$

The general solution of the solved differential equation in (4.29) and the equation (5.6) describe the same curve, if the coefficients are identical.
Substitute the constant K_0 (see equation (4.30)) into relation (4.29):

$$r_g = K \cdot e^{A \cdot \theta} - r_b = K \cdot e^{-\theta \cdot tg\,\alpha} - r_b = (r_{g0} + r_b) \cdot e^{\theta_0 \cdot tg\,\alpha} \cdot e^{-\theta \cdot tg\,\alpha} - r_b \,, \tag{5.7}$$

namely

$$r_g = (r_{g0} + r_b) \cdot e^{(\theta_0 - \theta) \cdot tg\,\alpha} - r_b \,. \tag{5.8}$$

We must prove agreement of the following coefficients while comparing the equations (5.6) and (5.8):

$$R_0 = r_{g0} + r_b \tag{5.9}$$

and

$$-\theta \cdot ctg\,\varepsilon = (\theta_0 - \theta) \cdot tg\alpha \,. \tag{5.10}$$

Fulfilment of condition (5.9) is easy to show. In the initial position (when $\theta_0 = 0$) the value of R_0 can be defined as the sum of the constant inner ring radius (r_b) and the initial roller radius (r_{g0}). In case of condition (5.10), when $\theta_0 = 0$ the equation ctg ε = tan α must be satisfied.
After conversion using formula (5.2) the following equation is indeed satisfied:

$$ctg\,\varepsilon = ctg\,(\frac{\pi}{2} - \alpha) = tg\alpha\,. \tag{5.11}$$

The conclusion is that both methods have reached the same solution. This proves that the derivation is correct. It is proved, that if the path of the roller centre is a logarithmic spiral, the described ideal curve cannot be a logarithmic spiral because of the changing roller radius. The shape of inner ring, the ideal curve and the path of the roller centre are shown in *Figure 7*.

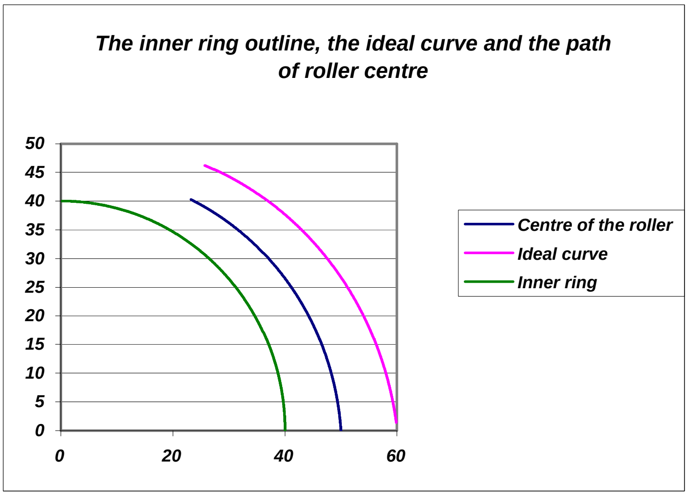

Figure 7. The inner ring outline, the ideal curve and the path of roller centre

Acknowledgements

"This research was carried out as part of the TAMOP-4.2.1.B-10/2/KONV-2010-0001 project with support by the European Union, co-financed by the European Social Fund."

REFERENCES

[1] Z. Terplán–G. Nagy–I. Herczeg: *Különleges tengelykapcsolók*. Műszaki Könyvkiadó, Budapest, 1971.
[2] K. Stölzle–S. Hart: *Freilaufkupplungen*. Springer Verlag. Berlin, 1961.
[3] G. Niemann–H. Winter: *Machinen Elemente. Band III., Springer Verlag,* 1983. pp. 270–290.
[4] Z. Bihari–J. Szente: *Az állandó zárószög feltétele görgős szabadonfutóknál*. Gép, LXI. évf., 2010/9–10. pp. 11–13.
[5] J. Szente–Z. Bihari: *Szabadonfutó tengelykapcsolók vizsgálata*. Gép, LVI. évf., 2005/11–12. pp. 161–166.
[6] F. Latka: *Matematikai képletgyűjtemény.*. Műszaki Könyvkiadó, Budapest, 1989.

Design of Machines and Structures, Vol. 2, No. 1 (2012), pp. 25–34.

DEVIATION FROM STANDARDS IN RELATION TO CYLINDRICAL GEARS WITH EXTERNAL STRAIGHT TEETH

ZSUZSA DRÁGÁR–LÁSZLÓ KAMONDI
Department of Machine and Product Design, University of Miskolc
H-3515 Miskolc-Egyetemváros
machdzs@uni-miskolc.hu; machkl@uni-miskolc.hu

Abstract. In propulsion technique applied in every day practice the load of gears is usually one directional or two directional, but the stresses on the tooth sides are not the same degree. Numerous researches verify that departing from standard symmetric toothed wheels, the loading capacity of gears can be increased by asymmetric teeth. Effects of deviation from standard have numerous consequences, which have to be examined.

Keywords: tooth shape, tooth root curve, tooth root stress, asymmetric teeth

1. Application of gears

Functional units and gear drives, which modify parameters of movement, take a great part in energetic chain realized in mechanical products. In gear drives continuous one-directional rotation of the toothed element pairs can be ensured by a suitably integrated rotation reversing facility. These transmission elements of movement realize either exact map of movement or large load transfer. The tooth shape plays a great role in determination of transmission parameters. Deviation from symmetric tooth shape generates questions about design, manufacturing and certification (proportioning, reliability). [9] The most important function of gear drives applied in driving mechanisms is steady transmission of movement during working. [1] Considering the single forms of motion, rotation would be changed, for example by reduction of revolutions.

Gearings can essentially be divided into two groups, kinematical and load transfer drives. [1] These functions mean different requirements for the teeth. Kinematical drives ensure precise angle rotation. These drives are characterized by small pitch. In load transfer drives pitch is larger, which helps accommodation to the fluctuation of temperature during working respectively inaccuracy of gears.

In the drive train of mechanical systems there is a usual functional claim, where the energy in a unit of time, which is the source of power, should be available for any working machine. This availability taking the energy components into consideration can be changed discreetly or continuously in a range. These functional units are driving mechanisms.

One element of the system is denoted functionally by the structure element in *Figure 1.*, which can be examined from inside as if it would be an unknown construction.

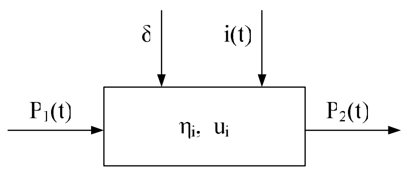

Figure 1. Functional unit describing driving mechanism

The input is described by the effect $P_1(t)$, with its components in the energy chain that are the moment $M_1(t)$ and the angular speed $\omega_1(t)$. This characterizes the source of energy at the same time.

The output is marked by the effect $P_2(t)$, which due to construction of the system element depends on the system controller information. These are the stage contact (i), which can be discreet or time control and it gives the system transmission, and the functional δ, which denotes the direction of rotation inside the system.

Based on the above mentioned it can be written that

$$P_1(t) = M_1(t) \cdot \omega_1(t), \tag{1}$$

$$P_2(t) = M_i(t) \cdot \omega_i(t), \tag{2}$$

$$\frac{\omega_1(t)}{\omega_i(t)} = u_i = f(i), \tag{3}$$

together with appropriation the formulas (1), (2), (3).

$$M_i(t) = \eta_i \cdot M_1(t) \cdot u_i, \tag{4}$$

where η_i is the efficiency which belongs to the controlled settings (stages) of the system element. Examining the system so that in point $\omega_i(t)$ regulated rotating movement should be mapped as well, from formula (3) it follows that

$$\omega_i(t) = \delta \cdot u_i \cdot \omega_1(t), \tag{5}$$

where δ is a $\{ -1,0,1 \}$-value function, which is a further directional input and defines the rotation direction character of the input (given direction, stillness, change of direction).

To the outgoing moment of the system generally it can be written that

$$M_2(t) = \delta \cdot \eta_i \cdot M_1(t) \cdot u_i. \tag{6}$$

Figure 1. can be transformed in view of formula (6) so that it can be seen in *Figure 2.*, which shows that one group of the driving mechanism (for example gradual) elements can characterised by the unchanging rotation direction movement, while the reversing can be solved by insert a functional element.

This recognition lead the researchers for example at the driving gears of the vehicles or wind turbines that the unvaried rotation direction for instance at loading capacity, efficiency of gears can result regular working, if deviating from symmetric tooth shape non-symmetric tooth form is applied. This motivated rows of researches for the practical application, on the one hand to the description of geometry, on the other hand towards the static and the dynamic examinations, and the manufacturability as well.

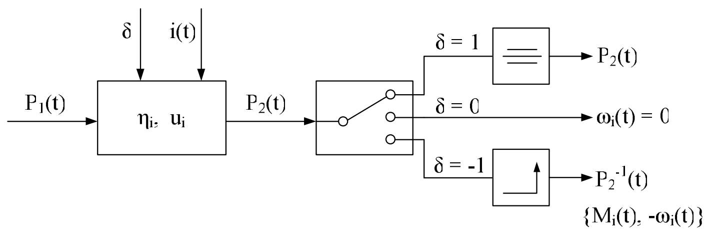

Figure 2. Reversing function built in the driving mechanism

2. Damage of gears and modification of loading capacity

Damage forms of gears can be divided into two groups. Tooth breaks caused by fatigue or aggressive origin breaks belong to one of the largest group. [1, 2] When it is caused by fatigue in connecting point perpendicular to the tooth surface tangential direction component of the normal tooth force results in complex stresses (bending and shearing) in the tooth root. Through bending stress mainly in the tooth root on the loaded tooth side i.e. on the drive side tensile stress wakes, while on the unloaded side i.e. on the coast side pressure rises. These pulsating fatigue stresses are responsible for development of cracks, which can cause break later.

Another large part of damages are caused by casualties of the tooth surface. [1, 2] Abrasion, pitting, different scratches and scoring, cracking and other tooth surface damages belong here. Damage of the tooth surface can be caused by several reasons, but here we would like to talk about damages caused by fatigue first of all. During contact of curved surfaces because of surface pressure Hertzian-stress is consorted with sharing stresses, therefore fatigue of tooth surface occurs above a loading period number (as in case of tooth root fatigue). These stresses are pulsating pressure stresses and this process causes pitting of the tooth surface.

The shape of tooth influences remarkably loading capacity of gears, extent of stresses in the tooth, which develop in meshing because of loading. Having the tooth manufacturing realized by extracting principle in sight by changing the tool basic profile modified teeth can be produced. [9] Shaping the tool cutting edge or changing it we can affect the shape of tooth root. With increase or decrease the tool basic profile angles we can modify the radius of curvature of the tooth evolve profile arcs, thus extent of Hertzian-stresses as well.

3. Concerning standards

The established manufacturing processes and the requirements of application define basic profile symmetric, which is standard. It is because of economy; integrate of cutting tools, changeability of gears, given kinematics of manufacture instruments, standard forms of calculating procedures, demand of changes of direction in drives.

The basic profile determines the exact geometry of gear teeth, which is a fictive rack profile. This can mesh with teeth of a given gear-family. [1] On the middle line of the basic profile the tooth thickness and the tooth cut width are the same. The acute angle between parts of the straight profiles, determine the sidelong edges, and the straights perpendicular to the middle line is the basic profile angle (α). Value of the standard basic profile angle is usually 20° but in special applications it can be different from this as well. We can express the odd sizes of the basic profile with module (m), which is nationally standardized too.

The basic profile of the evolve teeth determines the basic profile of the cutting tool, which is called tool basic profile. [1] If we put these two kinds of basic profile to each other, then their middle lines cover each other. The head line of the tool basic profile corresponds to the foot line of the teeth basic profile. It means that the shape of the tool head edge determines the tooth root profile of the gear teeth. In case of little module (smaller than 1 mm) the foot line of the tool basic profile agrees with the head line of the teeth basic profile. In the other cases the tooth height of the tool basic profile is larger than the tooth height of the teeth basic profile.

In our country the basic profile of cylindrical gears with evolves teeth and its tool basic profile to manufacture are described by standards MSZ 433 and MSZ 17154. Standard MSZ 310 decrees module series.

4. Increasing the loading capacity and the lifespan as a new possibility

Researches tending to increase loading capacity of gears are in connection with asymmetric tooth shape mainly. In these studies tooth sides are distinguished. One of them is the loaded tooth side (drive side) another is the unloaded side (coast side). The profile angles of both sides are different, that causes asymmetry particularly. Various advantageous or disadvantageous properties come to the front depending on whether profile angle on the drive side or on the coast side is larger. Greater parts of the researchers prefer that case, when the profile angle on the drive side is larger. Circumstances and marginal conditions of the researches have to be taken into consideration in each case.

Kapelevich [3] realizes computer aided simulation of the gear design in his method. This way special pair of gears can be solved widely. Increase of loading capacity of gears can be reached by application of larger profile angle of the drive side beside size and mass reduce. Furthermore he showed decrease of vibration level, which was available by decreasing meshing stiffness.

Working gears at big revolutions per minute dynamic load and vibration cause the main problem. Karpat et al. in [5] investigated behaviour of asymmetric gears during dynamic load. With enlarging the profile angle on the drive side dynamic factor of the asymmetric toothed gears was grown. However this factor reduced remarkably by increase of addendum, item the area on the tooth surface was grown where one pair of tooth meshes with each other and extent of static transmission errors reduced at the same time. Design of asymmetric teeth can be optimized by decrease of dynamic effects. These results are significant mainly in relation with aircraft industry, automotive industry and wind turbines.

Results of Pedersen [6] showed that in order to decrease the bending stresses in the tooth root it is necessary to apply asymmetric teeth. The greatest effect can be reached by this way. Reduction of bending stresses can be reached by two methods: either by thickening of tooth root or changing the shape of tooth root where the stress density is the largest one.

In Senthil Kumar et al.’s study [4] the asymmetry enlarges the loading capacity of the tooth root in contradiction to traditional symmetric gears. The asymmetry means larger profile angle on the drive side in this case.

Researches can be found, in which the authors propose shaping of the cutting tool (rack), because the shape affects the gear teeth (evolve profile and tooth root curve). Rack profiles proposed by Senthil Kumar et al. [4] have one circle arc on its head edge. In this case by application of profile angles differ from each other the radius of tool head edge decreases to a lesser degree than in case of symmetric. The positive effect on the bending stresses is in connection with widening of the tooth. In this study at designing of non-standard tools the authors considered only standard module and standard profile angle on the coast side, which makes the process of the tool engineering easier.

Pedersen [6] proposed new shape of standard rack. He made a difference in between the parts of the tool head edge according to which root of the tooth profile side it forms. On the coast side of the tool head edge there is circle arc, on the drive side there is ellipse arc. He guaranteed the continuity of the tool profile with an initiated factor μ, which modifies the width of the tooth at the same time.

Alipiev [7] generated variations of rack tool profiles in case of different profile angles on the drive and on the coast side, while he changed the size of the head edge radius and its positions.

These results are not complete, only a short summary can be read above.

5. Generalization of the tool basic profile

In order to study of effects of asymmetry, one of the first steps is to determine the basic profile of the tool, which generates the gear teeth. [10] Later changing possibilities of the meshing characteristics can be examined with this. [8] Points of the basic profile are arranged in an xy orthogonal coordinate-system in such a way that the middle line of the basic profile overlaps with the x axis of the coordinate-system, the y axis divides longitudinal the tooth of the basic profile into halves. This arrangement was shown in *Figure 3*.

The basic profile is constituted by straights and curves connected to one another, equations determining them must be described in the xy coordinate-system. The straights construct the edges at the sides, head and at foot line of the basic profile. The curves are the rounding between the straight parts. The rounding between the side edge and the head edge has a great influence on the shape of the tooth root profile. [1] The equations of the straights can be given as a function of x in the xy coordinate-system. These straights are marked I. and II. in *Figure 3*. The straight I. which forms the edge at the side of the tool basic profile crosses the point P_3 on the x axis in a given direction. The straight I. encloses (90°+α) with the x axis, where α means profile angle. The coordinates of the point P_3 (7) can be read from *Figure 3.* and by this the equation of straight I. can be written (8).

$$P_3(x_3; y_3) = P_3(-\frac{\pi \cdot m}{4}; 0)\,, \tag{7}$$

$$y_I = -\frac{1}{\tan\alpha}(x + \frac{\pi \cdot m}{4})\,. \tag{8}$$

The straight II., which defines the straight part of the tool basic profile, is parallel with the x axis, and the distance between them is equal to the sum of clearance and module. The equation of the straight II. can be given by formula (9).

$$y_{II} = -(m + c) = -(m + c^* \cdot m) = -m \cdot (1 + c^*)\,. \tag{9}$$

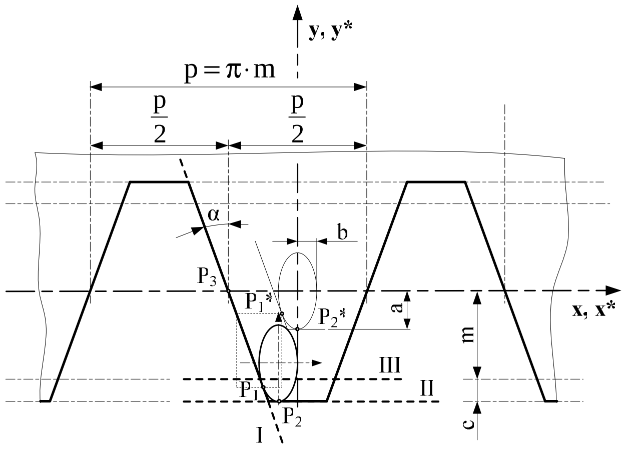

Figure 3. Tool basic profile with ellipse curve [10]

To the rounding of the head edge and the side edge for example an arch of a round or an ellipse can be taken. Another curve can be used as well, which is attached to a suitable reference point. Another x*y* coordinate-system can be used to write down the equation of the curve. The origin of this new coordinate-system overlaps the origin of the xy coordinate-system. As an example, let the rounding of head edge and side edge be an ellipse arc, which's major axis (2a) to the y axis, and minor axis (2b) to the x axis is fitted. From well known equation of the ellipse value of y can be expressed (10).

$$y^* = \sqrt{\left(1-\frac{(x^*)^2}{b^2}\right)\cdot a^2}\,. \tag{10}$$

After tangents of the curve are defined (11.) on the understanding that gradients of the tangents be equal with gradients of the straights I. and II. Thus the tangents are parallel with the straights I. and II. The tangents on the points P_1* and P_2* are tangential to the curve (12). After differentiation formula (13) is offered.

$$\frac{dy^*}{dx^*} = (y^*)'\,, \tag{11}$$

$$\frac{dy^*}{dx^*} = \frac{dy_{I,II}}{dx} \rightarrow P_{1,2}{}^*(x_{1,2}{}^*; y_{1,2}{}^*)\,, \tag{12}$$

$$\frac{dy^*}{dx^*} = (y^*)' = \frac{-\frac{a^2}{b^2}\cdot 2x^*}{2\cdot\sqrt{a^2-\frac{a^2}{b^2}\cdot(x^*)^2}}\,. \tag{13}$$

If the formula (13) equals with gradient of the straight I. and x* is expressed from the equation, then formula (15) is given. From the result of the extraction of root the negative value is considered. This equals to the coordinate x_1* of the usual point P_1* later.

$$(y^*)' = -\frac{1}{\tan\alpha}, \tag{14}$$

$$x^* = -\frac{1}{\sqrt{\frac{1}{b^2}\left(\frac{a^2}{b^2}\cdot\tan^2\alpha+1\right)}}. \tag{15}$$

After this the origin of the ellipse curve is moved (shifting in the direction of x and y) in the xy coordinate-system so that the tangents and the straights I. and II. are covered with one another. At this time the rounding between the head edge and the side edge which are straights, is generated by the arc of the given curve now between the contact points P_1 and P_2 as it can be seen in *Figure 3*.

The shifting in the direction y of the ellipse (point P_2* is moved to the straight II. → point P_2 is offered) is given by the difference between the y coordinates of the definite tangent and the straight II. The gradient of the straight I. influences the shifting in the direction x (point P_1* is moved to the straight I. → point P_1 is offered). Given from geometry the coordinates of the point P_2* can be read from *Figure 3*. On the basis of this the correct shifting in the y direction of the ellipse can be given by formula (16).

$$O'y = -(m+c)+a \tag{16}$$

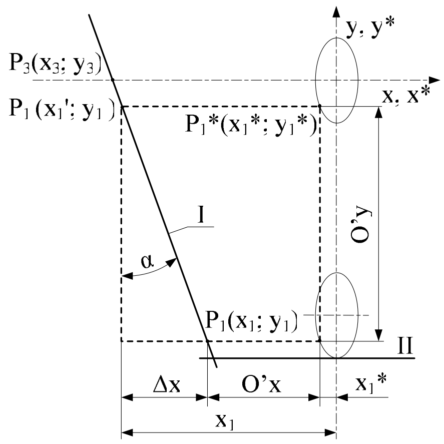

Figure 4. Tool basic profile with ellipse curve [10]

To the determination of the shift in the x direction through the y_1' coordinate of the point P_1' on straight I., which equals to the y_1* coordinate of the point P_1*, the x_1' coordinate can be written by formula (17). Considering the *Figure 4.*, formula (18) gives the correct shift in the y direction. By adding the correct shift values under formulas (16) and (18) to the corresponding coordinates of the point P_1* we get the coordinates of the point P_1 on straight I. In case of the point P_2 it can be done in similar way.

$$x_I' = y_I' \cdot (-\tan\alpha) - \frac{\pi \cdot m}{4}, \tag{17}$$

$$O'x = x_1' + \Delta x + x_1^*. \tag{18}$$

By the definition of these straights (head edge, side edge), the optional arc (rounding) and the coordinates of the connection points of these curves the half of the tool basic profile can be determined. The whole profile can be given exactly by reflection to the y axis the profile got this way or by application of a different curve.

By exact description of the tool basic profile definite teeth can be generated. In the course of generalization by changing the parameters of the basic profile for example the profile angle, the rounding of the head edge, the combination of the rounding curves, just in different way on the two sides of the profile, rows of asymmetric non standard teeth can be originated.

6. Determination of the maximum stress location at the tooth root

The international and national standards (DIN, ISO and so on) give precise directives to the static examination of cylindrical gear pairs in case of symmetric teeth. At research of tooth root fatigue the calculation methods set out always from a base model. These models present deviation in each standard (for example account the friction). These differences are not significant but they can not be left out of consideration. The models define parameters, which depend on the geometry of the model. The established parameters determine factors suitably. These factors help describing the maximum of the tooth root stress in a maximum stress location supposed and fixed in the model. A base model can be seen in *Figure 5. a)* in case of symmetric tooth shape.

Base models can usually handle specific geometrical constructions only. That is why the designer runs into difficulty of the calculation method immediately, mainly when the axial distance is smaller or larger than the elementary axial distance. At this time teeth has to be done free from clearance so profile removals has to be applied. Determining of the profile removals can be solved by dividing of the common tooth height (h_w) when it is defined by some kind of principles (equal tooth root fatigue endurance, minimal slip lost effect and so on). Because of the differences among tooth heights the static examinations supporter software are not able to handle the tooth root stress modifier factors.

In case of non-symmetric tooth shape [*Figure 5. b)*] the accuracy of the model itself can be questioned because it is not sure that the maximum stress locations take place in the contact points on the 30 degrees tangents of the tooth root curve.

In the tooth root the maximum tension place can be defined by experimental model methods beside classical mechanical procedures. These can be the followings.

- Fatiguing experiment affected on real model, from which after tooth break the position of the broken piece cross section let conclude the maximum stress location but not the effective magnitude of the maximum tension.
- The examination is possible on CAD virtual model with FEM analysis where the maximum stress place and the maximum tension can be calculated.
- With optical stress analysis where with the help of suitable matter on real model near static load the maximum stress location and tension can be defined.

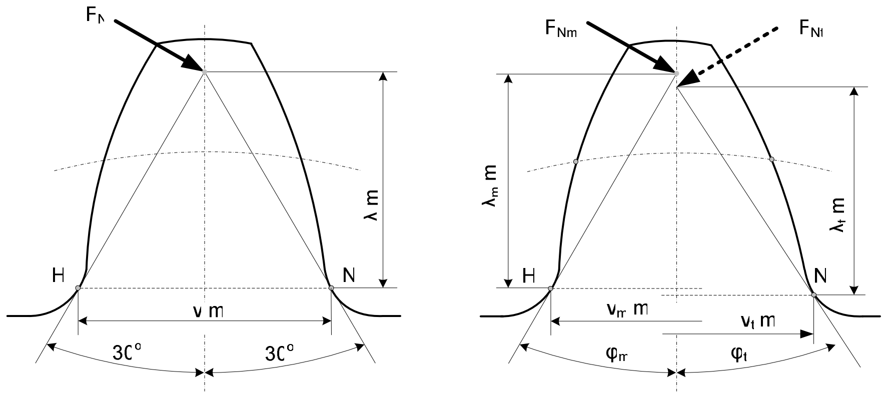

a) symmetric shape b) non-symmetric shape

Figure 5. Geometric base model

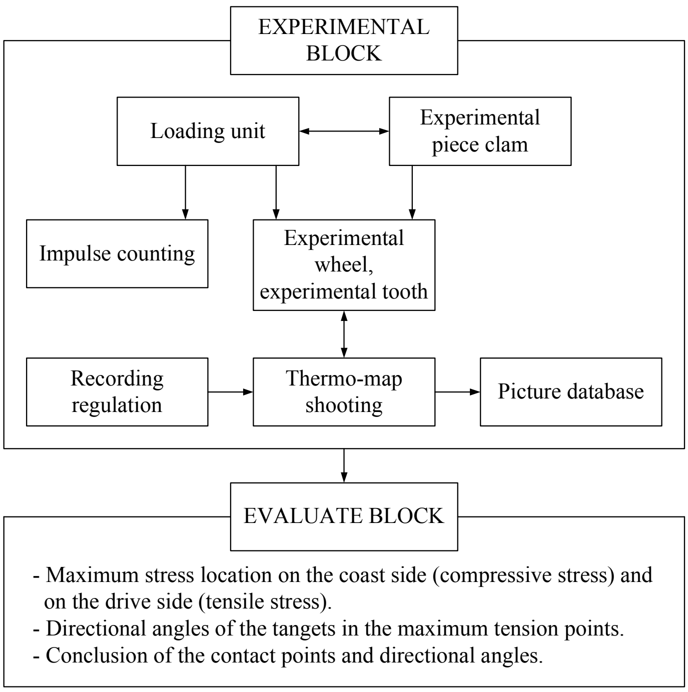

Figure 6. Shoot of thermo-map

– Thermo-map shoot on real model effect of fatigue load. Essence of the method is that the tooth exposed to the fatigue load under effect of the developed stresses because of the transformation limit formed in the tooth root the loss of energy originating in the internal friction changes the thermo-map of the tooth. The thermo-map gives the critical stress locations thus the maximum stress location, too. *Figure 6.* presents a principled solving on this measuring method.

Locating the maximum stress position and determination of the maximum tension is necessary to give a fast and confirmed proportioning and controlling method to the designers' hand in case of non-symmetrical tooth shape as well, which method is a nominal stress determination of an approximate model and a joint of geometry dependent stress modifying parameters.

7. Summary

In propulsion chain of mechanical constructions the toothed element pairs, mainly gear pairs with evolve tooth profile play an important role. Constructional solving come to foreground increasingly tending to fulfil the function. Becoming the one directional energy transfer (there is no rotation direction change) in the centre of interest proposed the request at tooth shapes the deviation from symmetrical form. This study is tending to sum up several results that have been achieved so far. It presents the generalization of the deductive base profile to mapping the non-symmetrical teeth. At static examinations it calls the attention to the difficulties caused by the divergence from symmetrical tooth shape, for example at applying the standards recommendations. It shows an adoption of thermo-map like new method, which can make it easier to create the approximate models.

Acknowledgement

"This research was carried out as part of the TÁMOP-4.2.1.B-10/2/KONV-2010-0001 project with support by the European Union, co-financed by the European Social Fund."

REFERENCES

[1] Gy. Erney: *Fogaskerekek*. Műszaki Könyvkiadó, Budapest, 1983.
[2] Á. Zsáry: *Gépelemek II.* Nemzeti Tankönyvkiadó, Budapest, 1990.
[3] A. Kapelevich: *Geometry and design of involute spur gears with asymmetric teeth*. Mechanism and Machine Theory 35 (2000), pp. 117–130.
[4] V. Senthil Kumar–D. V. Muni–G. Muthuveerappan: *Optimization of asymmetric spur gear drives to improve the bending load capacity*. Mechanism and Machine Theory 43 (2008), pp. 829–858.
[5] F. Karpat–S. Ekwaro-Osire–K. Cavdar–F. C. Babalik: *Dynamic analysis of involute spur gears with asymmetric teeth.* International Journal of Mechanical Sciences, 50 (2008), pp. 1598–1610.
[6] N. L. Pedersen: *Improving bending stress in spur gears using asymmetric gears and shape optimization*. Mechanism and Machine Theory, 45 (2010), pp. 1707–1720.
[7] O. Alipiev: *Geometric design of involute spur gear drives with symmetric and asymmetric teeth using the Realized Potential Method*. Mechanism and Machine Theory, 46 (2011), pp. 10–32.
[8] Zs. Drágár–L. Kamondi: *Nem szabványos alapprofilú fogaskerekek tervezésének kérdései*. Géptervezők és Termékfejlesztők XXVII. Szemináriuma, Miskolc, 2011. november 10–11. GÉP, LXII., 2011/7–8., I. kötet, pp. 35–38.
[9] Zs. Drágár–L. Kamondi: *Design questions of gears with non-symmetric teeth*. 13th International Conference on Tools, ICT-2012, Miskolc, Hungary, 27–28 March 2012, pp. 329–332.
[10] Zs. Drágár–L. Kamondi: *Szerszám-alapprofil leírása fogaskerekekhez analitikus geometria alkalamazásával*. XX. Nemzetközi Gépészeti Találkozó. OGÉT 2012, Romania, Kolozsvár, 2012. április 19–22., pp. 105–108.

Design of Machines and Structures, Vol. 2, No. 1 (2012), pp. 35–51.

RESULTS OF LABOARATORY TESTS OF HARMONIC GEAR DRIVE

JÓZSEF PÉTER–GÉZA NÉMETH
Department of Machine and Product Design
3515 Miskolc-Egyetemváros
machpj@uni-miskolc.hu; machng@uni-miskolc.hu

Abstract
The constraint of the reliable operation of a gear drive is the proper stiffness of the structural elements, so the stiffness of the gears. One of the variant of the planetary gear drives is the harmonic gear drive, which essence is the flexibility of one or both elements of the gear pair. The flexible gear body changes its shape due to the structure of wave generator and gear pair, and also due to the external loads of the drive. The mesh of the gears is the function of the degree and nature of deformation. This paper is dealing with the laboratory test of a drive produced for experimental purposes.

1. Introduction

Since the foundation of the Department of Machine and Product Design (formerly the Department of Machine Elements) at the University of Miskolc there has been research works in relations with planetary gear drives. One of the variant of the drive is the harmonic gear drive that has been belonging to the area of examined drives since the middle of 1970s. One of the constraints of the design and production of the harmonic gear drive (hereinafter referred to as harmonic drive) is the knowledge of the meshing and the interaction of the rigid and flexible gear pair. In paper [2] the author dealt with the theory and laboratory test of the meshing of harmonic drive, in paper [3] the analysis was expanded by the study of the waving gear coupling and the calculations of the deflection of flexible gear due to loads. In the paper the authors summarize all the knowledge necessary to the interpretation of the laboratory test results and the newer results of the analysis of test results.

2. Elastic deflection of bodies

Although the relation between load and the elastic deformation of bodies due to load has been widely known there are relatively few mechanisms the operation of which is based on this recognition. The majority of mechanisms is based on the rigid body model to the present day. Clerence Walton Musser was the inventor who summarized in paper [1] the principles that can be the basis of the operation of mechanisms, starting from Robert Hooke's well known formula which states that the elastic deflections of bodies are proportional to the loads. These principles are the arcuation, the integration, the scalloping, the differentiation, the interfacial strain, the Poisson's wedge, the torsion lever and the twisted strip. In [5] the authors dealt with the arcuation, the integration and the scalloping in detail, keeping the harmonic drive and the waving gear coupling in mind.

3. The arcuation

At *Figure 1*. the neutral line, k of a prismatic flat curved beam is visible which is transformed to k' curve, due to load. The neutral line, k is an arc with radius, r. The tangential displacement of one of its arbitrary point having φ coordinate is $w = w(\phi)$ and its curvature is $\kappa(\phi) = \dfrac{1}{\rho(\phi)} = -\dfrac{1}{r^2}\left(\dfrac{d^2 w}{d\phi^2} + w\right)$. By increasing the curvature of the beam the chord length, AB is decreasing. The increment of the chord length is the function of curvature, i.e. $s_1 - s = f(\rho(\phi) - r)$.

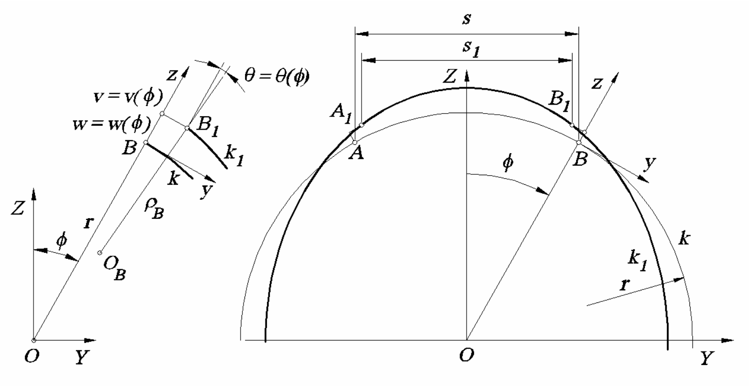

a) *b)*

Figure 1. Arcuation. a) The displacement of an arbitrary point and b) the change in chord length

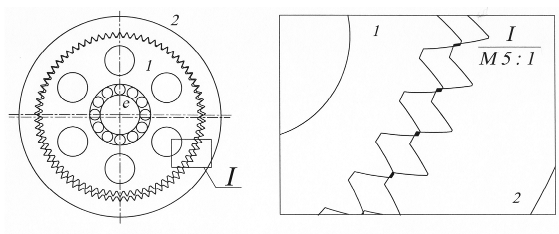

a) *b)*

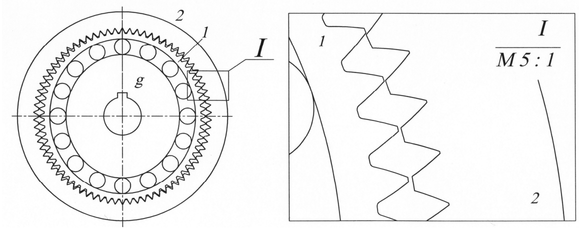

c) *d)*

Figure 2. a) and b) Planetary gear drive, c) and d) Harmonic gear drive

In *Figure 2. a)* a planetary gear drive having an internal connection gear pair *1* and *2* and an eccentric, *e* connecting them is visible. In *Figure 2. c)* a harmonic gear drive consisting of an internal connection gear pair *1* and *2* and a wave generator, *g* deflecting the external toothed gear to elliptic shape is visible. The gears *1* and *2* and the eccentric, *e* of the planetary gear drive is regarded as rigid. The circular spline, 2 and the wave generator, g of the harmonic drive is also rigid. The external toothed gear (flexspline), *1* of the harmonic drive is deflected elastically due to the wave generator, *g*.

The angular velocities of the elements of planetary drive relatively to the housing are ω_1, ω_2 and ω_e, that of the gear pair relatively to the eccentric are $\omega_{1e} = \omega_1 - \omega_e$ and $\omega_{2g} = \omega_2 - \omega_g$. The ratio of angular velocities ω_{1e} and ω_{2e} is defined by the ratio of number of teeth, z_1 and z_2, i.e. $u = \dfrac{z_2}{z_1}$. If gear 1 drives gear 2, ($1 \to 2$), the ratio of angular velocities relatively to the eccentric, e is $i_{12} = \dfrac{\omega_1 - \omega_e}{\omega_2 - \omega_e} = u$. In case of $\omega_2 = 0$ and $e \to 1$ the ratio is $i_{e1} = \dfrac{\omega_e}{\omega_1} = \dfrac{1}{1-u}$. To increase the ratio, the number of teeth, z_1 should be increased and/or the difference of tooth numbers, $z_2 - z_1$ should be decreased. The increment of tooth numbers increases the radial dimensions and the decrement of the difference of tooth numbers causes interference between root and crest as *Figure 2. b)* shows.

The external toothed gear, *1* of the harmonic drive is deflected to elliptic shape by the wave generator, g and the curvature along its circumference is changing similarly to the beam shown in *Figure 1. b).* The teeth of the flexible spline, 1 can mesh the teeth of circular spline, 2 in the stage having greater curvature. At this stage the chord lengths among the tooth tip edges of the flexible spline are decreased and **there is no interference between the teeth** of the gears, as shown in *Figure 2. d).* The tooth number difference is integral multiple of the wave number, for symmetry. When the wave number, $N = 2,$ the minimum of the tooth number difference, $z_2 - z_1 = 2.$

4. Harmonic gear drive or gear drive service

The planetary drive shown in *Figure 2. a)* can be studied **in both gear drive and planetary gear drive service**. In gear drive service the frame of reference is fixed to the eccentric, e and the interaction of the gears turned relatively to the eccentric is analysed. In planetary gear drive the frame of reference is fixed, e.g. to the circular spline, *2* and the interaction of external gear, 1 and internal gear 2 is studied in the slewing of the eccentric.

On the analogy of planetary drive the harmonic drive can be analysed **in gear drive or harmonic gear drive service**. First case, the swivel of pair of gears is analysed in the frame of reference fixed to the wave generator, in harmonic gear drive service the weaving motion of the external gear is examined in the frame of reference fixed to the circular spline. As the investigation of gear pair meshing, the occurrence of interference disturbing the meshing and the interaction of the elements of the drive are more clear in gear drive service, **the following analyses are made in the frame of reference fixed to the wave generator**.

5. Reducing and multiplying drive

The gear drive speeds down when the ratio, $i = \dfrac{\omega_{driving}}{\omega_{driven}}$ is $i < -1$, or $i > +1$, and seeds up when $-1 < i < 1$. The harmonic gear drive speeds down when the wave generator, *g* is the driving element and the gear *1* or *2* is driven besides the fixed *2* or *1* gear to the frame. In this case the driving direction is $g \rightarrow 1$ or $g \rightarrow 2$. The harmonic gear drive speeds up when the direction of drive is $1 \rightarrow g$, or $2 \rightarrow g$. The relations are summarized in *Table 1*.

Table 1.

Speeds down	*Gear drive*	$1 \rightarrow 2$	$i_{12} = u$	*Speeds up*	*Gear drive*	$2 \rightarrow 1$	$i_{21} = \dfrac{1}{u}$
	Harmonic gear drive	$g \rightarrow 1$	$i_{g1} = \dfrac{1}{1-u}$		*Harmonic gear drive*	$1 \rightarrow g$	$i_{1g} = 1-u$
		$g \rightarrow 2$	$i_{g2} = \dfrac{1}{1-\dfrac{1}{u}}$			$2 \rightarrow g$	$i_{2g} = 1-\dfrac{1}{u}$

The comparison of mechanical powers gives the feasibility of decision if which sence of power flow of the gear drive $1 \rightarrow 2$ or $2 \rightarrow 1$ is the equivalent of the sence of power flow in harmonic gear drive service. The basis of analysis is the equilibrium of the drive and the assumption stating that the magnitude and sense of torques M_g, M_1 and M_2 are acting to the elements of *g*, *1* and *2*, respectively, are not dependent on the frame of reference.

In the frame of reference fixed to the housing the mechanical power flowing through the gears *1* and *2* are $P_1 = M_1 \omega_1$ and $P_2 = M_2 \omega_2$, respectively, and that of the powers in the frame of reference fixed to the wave generator $P_{1g} = M_1(\omega_1 - \omega_g)$ és $P_{2g} = M_2(\omega_2 - \omega_g)$. On the basis of *Table 2.* the sign of power ratios and their consequences are studiable. In case *(1)* the ratio of powers P_{1g} flowing on the gear *1* with $\omega_{1g} = \omega_1 - \omega_g$ angular velocity relative to the wave generator and P_1 flowing on the gear *1* with ω_1 angular velocity relative to the frame is positive so in the services of both gear drive and harmonic gear drive the gear 1 is the driving or the driven element. The senses of power flow are $1 \rightarrow 2$ and $1 \rightarrow g$, or $2 \rightarrow 1$ and $g \rightarrow 1$.

In case *(2)* the ratio of powers P_{2g} flowing on the gear *2* with $\omega_{2g} = \omega_2 - \omega_g$ angular velocity relative to the wave generator and P_2 flowing on the gear *2* with ω_2 angular velocity relative to the frame is negative. In this case the power flow $1 \rightarrow 2$ suits $2 \rightarrow g$, and that of $2 \rightarrow 1$ suits $g \rightarrow 2$.

Table 2.

Power ratio		Power flow	
		Harmonic gear drive	*Gear drive*
(1)	$\frac{P_{1g}}{P_1}=\frac{M_1(\omega_1-\omega_g)}{M_1\omega_1}=\frac{u}{u-1}>0$	$1 \rightarrow g$	$1 \rightarrow 2$
		$g \rightarrow 1$	$2 \rightarrow 1$
(2)	$\frac{P_{2g}}{P_2}=\frac{M_2(\omega_2-\omega_g)}{M_2\omega_2}=\frac{1}{1-u}<0$	$2 \rightarrow g$	$1 \rightarrow 2$
		$g \rightarrow 2$	$2 \rightarrow 1$

6. The meshing of harmonic gear drive

The paper [4] deals in detail with both the mechanical model used to the analysis of meshing of harmonic gear drive and the occurrence of interference disturbing the meshing.

6.1. Tooth profile

Te applied tooth profile is an involute curve, the base profile angle, $\alpha = 20^o$, the addendum factor, $h_a^* = 1,$ the radial clearance factor, $c^* = 0,25.$ In the course of tests **the flexible gear was manufactured as a cylindrical gear by hobbing and the internal gear was generated by pinion cutter**.

6.2. Flexible gear, flexspline

The flexible gears are cup shaped. The profile correction factors, x_1 of the flexible gears, *H21* and *H22* were chosen larger than it was recommended (in the range of number of teeth, $z_1 = 100...800 \quad x_1 = 3...4$). The *Table 2.* in paper [7] contains the profile correction factors both as intended, (x_1) and as determined by measurement over pins, (x_{1m}). The recommended height of the tooth of flexible gear, $h_1 = 1,4...1,6\ m$ In case of the *gear, H21* this tooth height is less than the offered one and in case of the *gear, H22* it is bigger. The relation between the tooth height and the number of teeth meshing at one time are examined by the tooth height deviated from the recommended value. The offered value of the face width of flexible spline, $b_1 = 0,2...0,4D$. The face width was chosen less than offered to avoid the interference appeared at the back part of the tooth tip.

In the course of dimensioning and strength calculations the flexible gear was substituted by a hollow cylinder having a wall thickness, h_{e1} and length, L_{e1} to simplify the problem. The neutral surface of the hollow cylinder is a straight cylinder with radius, $r_0 = \frac{D+h_{e1}}{4}$. The wall thickness underneath the teeth, $h_0 = \frac{d_{f1}-D}{2}$, the equivalent thickness considering the effect of the teeth due to flexural rigidity, $h_{e1} = h_0 + m,$ where m

is the module. The length of the hollow cylinder, $L_{e1} = b_1 + \frac{L_1 - b_1}{3}$ comprises also the superficies following the teeth and having the role of a compensating coupling where b_1 is the tooth width of the flexible gear.

6.3. The circular spline

The flexible spline and circular spline are meshing in the vicinity of the semi major axis, prior to the appearance of the external loads, as shown in *Figure 3*. **Along the semi major axis of the wave generator the centre distance,** $O_1 O_2 = a_w$ **is equal to the radial deflection of the flexible spline**, $a_w = w_0$. When the profile correction factor of the circular spline along the major axis is calculated by the constraints of backlash-free mesh, $x_2 = \frac{z_2 - z_1}{2} \frac{inv\alpha_{wt} - inv\alpha}{tan\,\alpha} + x_1$ is obtained, where the pressure angle, $\alpha_{wt} = arc\,cos \frac{z_2 - z_1}{2} \frac{m}{w_0}$. The revealing dimensions of circular splines, *G22* and *G23* are collected in *Table 4*. of paper [7].

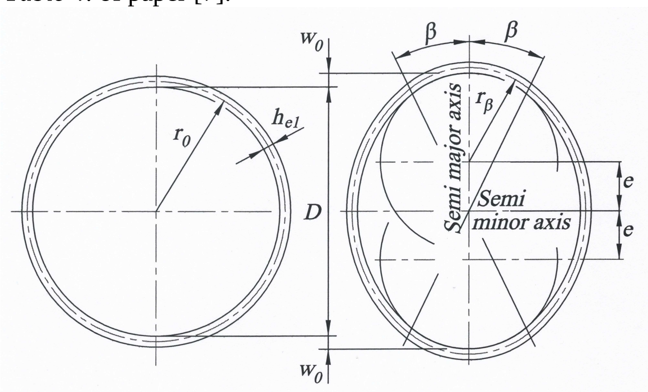

a) *b)*

Figure 3. a) Ring substituting the flexspline b) Ring deflected by two disks with eccentric bearing support

6.4. Wave generator

The elliptically deformed fleible spline and the rigid circular spline are brought in connection by the wave generator. Two wave eccentric disk wave generator (and elliptical cam wave generator, not discussed in present paper) were used. The two wave eccentric disk wave generator consists of two eccentric, two disks and commercially available rolling bearings.

a) In the course of research the ratio of radial deflection/module, w_0 /m wa changed to the values of $0.6, 0.7, 0.8, 1.1, 1.2, 1.3$ by altering the flexible spline, the eccentric and the disks due to *Table 3.* [7]. **By changing the element of the drive the relation between the radial displacement, w_0 the semi arc of contact between the flexspline and wave generator disks, β, shown in *Figure 3.* and the deflection of flexspline, described by the radius of curvature, ρ were inspected.**

b) The flexible spline is influenced by the disk which has bearing support with eccentric, e, and diameter, d_t, along an arc of central angle, 2β. The suggested range of β, considering the magnitude of the bending stress in the vicinity of the semi major and semi minor axes is $\beta = 20^o ... 40^o$. Along the arc of contact the radius of curvature of the neutral line, $r_\beta = r_0 + w_0 - e$ is constant, the radius of disk is $r_t = r_\beta - \frac{h_{e1}}{2}$. The relation between the data of w_0, r_0, r_β and β can be expressed by the formula

$$\frac{(r_0 - r_\beta) r_0}{w_0 \, r_\beta} = \frac{\frac{4}{\pi}(\cos\beta + \beta\sin\beta) - 2\sin\beta}{\frac{\pi}{2} - \sin\beta\cos\beta - \beta - \frac{4}{\pi}(\cos\beta + \beta\sin\beta) + 2\sin\beta}.$$

The values of β computed by given w_0, r_0 and r_β data are collected in *Table 3.* [7].

6.5.The mesh of the elastic external teeth gear (flexsline) and the rigid internal teeth gear (circular spline)

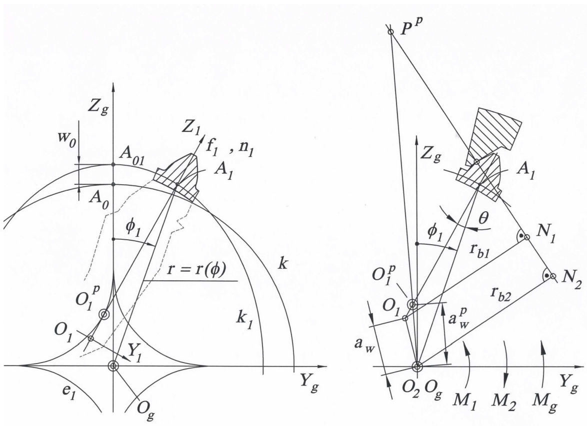

a) *b*

Figure 4. a) Deflected flexspline, b) Profile mesh, c) Edge mesh

The deflected elastic gear (flexspline) is shown in *Figure 4. a).* There are some assumptions around the tooth. Its axis of symmetry, f_1 is the normal of neutral line, k_1. The centre of base circle, O_1 belonging to the involute tooth profiles is situated along the axis of symmetry, f_1. The momentary centre of rotation of the tooth during the traverse of flexspline in relation to the wave generator is O_1^p.

The engage of one pair of tooth of the flexible-rigid pair of gears can be studied in *Figure 4. b).* It can be traced back to the engage of an external teeth gear with geometric centre, O_1 and a shifted centre of rotation O_1^p, and an internal teeth gear with coincident geometric centre and centre of rotation, O_2.

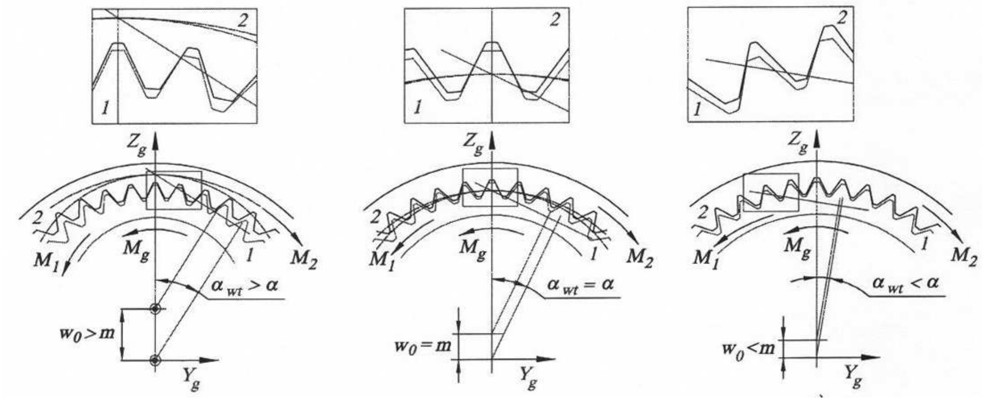

a) *b)* *c)*

Figure 5. The location of meshing teeth in relation to the semi major axis of the wave generator as the function of radial deflection, w_0

The location of meshing teeth in relation to the semi major axis of the wave generator is changing in the function of radial deflection, w_0, as shown in *Figure 5.* The suggested range of w_0 is $1{,}1...1{,}2\ m$, which is reduced due to the elastic deflection of the elements and the rearranging of clearances.

In front of and behind the profile mesh the gap in direction of the normal between the tooth profile and the tooth tip edge, is so small in a relatively wide range, that the elastic deflection of **the elements are meshing edge-like way too**. The basis of the investigation of the edge mesh is **the knowledge of the gap in normal direction and the elastic deflection due to loading of the drive elements**. The papers [2, 3] deal in detail with the components of elastic deflection of harmonic gear drive and the edge mesh.

7. The typical data of the elements of test drive

The typical size of the harmonic gear drive is the nominal (N) inner diameter (ND), which is approximately identical with the actual inner diameter (D) of the flexible gear drive. The elements of harmonic drive with the nominal diameter of ND 120, 160 and 190 are shown in *Figure 6*. These elements were manufactured in the laboratory of Department of Machine Elements, University of Miskolc, and the tests were made on the elements having the nominal diameter $ND190$. The geometry data of drive element were summarized in paper [7], *Table 2., 3.* and *4.*

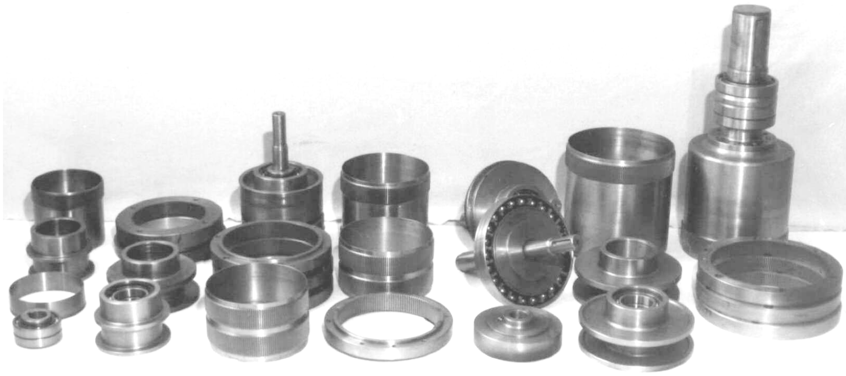

a) b) c)

Figure 6. Basic elements of the Harmonic drive.
a) $ND120$, b) $ND160$, c) $ND190$ drive elements

7.1. The test place building up

The drive box shown in *Figure 7.* was fixed on a machine base and the circular spline, 2 was fixed to the drive box $(\omega_2 = 0)$. The wave generator, g was revolved in relation to the drive box through a torque measuring shaft. The torque M_1 acting to the flexspline, 1 was changed by the loading disks, 6. With regard to the end face of the drive the M_1 acts counter clockwise as shown *in Figure 8.* and *9.* The wave generator was revolved counter clockwise in slow down service $(g \rightarrow 1)$ and clockwise in speed up service $(1 \rightarrow g)$.

7.2. Recording the test data

The radial displacement of flexspline, the change of its radius of curvature and the load acting to the tooth of flexspline was recorded according to *Figure 8.*, as the function of deviation, φ_g in relation to the circular spline.

7.3. Measurement of the radial displacement

The radial displacement of the fexspline, w was measured next to the tooth, in a plane parallel to the end face of the flexspline. The measuring gauge that consist of feather and feeler, wes fixed to the circular spline. The displacement was recorded by strain gauges glued to the two sides of the feather, in the function of the wave generator deviation relatively to the circular spline. The dicplacement of $w = 0$ was recorded previously to putting the wave generator into the flexspline. The unit of displacement was determined at the tip of deformational wave, $(\phi_g = 0)$ on the basis of generator geometry $\left(w_0 = e + \frac{d_t}{2} - \frac{D}{2} \right)$.

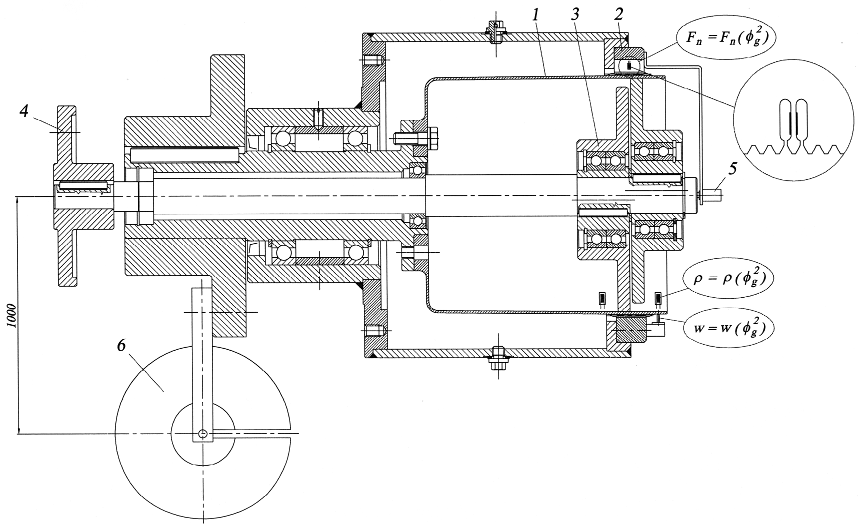

Figure 7. Experimental drive. 1 flexspline, 2 circular spline, 3 wave generator, 4 coupling, 5 rotating transducer, 6 loading disk

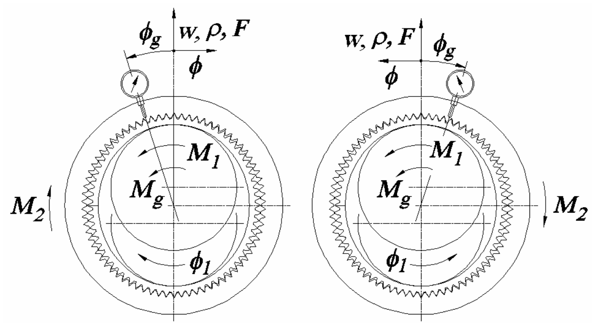

a) b)

Figure 8. The wave generator deviation and the recording of measured amounts in harmonic gear drive service. a) The harmonic drive slows down, b) speeds up

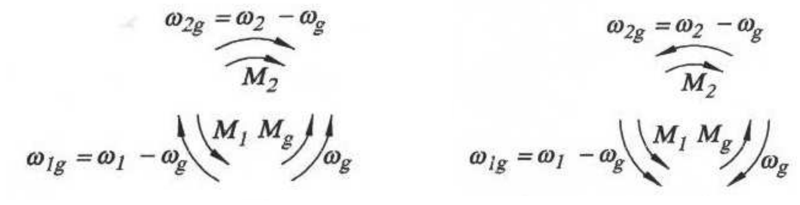

a) *b)*

Figure 9. Torques acting to the elements of the drive and the angular velocities in gear drive service.
a) The gear drive slows down, b) speeds up

7.4. Measuring the radius of curvature

During the tests the tangential elongation of the cenre layer of the flexspline is supposed to be negligibly small ($(\varepsilon_{\phi 0} \approx 0)$). In normal direction, at $\frac{h_0}{2}$ distance from the centre surface of flexspline, parallelly to the end surface of flexspline, the strain $\varepsilon_\phi = \varepsilon_\phi(\phi_g)$ originated from the bending is measurable by strain gauges. Knowing the strain the radius of curvature is $\rho = \dfrac{1}{\dfrac{1}{r_0} + \varepsilon_\varphi(\varphi_g)\dfrac{h_0}{2}}$.

The change of the radius of curvature is measured in a plane, parallel with the end surface of the flexspline, next to the teeth. The strain gauges are glued next to the teeth. The strain complied with the radius of curvature, r_0 is allocated prior to putting the generator into the flexspline ($\varepsilon_\phi = 0$). The change of unit of radius of curvature is determined by a measurement at the tip of wave, ($\phi_g = 0$, $\rho_\beta = r_\beta$, in paper [7] *Table 3.* with a generator disk havingknown radius. The radius of curvature is recorded during the deviation of generator relatively to the circular spline.

7.5. Measuring the force acting to the tooth of circular spline

To determine the load acting to the tooth of tha circular spline, a measuringh tooth was shaped on the circular spline, on a way shown in *Figure 7*. The measuring tooth is supported by a slender feather, gluing strain gauges on both the sides. The load acting to theteeth is recorded in the function of generator deviation relatively to the circular spline. The load acting to the teeth is determined knowing the load distribution, the number of meshing teeth and the torque acting to the flexspline, M_1.

8. The measured amounts and the conclusions

The measured amounts in gear drive service are shown in *Figure 10–13*. The power flow of $2 \to 1$ belongs the left hand side and that of $1 \to 2$ belongs the right hand side column. In the case of the power flow $2 \to 1$ the wheels are revolving clockwise relatively to the generator, the teeth of flexspline enter into the spaces of the circular spline on the arc belongs to the angle range of $-\frac{\pi}{4} \le \phi \le 0$ and come out on the arc belongs to the angle range of $0 \le \phi \le \frac{\pi}{2}$. In the case of the power flow $1 \to 2$ the wheels are revolving counter clockwise, the teeth of flexspline enter into the spaces of the circular spline on the arc belongs to the angle range of $0 \le \phi \le \frac{\pi}{2}$ and come out along the section $-\frac{\pi}{4} \le \phi \le 0$.

The number of teeth of the gears and the inner diameter of the flexspline in the inpected cases are $z_1 = 190$, $z_2 = 192$, and $D = 191{,}7\ mm$, respectively. In the cases shown in *Figure 10. a) and c)* the torques acting clockwise to the flexspline are $M_1 = 0\ Nm, 200\ Nm, 400\ Nm, 600\ Nm,$ and that of *Figure b)* $M_1 = 0 Nm, 200\ Nm, 400\ Nm$ *és 600 Nm.* In *Figure d)* $M_1 = 0\ Nm, 200\ Nm, 400\ Nm$, and *Figure e)* and *f)* the torque is $M_1 = 600\ Nm$.

In the function of angle ϕ, measured from the major axis of the generator, the radial displacement, w, measured next to the teeth of flexspline is shown in *Figure10. a)* and *b).* The radius of curvature, ρ, inspected also next to the teeth of flexspline is shown in *Figure 10. c)* and *d).* In *Figure 10. d)* and *e)* the force acting to the tooth of circular spline is shown.

a) *Figure 10. a) and b)* show the radial displacement of the flexspline. **Applying the load on the drive the flexspline is deflected and the gaps are rearranged and as a consequence, the radial displacement of the flexspline decreases.**

b) *Figure 10. c)* and *d)* show the alteration of the radius of curvature. In case of $M_1 = 0 Nm$ the flexible spline is fitted to the disk along the arc belongs to 2β as shown in *Figure 3*. **The measured value of the radius of curvature is approximately constant.**

c) In the case of $M_1 > 0,\ 2 \to 1\ \text{and}\ 1 \to 2$ the alteration of the radius of curvature is different. **In the case of $2 \to 1$ the disk acts in two stage to the flexible spline. Between these two stages the flexspline is bent and become detached from the disk.**

d) In the case of $M_1 > 0$ and $1 \to 2$ **three special stages can be observed** on the wave. The generator supports the flexspline only on the left hand side of the wave, at the stage of penetration of the teeth of flexspline into the spaces of circular spline. At the tip of wave the flexspline separates from the disk and the circular spline will cause the radius of curvature of the flexspline to be decreased. Emerging from the engagement the radius of curvature of the flexspline is increasing. This stage is followed by another one which has an approximately constant radius of curvature.

Gear drive service $2 \rightarrow 1$ *Gear drive service* $1 \rightarrow 2$

$x_1 = 4{,}555$, $x_2 = 4{,}958$, $w_0 = 1{,}2\,mm$, $e = 3{,}9\,mm$, $d_t = 186{,}3\,mm$ $\beta = 34{,}757^{\,o}$

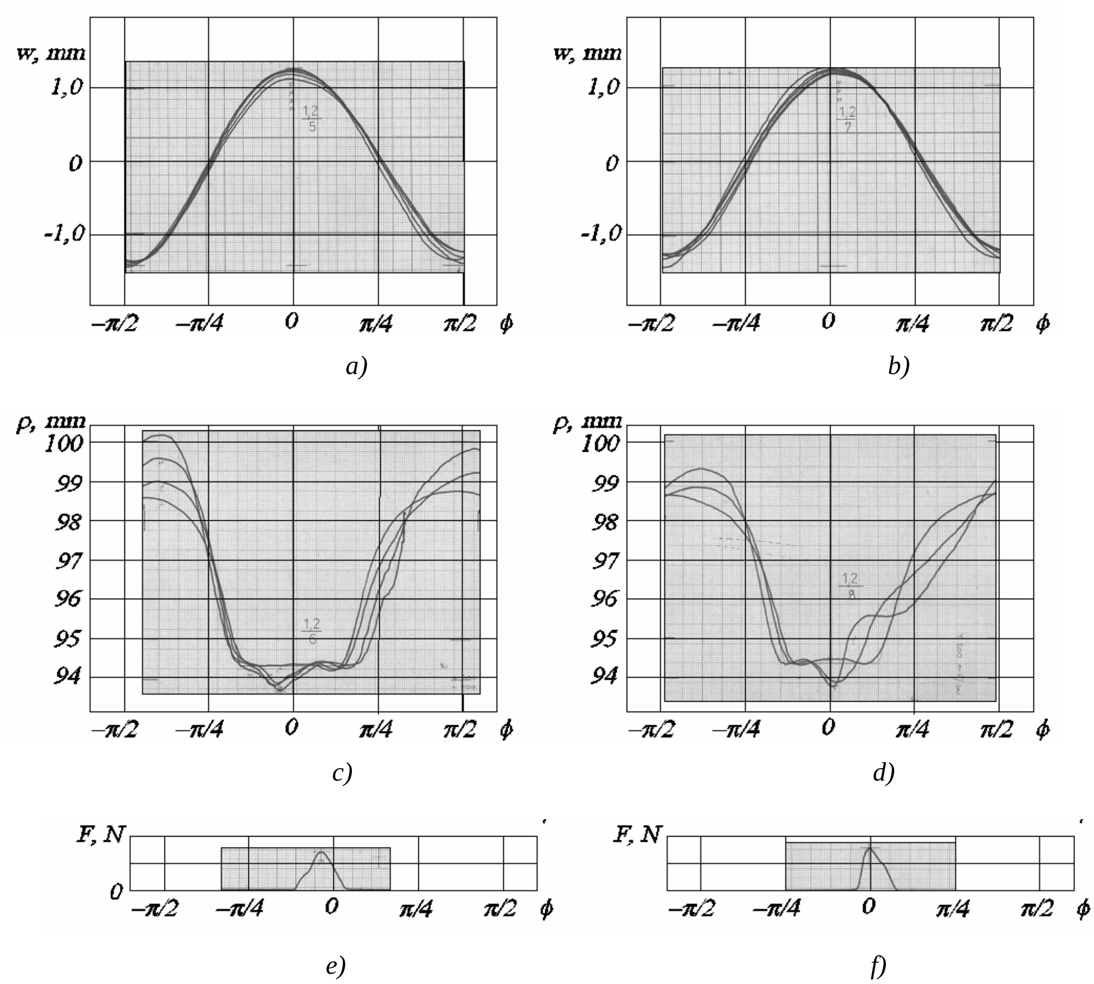

Figure 10. a) and b) Radial displacement of the flexspline,
b) and d) ρ *is the radius of curvature, e) and*
f) F *is the force acting to the tooth of the circular spline*

Gear drive service, $2 \to 1$ *Gear drive service,* $1 \to 2$

$x_1 = 4,555$, $x_2 = 4,958$, $w_0 = 1,1\,mm$, $e = 3,9\,mm$, $d_t = 186,1\,mm$, $\beta = 24,811^o$

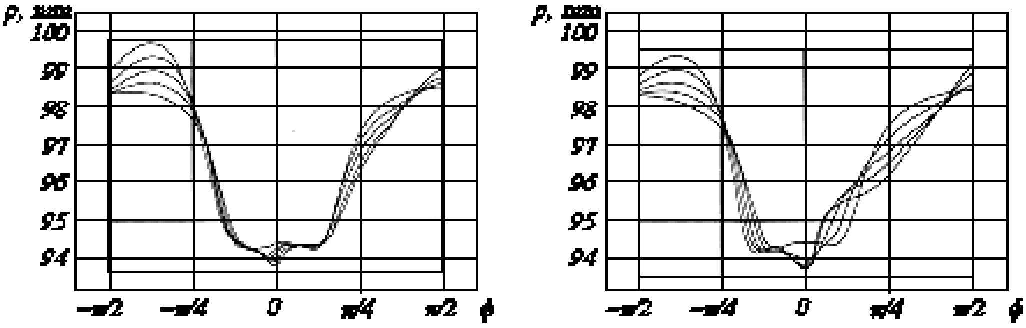

a) b)

Figure 11. The radius of curvature, in the function of deviation relatively to the major axis

e) *Figure 10. e)* and *f)* show the forse acting to the teeth of circular spline in case of the torque value of $M_1 = 600\ Nm$. **In both power flow the simultaneously engaging teeth and the largest tooth force are approximately the same**, and the distribution of forces acting to the engaging teeth is also similar.
f) In the case shown in *Figure 11*. the disks of the generator were changed from $d_t = 186,3\ mm$ to $d_t = 186,1\ mm$. The radial displacement decreased from $w_0 = 1,2\,mm$ to $w_0 = 1,1\,mm$, the semi arc of contact also decreased from $\beta = 34,757^o$ to $\beta = 24,811^o$, **the effect to the radius of curvature is negligible**.
g) In the case shown in *Figure 12*. the disks of generators were changed from $d_t = 186,3\,mm$ to $d_t = 186,1\ mm$. The radial displacement decreased from $w_0 = 1,2\ mm$ to $w_0 = 1,2\ mm$, and the semi arc of contact also decreased from $\beta = 34,757^o$ to $\beta = 24,811^o$. Relatively to the variant shown in *Figure 11*. the circular spline was also changed, instead of $x_2 = 4,958$ the profile correction factor altered to $x_2 = 5,098$. **The increment in the number of simultaneously engaging teeth is shown by the alteration of the radius of curvature.**
h) In the variant visible on *Figure 12*. the eccentric and the disks were changed, **the arc of contact between the flexspline and the disks was increased** $(2\beta = 85,06^o)$. The radius of curvature of the flexspline, relatively to the previously mentioned cases, was changed slightly in the power flow $2 \to 1$, and in the power flow $1 \to 2$ **it was changed significantly, due to the influence of the disk to the flexspline**.
j) In the cases discussed with the help of *Figure 9–12*. it is obvious that **the shape of flexspline diverges depending on the power flow of the drive**.
k) At the power flow of $1 \to 2$ the deflection of flexspline can be limited by increasing the disk diameter.
l) Increasing the normal gap the limitation of deflection of flexspline is reduced.

Gear drive service, $2 \rightarrow 1$ *Gear drive service,* $1 \rightarrow 2$

$x_1 = 4{,}555$, $x_2 = 5{,}098$, $w_0 = 1{,}2\ mm$, $e = 3{,}9\,mm$, $d_t = 186{,}3\,mm$, $\beta = 34{,}757^{\,o}$

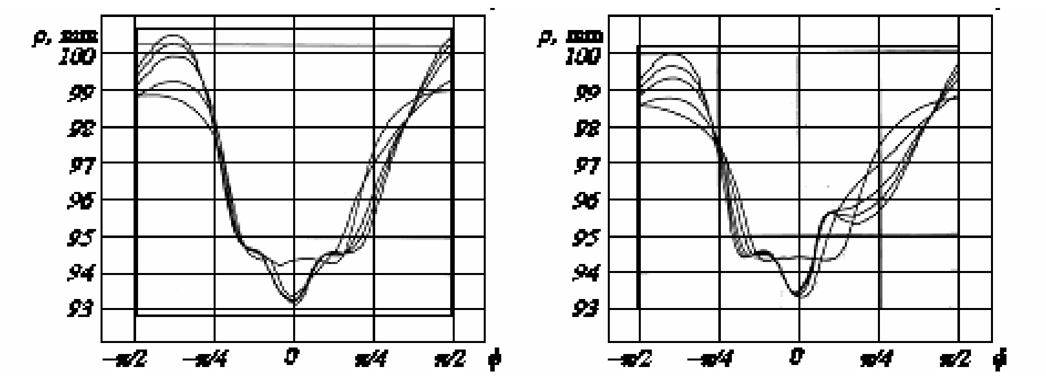

a) b)

$x_1 = 4{,}555$, $x_2 = 5{,}098$, $w_0 = 1{,}2\,mm$, $e = 3{,}9\,mm$, $d_t = 186{,}1\,mm$, $\beta = 24{,}811^{\,o}$

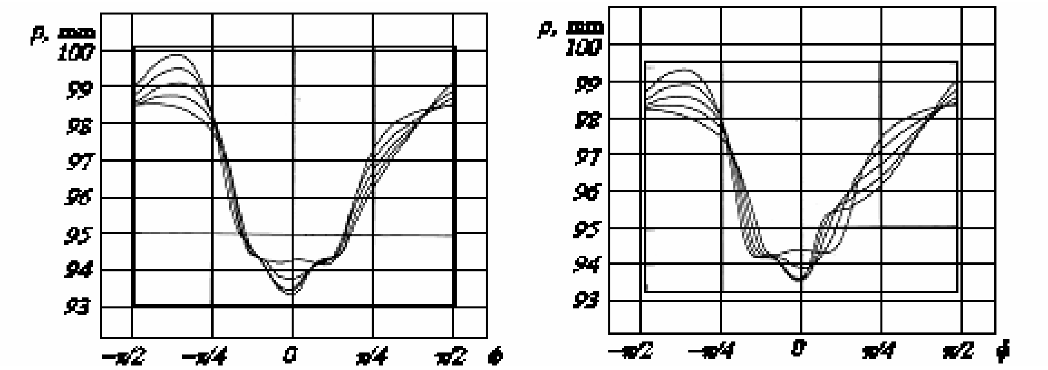

c) d)

Figure 12. The radius of curvature, in the function of deviation relatively to the major axis of the generator.

Gear drive service, $2 \rightarrow 1$ *Gear drive service,* $1 \rightarrow 2$

$x_1 = 4{,}555$, $x_2 = 4{,}958$, $w_0 = 1{,}2\,mm$, $e = 3{,}4\,mm$, $d_t = 186{,}9\,mm$, $\beta = 42{,}53^o$

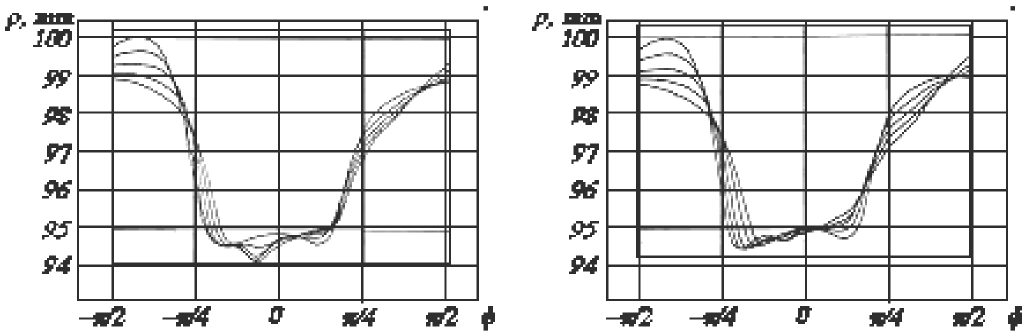

a) *b)*

$x_1 = 4{,}555$, $x_2 = 5{,}098$, $w_0 = 1{,}1mm$, $e = 3{,}4\,mm$, $d_t = 186{,}9\,mm$, $\beta = 42{,}53^o$

Gear drive service, $2 \rightarrow 1$ *Gear drive service,* $1 \rightarrow 2$

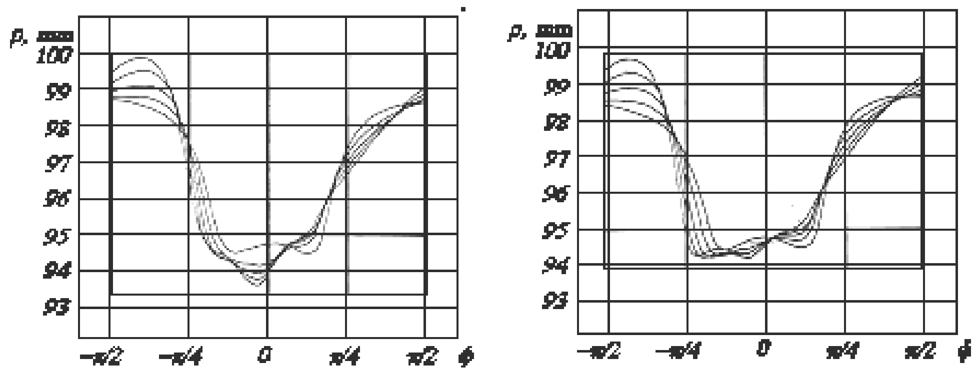

c) *d)*

Figure 13. The radius of curvature, in the function of deviation relatively to the major axis

10. Summary

In the present paper the authors examined the relationship among the geometry and load characteristics of a harmonic gear drive containing eccentric disk wave generator. The characteristics were the radial displacement measured next to the back surface of the flexspline, the radius of curvature, the force acting to the tooth of circular spline, the data of geometry and the load of the drive. The conclusions was restricted to the effect of the changed driving elements on the curvature of flexspline.

Acknowledgement

"This research was carried out as part of the TAMOP-4.2.1.B-10/2/KONV-2010-0001 project with support by the European Union, co-financed by the European Social Fund."

REFERENCES

[1] C. W. Musser: *Elastic-Body Mechanics*. Machine Design, 1961. No. 6. 150–156 p.
[2] J. Péter: *Fogazott hullámhajtómű kapcsolódásának vizsgálata*. (A Miskolci Műszaki Egyetemen elfogadott egyetemi doktori értekezés.) 1981, 174. p.
[3] J. Péter: *Fogaskerék-hullámhajtómű és tengelykapcsoló kapcsolódásának vizsgálata*. (Az MTA Tudományos Minősítő Bizottsága által elfogadott kandidátusi értekezés.) 1992, 111. p.
[4] J. Péter–G. Németh: *A fogaskerék-hullámhajtómű geometriai viszonyai*. Gép, 2005/11–12. 133–137. p.
[5] J. Péter: *A fogaskerék-hullámhajtómű rugalmas alakváltozásának összetevői*. Gép. 2008, 10–11. 111–118. p.
[6] J. Péter–G. Németh: *Rugalmas mechanizmusok*. Gép, 2010/11. 77–82 p.
[7] J. Péter–G. Németh: *Fogaskerék-hullámhajtómű laboratóriumi vizsgálata I.* Gép, 2011.
[8] J. Péter–G. Németh: *Fogaskerék-hullámhajtómű laboratóriumi vizsgálata II.* Gép, 2011.
[9] Sz. A. Suvalov–A. D. Volkov: *Deformacija gibkogo zubcsatogo kolesza dvumja diszkami*. Izv. vuz. Mas. 1971. No 10. 44–49. p.

Design of Machines and Structures, Vol. 2, No. 1 (2012), pp. 53–62.

ON COMPUTATIONS OF VIBRATIONS AND FREQUENCIES OF ROLLING BEARINGS

FERENC SARKA
University of Miskolc, Department of Product and Machine Design
3515 Miskolc-Egyetemváros
sarkaferenc@yahoo.com

This paper summarises the sources and the reasons of developed vibrations in rolling bearings. Equations are given to compute the developed vibrations according to the professional literature. The behaviour of rolling bearings is analysed detailed in different frequency range

1. Introduction

Rolling bearing as a mechanical element or machine element has been used in the Ancient Rome. It has a very different shape than it has nowadays, but the principle of the operation was the same. It had wooden rolling elements and it was used in the wheels of coaches. After the fall of the Roman Empire, many magnificent scientific results were forgotten, like bearings in wheels of coaches. [1]

Leonardo da Vinci the grate scientist of the Middle Ages dealed with shaft mountings, that is to say bearings. Unfortunately as with many other ideas of his own, he just made sketches about the bearing, there is no known prototype of them.

In our days the bearing is one of the most often used machine element in machines and equipments. Bearings after the patent of Philip Vaughan (1794) have been made significant expression to the engineers in the meaning of their different operation circumstances and rolling problems. Judging their condition and defining the rest of their lifetime have caused a huge headache for the engineers.

2. Beginning steps

The first large scale examination to estimate the state of heavy machines and judge their running conditions was made by T. C. Rathbone. Scientific vibration diagnostic of our days was built upon their work. The scientific level of the modern vibration diagnostic was generated by the development of computing equipments and the claims of the industry.

Rathbone was the chief engineer of Turbine and Machinery Division, for the Fidelity and Casualty Company of New York. He started to deal with the measurement and the documentation of the machine vibration at the beginning of the 1930's. He first publicated his results in 1939 with the title of „Vibration Tolerance" in the periodica Power Plant Engineering. This paper was about the diagnostic of the vibration level rising in case of rough operation deriving from unbalancing machines. [2] His results were summarised in a chart (*Figure 1.* Rathbone chart).

The Rathbone chart classifies machines into seven divisions:

- 1. Sensory perception level,
- 2. Very smooth,
- 3. Good,

- 4. Fair,
- 5. Slightly rough
- 6. Rough – needs correction,
- 7: Very rough – correct immediately.

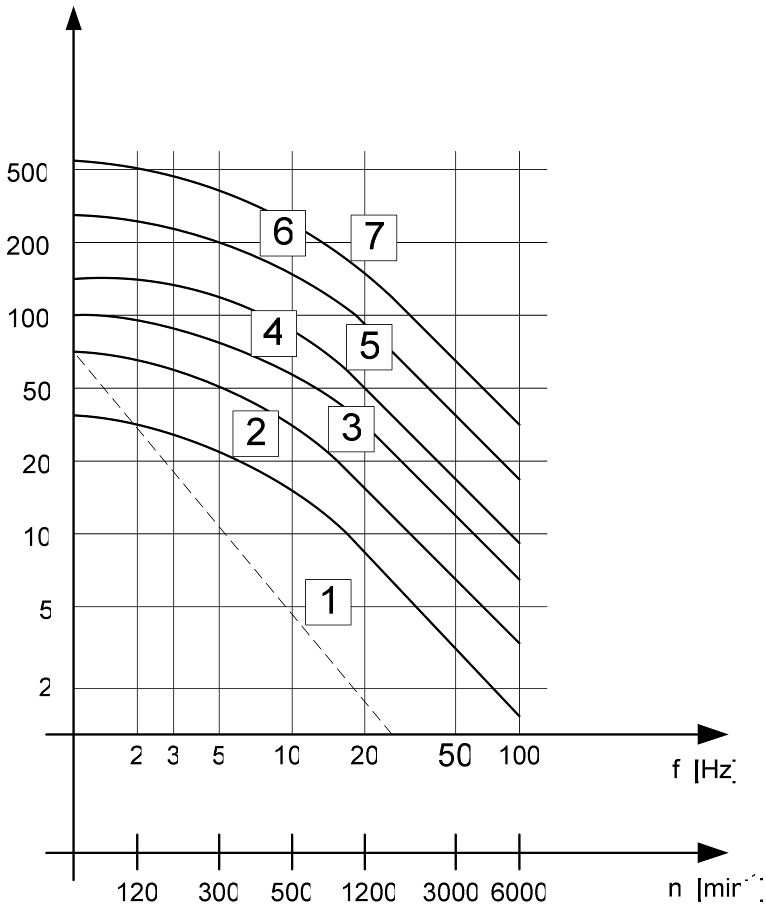

Figure 1. Rathbone chart [3]

Of course his results are not up to date and not proper for our days regulations, but his work was very significant milestone in this filed of science.

The determination of the acceptable vibration level in case of rolling bearings is still in use was based on this chart and the measuring results of the engineers working for ENTEK IRD. In Europe the chart for rolling bearings was signed as the original Rathbone diagram for many years (*Figure 2*.).

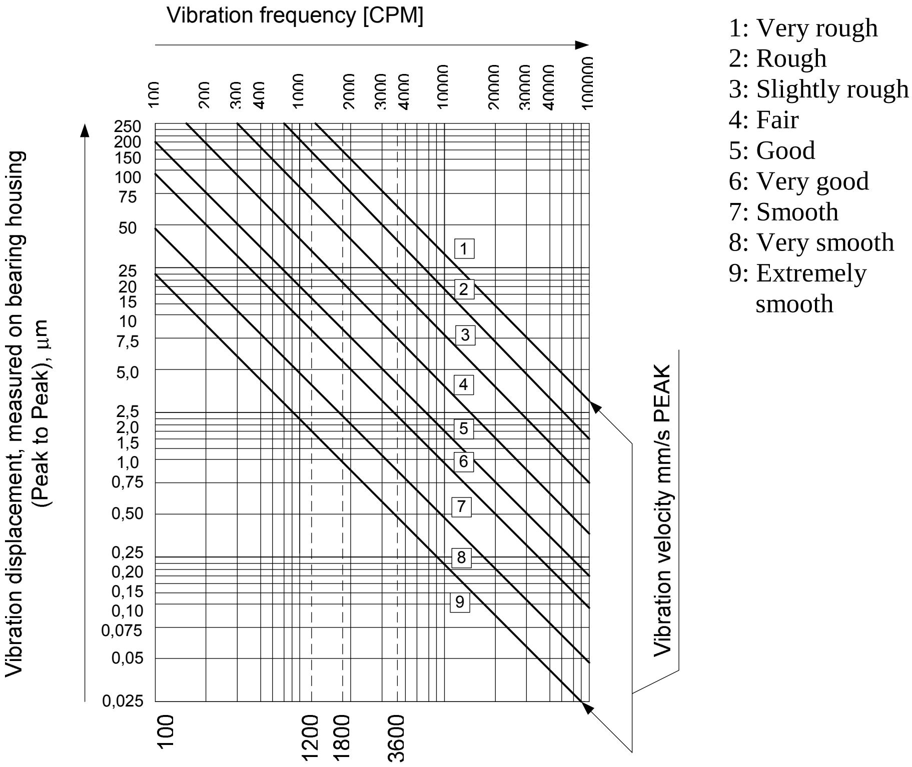

Figure 2. Chart summarising the results of ENTEK IRD [8]

3. The behaviour of rolling bearing is different frequency range

The vibrational behaviour of rolling bearings can be divided into several ranges according to the frequency. This can be seen in *Figure 3*. [4]

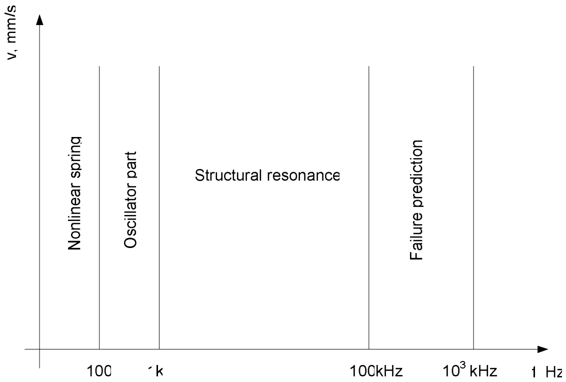

Figure 3. The vibrational feature of rolling bearing according to the frequency ranges [4]

3.1. Non-linear spring

The rolling bearing under 100Hz can be modelled by a nonlinear spring. This model consists of 3 masses. A spring element and an absorber element mean the connection between the masses. Mechanical model can be seen in *Figure 4.*

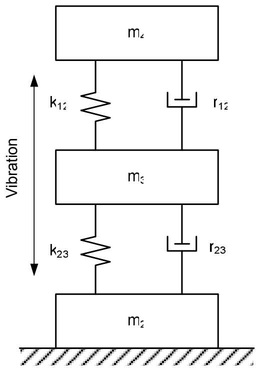

Figure 4. Mechanical model of rolling bearing

With the signs of *Figure 3.:*

- m_4: outer ring
- m_3: rolling elements
- m_2: inner ring
- k: rigidity of spring element
- r: the coefficient of absorber element

The connecting surfaces in the rolling bearing are extremely small. In a sense of mechanics the connection is a point (in ball bearing), or a line (in roller bearings). Bearing can be examined according to the Hertz theory. With the help of this theory the deformation can be determined in the connection point or line and around. Of course this theory uses simplification, but this is not means such a big difference as we should generate if we examine the model as a pure rigid body [4], [5].

The Hertz-theory uses a couple of conditions; examinations can be solved according to them.

Conditions:

- The size of the connecting surfaces is much smaller than the size of the connecting elements.
- The load is perpendicular to the common tangent plane of the connecting elements.
- The material of the connecting elements is homogeneous and isotropic.
- Friction between elements is eliminated.

3.2. Vibration emitter, planetary gear analogy, developed frequencies

On the horizontal axle of *Figure 3*. the next behavior stage can be seen. In this stage that has an interval from approximately 100 Hz to 1kHz, the vibration emitter behavior of rolling bearing is the determinative. This kind of behavior is the consequence of the structure the rolling bearings have. To understand the influence, let us see how the bearings are working.

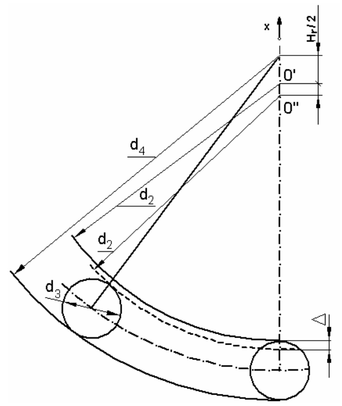

Figure 5. Seat evolved on one or two rolling body caused by the internal clearance of rolling bearings

It is known that bearings are built in with internal clearance. This means that the clearance between the inner ring and the outer ring is bigger than the featuring size of the rolling body. In cases like this moments can occur during the operation of the rolling bearings, when two rolling bodies prop the inner ring and there are moments as well, when only one rolling body provides the shoulder of the inner ring (*Figure 5.*). This phenomena results the Δ size movement of the inner ring in radial direction, so a kinematic excitation. Therefore polygon-frequency arises. Calculation of the polygon-frequency can be solved according to equation (1).

$$f_p = \frac{n_k}{60}\,[\,Hz\,] \qquad (1)$$

n_k is the revolution of the cage in min^{-1} unit.

When the internal clearance of the rolling bearing eliminated, then the kinematic excitation would be disappeared and the rolling bearing would be a pure rigid body. In circumstances like this rolling bearings could not be operated.

Of course the polygon-frequency is not the only frequency that features rolling bearings. In cases of bearings that are ensuring kinematic pure rolling other rolling frequencies can be divided into two groups, depending on whether the inner or the outer ring is rolling. [6]

In case of rolling inner ring:

– The frequency of the inner ring:

$$f_2 = \frac{n_b}{120}\left(1 + \frac{\cos\alpha}{\frac{d_k}{d_2}}\right)\cdot z_g\,. \qquad (2)$$

– Cage-frequency:

$$f_k = \frac{n_b}{120}\left(1 - \frac{\cos\alpha}{\frac{d_k}{d_3}}\right). \tag{3}$$

– The frequency of the rolling element:

$$f_3 = \frac{n_b}{120}\left(\frac{d_m}{d_g} - \frac{\cos^2\alpha}{\frac{d_k}{d_3}}\right). \tag{4}$$

In case of rolling outer ring:

– The frequency of the outer ring:

$$f_4 = \frac{n_k}{120}\left(1 + \frac{\cos\alpha}{\frac{d_k}{d_3}}\right)\cdot z_g. \tag{5}$$

– Cage-frequency:

$$f_k = \frac{n_k}{120}\left(1 - \frac{\cos\alpha}{\frac{d_k}{d_3}}\right). \tag{6}$$

– The frequency of the rolling element:

$$f_3 = \frac{n_k}{120}\left(\frac{d_m}{d_3} - \frac{\cos^2\alpha}{\frac{d_k}{d_3}}\right). \tag{7}$$

Quantities in (2)–(7) equations:

n_b : rev of the inner ring,

d_k : (featuring) diameter of the cage,

z_g : number of the rolling elements,

d_m : middle diameter of the rolling bearing,

d_g : diameter of the rolling element,

α: angle of action (in case of deep groove ball bearings $\alpha = 0°$),

Indexes 2, 3, 4 means inner ring, rolling element, outer ring.

Solving the computations rev of each elements of the rolling bearing is needed. Rolling bearing is able to be substituted by a OI planetary gear. Through this planetary gear analogy Kutzbach-construction can be applied for determining the revs (*Figure 6.*).

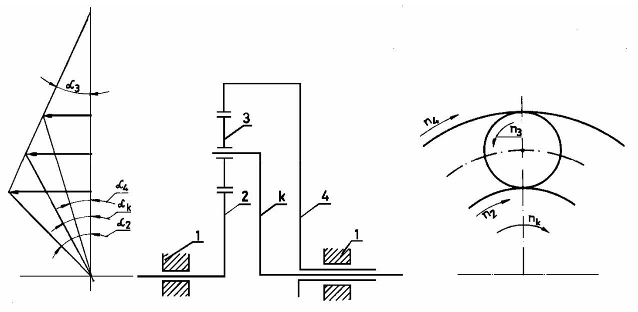

Figure 6. Rolling bearing substituted by planetary gear for defining revs

Besides the above mentioned frequencies others are also appears during the operation of rolling bearings originated from imbalance and the failures of the geometry.

3.3. Frequencies deriving from imbalance

In case of each element that has rolling movement vibration deriving from imbalance occurs. Sometimes this vibration is higher, sometimes it is lower. Even in case of the most perfect manufacturing a few imbalance is still rest in elements.

Evolving frequencies:

– Shaft frequency generated by forces:

$$f_t = \frac{n_2}{60}. \tag{8}$$

– Cage frequency generated by forces:

$$f_k = \frac{n_k}{60}. \tag{9}$$

– Housing frequency generated by forces:

$$f_4 = \frac{n_4}{60}. \tag{10}$$

– Roller frequency generated by forces:

This frequency usually can be eliminated. Rollers generally compensate the effects they have. If it cannot be eliminated computations can be solved according to the equations (11), (12).

From main movements:

$$f_{g1} = \frac{n_3}{60}. \tag{11}$$

From collateral movements:

$$f_{g2} = \frac{n_s}{60}. \tag{12}$$

Collateral movements evolving in those bearings that are not able to ensure kinematic pure rolling. Bearings like this are e.g.: angular contact ball bearing or deep groove ball bearings that are also loaded by axial force

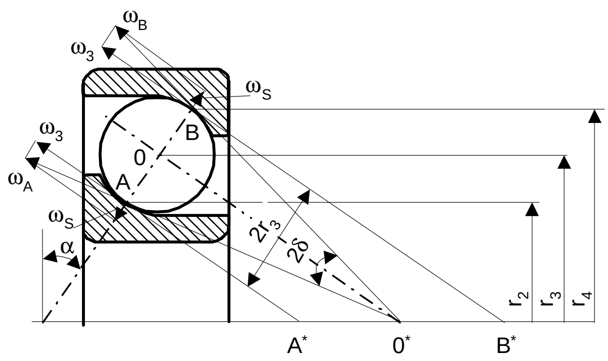

Figure 7. Sketch of an angular contact ball bearing

n_s can be counted according to *Figure 7.* by the next equation:

$$\omega_s = \omega_3 \frac{r_3}{r_k} \sin\alpha. \tag{13}$$

3.4. Frequencies deriving from the failures of the geometry

The running surfaces of real rolling bearings and the surfaces of the rolling elements are not pure true to type surfaces. According to this not perfect elements while rolling down on each other generate different sizes of irregularity.

The failure of running surfaces is usually waviness. This can be originated from the production and the circumstances of the assembly. The generated frequencies can be counted according to the following equations:

– Effect of the geometry failure in case of inner rings:

$$f_2 = i_2 \frac{n_{k2}}{60}. \tag{14}$$

– Effect of the geometry failure in case of outer rings:

$$f_4 = i_4 \frac{n_{k4}}{60}. \tag{15}$$

i_2 and i_4 in equation (14) and (15) are the number of the failures appearing on the given elements, in case of waviness i_2 and i_4 are the number of the waves. n_{k2} and n_{k4} are the rev of the cage related to the inner ring and outer ring.

Failures appearing on the surface of the rolling elements are polygon failure mainly. Counting the frequency generated by the polygon failure should be done according to equation (16):

$$f_3 = i_3 \frac{n_3}{30} . \tag{16}$$

Rev n_3 is the rev of the rolling body own shaft.

3.5. Eigenfrequencies (resonance frequencies)

In case of equipment consist of rotating machine elements eigenfrequencies of these elements should be kept in front of the designer's eyes. Permanent operation of an equipment like this on the rev that results an excitation proper for one of the elements' eigenfrequency is forbidden. Calculating eigenfrequencies on paper is to be solved only in case of those elements that has a very simple geometry. With the development of the computer technology finite element softwares are able to determine the eigenfrequencies even in case of difficult geometry as well. Eigenfrequency depends on the material and the size of the geometry. In case of rolling bearings eigenfrequencies of the inner and the outer ring are important. Frequency images of eigenfrequencies can be seen in *Figure 8.* Determining the eigenshapes was carried out by a FEM program.

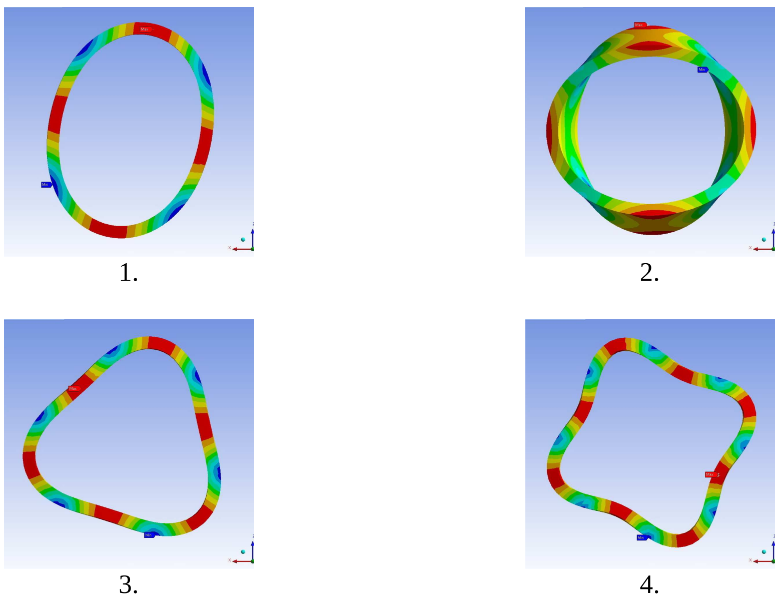

Figure 8. Resonance shapes of Eigen frequencies in case of rolling bearing rings (first 4)

3.6. Damage prognosis

In case of damages other frequencies appear over the above mentioned ones. These frequencies can be originated not only from the damage of the rolling bearing but it also can be caused by a false assembly, or an improper construction of the connecting elements (housing, shaft). Let us see a very simple example. Rolling bearing is positioned in a bore through an interference fit. Unfortunately the bore was made wavy. Because of the interference fit the outer ring of the rolling bearing adopts the wavy shape, so the running surface of the rolling elements also gets wavy.

The literature helps the engineers realising the failures of rolling bearings independent of the reason of the failure by different spectrum pictures determined by several measures and analysis.

On the field of vibration diagnostic there are a lot of measuring methods developed for determining the state of bearings. *Figure 9.* shows their application according to the frequency values.

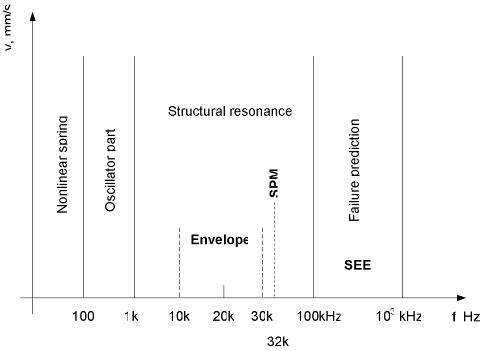

Figure 9. Suggested measuring methods in different frequency intervals [4]

4. Conclusion

The paper introduced how wide the range of frequencies a rolling bearing can perform is. It should be noticed that the above introduced calculations are only typical for normal operation. Frequencies generated by different failures were only mentioned. Analysing the spectrum of a bearing all above mentioned frequencies should be taken into account so the failures generated frequencies to be identified, and on this basis arrangements can be made.

Acknowledgement

"This research was carried out as part of the TAMOP-4.2.1.B-10/2/KONV-2010-0001 project with support by the European Union, co-financed by the European Social Fund."

References

[1] H. Hodges: *Technology in the Ancient World*. Barnes & Noble, 1992.
[2] J. S. Mitchell*: From Vibration Measurements to Condition Based Maintenance*. Sound And Vibration, 2007.
[3] http://www.tcf.com/docs/i-ms/rathbone-balancing-chart---es-5-1.pdf?Status=Master
[4] F. Dömötör: *Rezgésdiagnosztika I.* Dunaújvárosi Főiskola Kiadói Hivatala, Dunaújváros, 2010.
[5] A. Baksa: *Érintkezési feladatok numerikus vizsgálata.* PhD. Értekezés 2005, Miskolci Egyetem.
[6] A. Kováts*: Gépszerkezettan (műszaki akusztika).* Tankönyvkiadó, Budapest, 1985.
[7] Gy. Ludvig: *Gépek dinamikája*. Műszaki Könyvkiadó, Budapest, 1973.
[8] http://www.usedvibration.com/vibration_analysis_severity_charts.htm

Design of Machines and Structures, Vol. 2, No. 1 (2012), pp. 63–72.

OPTIMIZATION POSSIBILITIES AND METHODS IN PRODUCT DEVELOPMENT AND QUALIFICATION

FERENC JÁNOS SZABÓ
University of Miskolc, Department of Machine- and Product Design
H- 3515 Miskolc- Egyetemváros, Hungary
machszf@uni-miskolc.hu

Abstract
In this “state- of- the- art” paper the place and role of optimum design in product development process is described, based on the definition of products, definition of product quality and product qualification levels. Most important product characteristics and parameters are listed which can be subjected to optimization or multidisciplinary optimization (MDO) procedures. Case studies and numerical examples are shown for optimization, quality analysis, improvement and shape optimization of several industrial products and products designed by Industrial product and art designer students. The examples and case studies were selected from the industrial projects and students design and optimization works and results of the Department of Machine and Product Design at University of Miskolc, Hungary.

Keywords: product qualification, optimization methods, MDO, shape optimization of products

1. Introduction

In 1996 the Department of Machine Elements at University of Miskolc started the education of product development as a new formation course besides of machine elements and construction design. This resulted in the flare of the activity palette of the department. The education of product development invoked new disciplines as Product and Art Design, Integrated Product Design or Product Simulation. As a result of this new education activity, the name of the department changed the new name is: Department of Machine and Product Design since 2008.

During the design process of – not only industrial – products, besides the design of the shape, functionality and colours of the product, it is very important to keep the high standard of efficiency, reliability, economy (low material and manufacturing costs) or high load carrying capacity and longer life [1]. These characteristics could increase the added value content of the product or could give higher competitiveness. For the development and increase of these parameters of a product, it is unavoidable to apply and use the facilities and possibilities offered by multidisciplinary optimization (MDO) [2], the finite element method (FEM) [3], [4] and computer aided design (CAD).

In this paper the integration of these methods is presented into the product development process by showing several case studies and numerical optimization examples. Examples are shown for optimization, quality analysis, improvement and shape optimization of several industrial products and products designed by product engineering students.

The examples and case studies were selected from the industrial projects and student design and optimization works and results of the Department of Machine and Product Design at University of Miskolc, Hungary.

2. The place and role of MDO and FEM in the design and development of products

First of all, it would be necessary to repeat the well known definitions of product, product lifecycle, quality of product, product design, in order to place easier the FEM and MDO methods into this system. (The usage of a three dimensional CAD system is always necessary to create the models for FEM and MDO investigations.)

Product can be everything which is marketable, consumable, or usable, fulfilling a need, demand or request of the customers. As a simple approach, one can discuss three levels of the product:

a. Abstract product;
b. Manufactured product;
c. Complementary product.

The abstract level of product integrates all the advantages, provisions, services, supplies which can be associated to the image of the product and these will be the main reason to why buy the product (for example in case of food product the enjoyable taste, aroma, flavour, healthy effects, nutrition values, etc. or in case of furniture convenience, aesthetics etc.). At the level of abstract product, it is requested by the consumer that the product should work well and should carry the loads during the operation and usage. The verification of the product against these kinds of effects could be an entering point for FEM and MDO results into the product design process.

The product designer will transmit the abstract product into the manufactured product level. The manufactured product has its trade mark, name, form, characteristic colours, packing, technical parameters, quality, reliability, load carrying capacity, etc. The last four parameters already can be subjects of several finite element and optimization studies and improvement processes, the results of which can improve considerably some very important characteristics of the products. This is the most important point where the FEM and MDO methods could connect into the product design process.

The third level is the complementary product, which means some more or added services, characteristics of the manufactured product for example guarantee, assurance, set in operation, or in case of a software product the installation, upgrade, etc. If the manufactured product does not contain FEM or MDO results, this point could be also a possible place to call in these investigations into the product development process, for example by creating a new type of service as “optimized product” or “verified product”. Also it is possible to create some analysis, verification, optimization or improvement services for products after selling, similarly to the upgrade process, as “developed product”, “economic product” or “improved product”.

More detailed approach can be to define five levels of the product:

a. Elementary benefit;
b. Basic product;
c. Requested product;
d. Augmented product;
e. Potential product.

The “elementary benefit” level of the five level product definition could be associated to the abstract product” level of the three level product definition, therefore everything can be applied here what was mentioned for the abstract product level, concerning the possible entering way of FEM and MDO into the product design process.

The basic product incorporates all the advantages, characteristics, what where provisioned in case of the elementary benefit (for example yoghurt incorporates that it is healthy, enjoyable taste etc.).

The requested product contains all the requests, claims and demands of the customer concerning the product (for example easy to operate, practical, or in case of food good flavour etc.). This level could be associated to the "manufactured product" level of the three level product definitions, so this could be also an important entering point for the FEM and MDO methods into the product design process.

The "augmented product" collects more wishes of the customer above the "requested products" (for example more practical packing, more convenient delivery, better price/value ratio etc.) and the "potential product" contains all the characteristics and "dreams" which say how the product could be or will include future developments.

On the basis of the above mentioned things one can see that level d. and e. of the five level product definitions offer more possible ways for FEM and MDO investigation procedures to enter into the product design process.

2.1. Possible product characteristics which could be subjects of FEM and MDO investigations and qualification

The product lifecycle starts when the need for the product appears and ends with the end of the usage (when the product falls into oblivion). If the product development process results in newer and newer, better and better versions of the product, the "cycle" name is more and more appropriate, since the life process repeats cycle by cycle. In the lifecycle of every product one can find the design, experiment, analysis activity which helps the product development process from the beginning of the lifecycle until the starting of the manufacturing. This part of the lifecycle can be called as "product development". The most important possibilities for the application of FEM and MDO results are in this part of the lifecycle.

Let us overview the most important parameters or characteristics of products, which can be efficiently improved by the application of finite element and optimization results. The most important subjects of the machine- and product design could be the followings:

Drives:

- Gears, gear drives, gearboxes, conical gear drives, helical gears etc.
- Worm drives;
- Bevel gear drives;
- Belt drives, chain drives, friction drives;
- Harmonic drives, other special drives.

Bearings:

- Ball and rolling bearings, constructions containing bearings;
- Hydrodynamic, hydrostatic journal- and sliding bearings (axial, radial).

Shafts, couplings and their assembly elements:

- Behaviour of shaft- gear- bearing assemblies;
- Several couplings, having different operation concepts (mechanical, electrical, hydrodynamic etc).

Other important products and elements:

- Threaded connections;
- Seals;

- Brakes;
- Springs;
- Slider- crank mechanisms;
- Selected special elements for pipelines (pipe joints, valves, supporting structures for pipelines);
- Hand- tools and their elements;
- Household appliances, food processors;
- Tools to tinker and hobby;
- Cars and accessories or elements for cars;
- Furniture, artistic products;
- Children's toys and furniture;
- Office furniture and accessories;
- Computers and additional products;
- Medical tools, implants, accessories
- Etc.

Most important disciplines that could be involved and touched during the finite element analysis and multidisciplinary optimization of these elements are as follows:

Static:
- Linear static;
- Nonlinear materials;
- Large deformations.

Contact:
- Contact with or without friction;
- Lubricated contact;
- Wear and other forms of contact failure.

Dynamics:
- Eigenfrequencies, undamped and damped vibrations;
- Random vibrations, harmonic and random excitations;
- Transient response, response spectra analysis;
- Vibration reduction and supporting problems.

Sound and noise:
- Operation noise, noise reduction by the design and geometry modifications;
- Acoustics, handling of noise sources;
- Noise reduction, isolation problems.

Fluids, gases:
- Fluid- structure interaction;
- Flow of viscous fluids (oil or cooling liquids);
- Pressure distribution in fluid films;
- Fluid friction;
- Lubrication problems;
- In internal combustion engines: or wheel and tire design: interaction of gas and structure.

Thermodynamics:
- Heat exchange between elements of a construction;
- Cooling problems,

– Heat conduction and convection, radiation.

Electromagnetism:

– Forces acting on elements working in magnetic field;
– Elements of electric motors, effects of the electromagnetic systems;

Fabrication and operation conditions:

– Operation and fabrication interferences;
– Errors, quality requirements, tolerances;
– Requirements and constraints that one must fulfil for the good fabrication and operation.

A large variety of possible application variations can be provided by the combination of the products and applied disciplines for the realistic analysis and optimization of designed products. The disciplines can be considered as constraints (in this case the objective function could be the weight, fabrication costs, load carrying capacity etc. or their combinations in multiobjective problems) or they can be taken into consideration as objective function, this way it is possible to design noise minimized constructions or moving structures or products having minimum power consumption or minimum friction power loss, higher load carrying capacity etc.

The examples and case studies shown in this paper can be found also as a combination of products and disciplines.

The qualification of a product means that all the most important technical parameters will be verified, where possible by using FEM studies and at the end of this process the product will receive a qualification as “ineligible” or “eligible” or “safely eligible”. This qualification can be continued if the economy, efficiency or optimality of an important product characteristic is qualified, in this case it could be possible to use quality levels as “non- optimized” or “inefficient”, “optimized” or “efficient” and “Pareto- optimized” or “multiobjective optimized”. These could be the possible levels of product qualification.

3. Case studies for qualification and optimization of products

3.1. Minimization of strains in electronic panels (improvement of product reliability)

During the testing procedure of electronic panels, the test signal is driven to the attaching points of the panel by using measuring needles. Since the testing program contains several input and output signals and measurements, in our days this process is performed by industrial robots and up to date programmable NC machines.

In this unified and robotized process 300–400 measuring needles can press the panel in one time, depending on the type of the panel and on the type of the needle. Each needle is built with a spring, in order to assure the correct contact with the panel. These springs are calibrated so that 3–5 N load is present at the contact point. It is easy to calculate, that in case of several hundred needles the panel is loaded with 1000–2000 N .Regarding the panel sizes, (160 mm length, 100 mm width and 1.6 mm thickness approximately, the size depends on the panel type) this is a high load. This load sometimes is causing so large deformation and strain values in the panel, that some local failures occur in the electronic elements assembled onto the panel, therefore a number of supporting pins is applied to decrease the deformation and strain (*Figure 1.*).

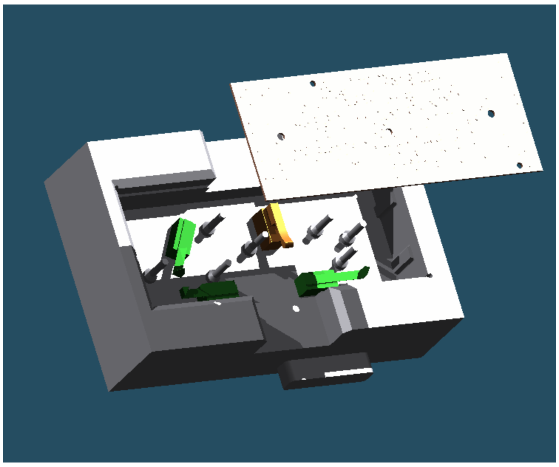

Figure 1. Supporting pins and the assembly of the panel into the measuring frame

Previous measurements and experiments show that a strain of value greater than a limit of 8×10^{-4} is dangerous for the local failure of the assembled elements. The experiments and measurements also show that the strain field in the panel is very sensitive for the arrangement and for the number of supporting pins (*Figure 2*.).

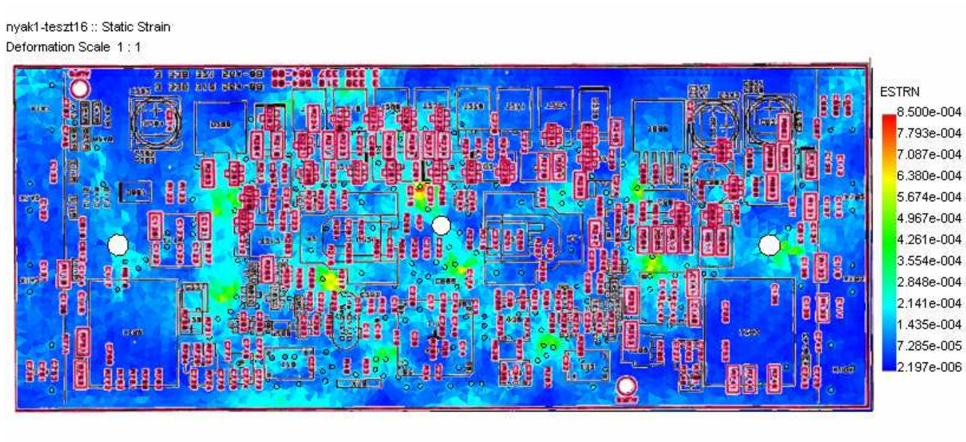

Figure 2. Strain contours shown on the assembly plan of electronic elements. This picture helps to decide which electronic element is in dangerous position

The assembly of the supporting pins sometimes can be very difficult, because electronic elements are assembled to the both sides of the panel, therefore one can find only a few place to apply supporting pins. This situation needs the optimisation of the number and position of supporting pins used for decreasing the maximum strain on the panel under the limit value $8x10^{-4}$. In the solution of this task the strain field was determined by using finite element calculations and for the optimization the Genetic Algorithm was used. As results in the investigated cases, because of the optimal support arrangement the maximum strain value was decreased under $6x10^{-4}$ with same number of supports as before the investigation, or in other cases the limit of $8x10^{-4}$ is fulfilled with a number of supporting pins 20% smaller than before the investigation. These results are useful during the fabrication, because the smaller number of supporting pins can decrease the fabrication cost, the preparation time for the measurement can be shorter. Eliminating high strain values in the panel can increase the reliability or elongates the fatigue life of the product, and the number of waste products and user- complaints can be decreased considerably.

This case study was an example of improvement product reliability and economy by applying the results of a multidisciplinary optimization process (MDO). This study shows the advantages of an "optimized product".

3.2. Verification and qualification of the product

The second case study shows the example of product qualification, based on a finite element analysis (FEM).

In chemical plants, stack gases are eliminated (burnt) in a burner link. When the link is started up (lighting), this is an explosion; the inner pressure in this part of the pipeline will be very high. It is very important that the igniter should be verified against this pressure value if it will bear the strains, stresses and deformations occurring when starting the burner link. *Figure 3*. shows the igniter chamber, stress and deformation contours are in *Figure 4*.

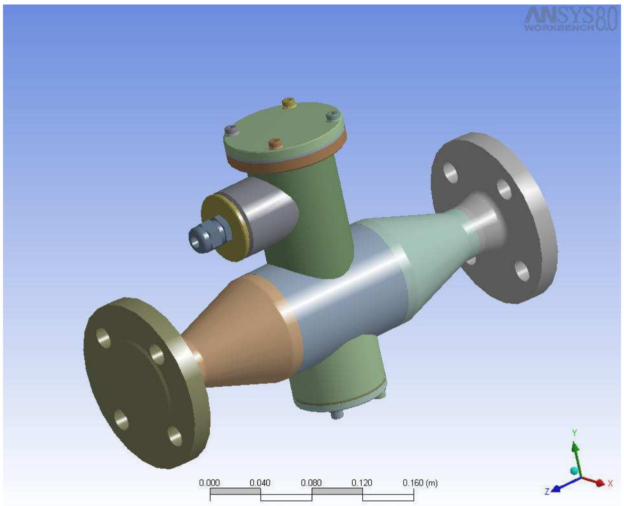

Figure 3. The igniter chamber

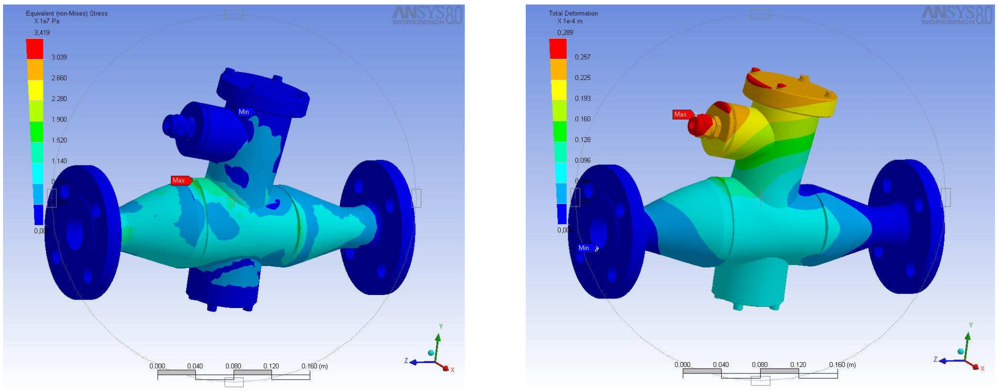

Figure 4. Stress (to the left) and deformation (to the right) contours of the igniter

On the basis of the finite element results, it was possible to draw the conclusion that the igniter is “safely eligible” under the operation circumstances during the lighting period. These results and some selected parts of the expert report were used by the manufacturer in the quality certificate of the product, which must be always part of the product documentation.

4. Student projects

4.1. Shape optimization of a product (pliers haft)

Figure 5. a) shows the initial three dimensional model of pliers, which has constant cross section shape regarding the haft. Shape optimization procedure in ANSYS DesignSpace program system shows the proposed material to eliminate (*Figure 5. b),* in red colour), the designer has to redesign the structure, eliminating the unnecessary material and giving a new form concept to the product (*Figure 6*.).

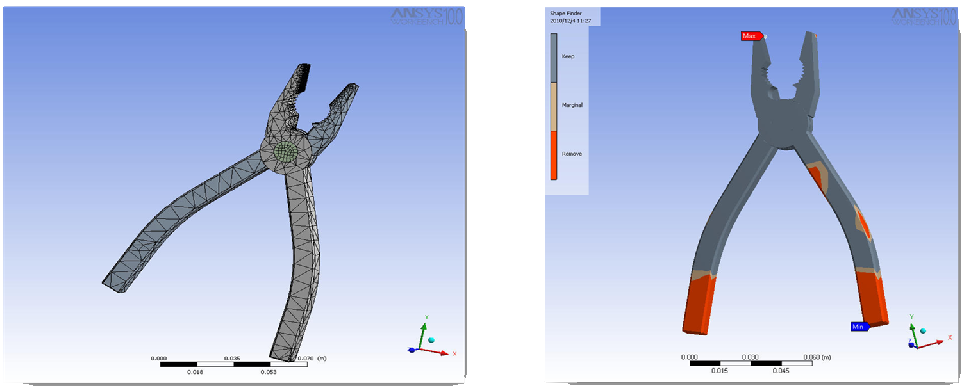

Figure 5. a) (Initial shape) and Figure 5. b) (materials to eliminate) of pliers model

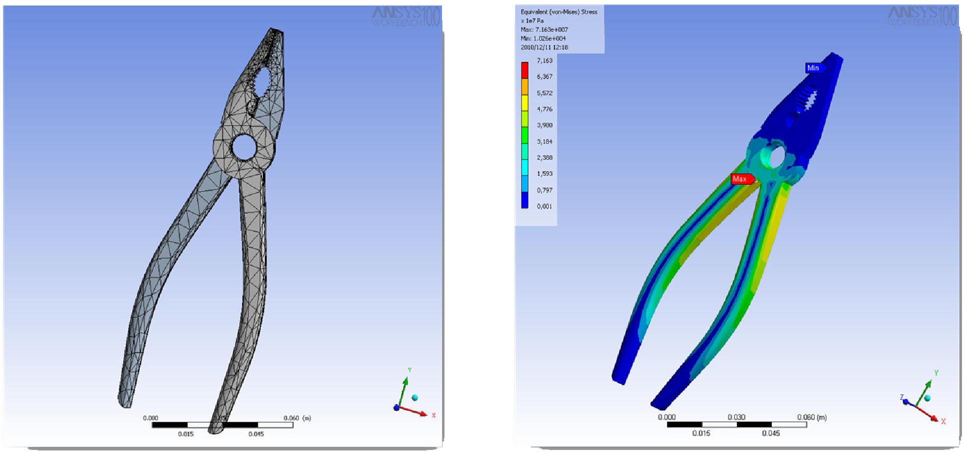

Figure 6. a) (New, improved form) and
Figure 6. b) (Stress state verification) of the product

As the result of the shape optimization procedure, 32% of the product material was spared. Finite element analysis of the new, optimized shape [*Figure 6. b*)] shows that the structure fulfils the operation requirements (in case of 200 N load, 71 Mpa is the maximum stress). The maximum deformation in this case is 0.2 mm.

4.2. Finite element analysis of a bar-chair

A new design of a bar- chair can be seen in *Figure 7. a)*, having the shape of DNA spiral. On the basis of several finite element analysis, the modified design is shown in *Figure 8.*, while stress contours under the load can be found in Figure *7. b).* The structural behaviour of the DNA shape column invokes a lot of future development and research possibilities, therefore these investigations will be continued in the future, within the frames of Student Research Work (TDK).

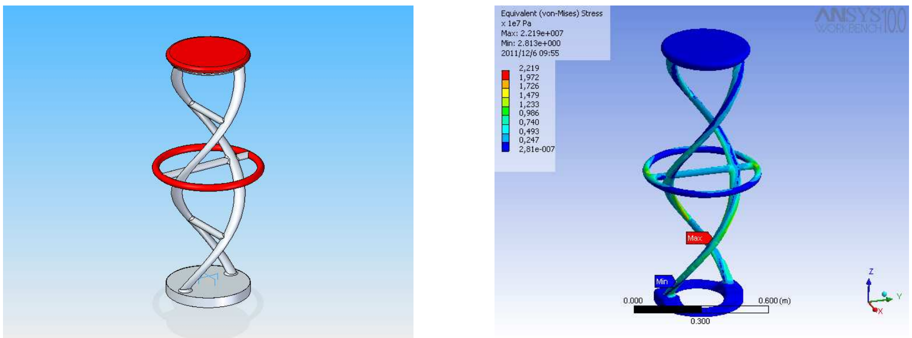

Figure 7. a) Original shape of the bar- chair and Figure 7. b) stress contours under the load caused by a sitting person

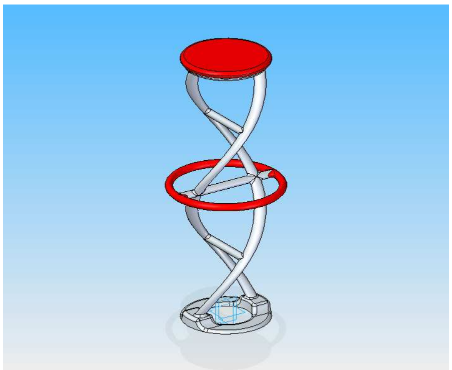

Figure 8. Modified design of the bar-chair after FEM analysis

5. Conclusion

On the basis of the definition of products, product quality and product qualification levels, the place and role of optimum design in product development process is described. Most important product characteristics and parameters are listed which can be subjected to optimization or multidisciplinary optimization (MDO) procedures. Case studies and numerical examples are shown for optimization, quality analysis, improvement and shape optimization of several industrial products and products designed by product designer students. The case studies and student works shown demonstrate the efficiency and advantages of applying FEM and MDO methods during the product design process.

Acknowledgements

"This work was carried out as part of the TÁMOP-4.2.1.B-10/2/KONV-2010-0001 project in the framework of the New Hungarian Development Plan. The realization of this project is supported by the European Union, co-financed by the European Social Fund."

The author would like to thank the helps of Judit Pintér 4th and István Nagy, 3rd year Industrial Product and Art Designer BSc students studying "Product Simulation" course given by the author of this paper, at the Department of Machine and Product Design, during this course they build-up the three dimensional CAD and FEM models shown in Chapter 4.

REFERENCES:

[1] F. J. Szabó–F. Sarka–Zs. Tóbis: *Numerical analysis, product simulation and qualification (in Hungarian).* Study aid, TÁMOP-4.1.2-08/1/A-2009-0001. Miskolc, 2011.
[2] F. J. Szabó: *Multidisciplinary optimization of a structure with temperature dependent material characteristics, subjected to impact loading.* International Review of Mechanical Engineering (IREME) Vol. 2. No. 3, pp. 499–505.
[3] Structural Research and Analysis Corporation (1997): *COSMOS/M User's Guide*, SRAC, Santa Barbara CA, USA.
[4] ANSYS, Inc. (2006): *ANSYS Workbench v. 10 Tutorial*, Canonsburg, PA, USA.

Design of Machines and Structures, Vol. 2, No. 1 (2012), pp. 73–82.

MATHEMATICAL MODELS FOR TOOTH SURFACES OF GEAR COUPLING

JÓZSEF SZENTE–LÁSZLÓ KELEMEN
Department of Machine and Product Design, University of Miskolc
3515 Miskolc-Egyetemváros, Hungary
machszj@uni-miskolc.hu; machkel@uni-miskolc.hu

Abstract. Gear couplings are used to eliminate the misalignments of the connected shafts. Most important components of the gear coupling are the hub and the sleeve. The hub is an external gear having crowned teeth. The sleeve is an internal spur gear. Both gears have equal number of teeth. In this paper the manufacturing methods are presented for the hub and sleeve and mathematical models are investigated for the tooth surfaces of both components.

Keywords: gear coupling, internal gear, crowning, gear hobbing, gear shaping

1. Introduction

Main components of the gear coupling (*Figure 1*.) are the sleeve and the hub. The sleeve is an internal gear and the hub is an external gear which has crowned teeth.

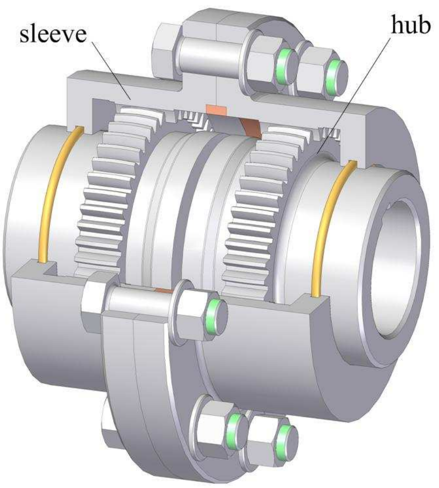

Figure 1. Gear coupling

The two toothed components compose a special gear pair, wherein both number of teeth are the same. The gear coupling is able to compensate the misalignment of the coupled shafts by the tooth crowning and backlash. Using a single hub and sleeve, the effect of angular misalignment may be eliminated. In the practice, generally two hub-sleeve pairs are built up as it is shown in Fig.1. In this case the compensation of the offset misalignment is possible in addition to the angular misalignment. Henceforward the possible manufacturing methods of these special gears will be examined. Mathematical models of the tooth surfaces will be set up, which can provide the basis of the further investigation for the operation of gear coupling.

2. Manufacturing of the crowned gear

The crowned teeth of the hub are produced by hobbing according to *Figure 2*.

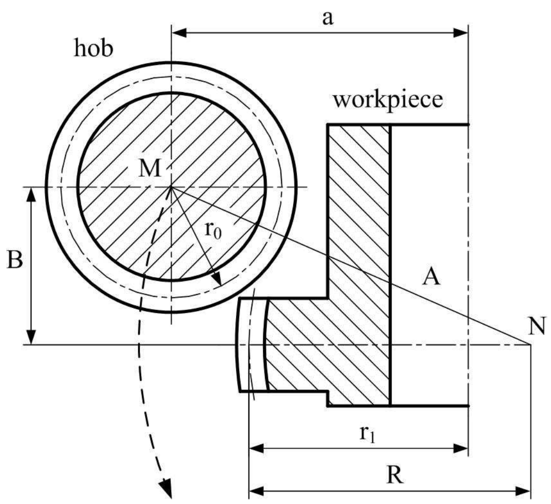

Figure 2. A conceptual sketch for manufacture of crowned tooth surfaces

In the hobbing of cylindrical gears the tool and the workpiece rotate permanently and the tool has a slow feed parallel to the axis of the workpiece. In the hobbing process the tool is called hob. To produce the crowned tooth surfaces the tool moves along a circular path as it is shown in *Figure 2*. The unique structure of the hobbing machine usually does not allow this motion of the tool, so the necessary relative movement is obtained by the radial motion of the workpiece-table and the axial movement of the tool. During production the centre distance varies continually. The maximum value of centre distance is:

$$a_{\max} = r_0 + r_1 , \tag{1}$$

where r_0 and r_1 are the radii of pitch circle for the hob and the workpiece respectively.

The circular arc of the relative movement between the tool and the workpiece can be characterized by the radius $A = \overline{MN}$, depending on the pitch radius of the hob and the distance R which is the typical size of tooth crowning (*Figure 2*):

$$A = r_0 + R . \tag{2}$$

In addition, the centre distance is determined by the current axial position of the hob denoted by B in *Figure 2*. Consequently, the actual centre distance:

$$a = \sqrt{A^2 - B^2} - R + r_1 . \tag{3}$$

3. The mathematical model of hobbing

The mathematical model of hobbing was presented by Litvin [1, 2] as an envelope with two independent parameters. This solution is suitable to describe the ideal tooth surfaces, but it includes some approximation, since the two parameters are not independent perfectly. Mitome [3] has reported a very expressive method for hobbing of conical involute gears. This method in modified form is suitable to determine the real tooth surfaces of cylindrical gears [4].

A conceptual sketch of the hobbing and the connection between coordinate systems are shown in *Figure 3.*

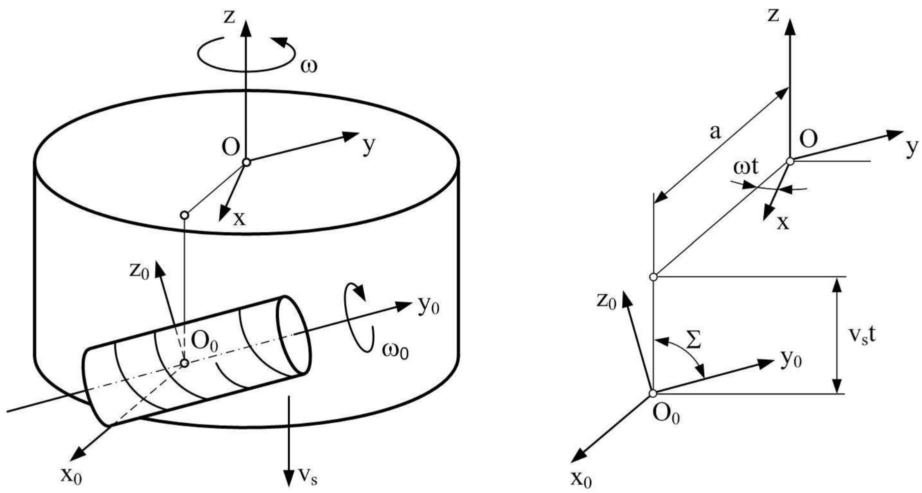

Figure 3. The sketch of hobbing and the used coordinate systems

The hob is considered as an involute worm wherein involute helicoid is fitted to the cutting edge of the hob. Thread surface of the worm has a virtual translation along the axis y_0 in coordinate system x_0, y_0, z_0 because of the angular velocity of rotation ω_0.

The equations of the resulted surface-series are

$$\begin{aligned} x_0 &= x_0(u,v), \\ y_0 &= y_0(u,v) + p\omega_0 t, \\ z_0 &= z_0(u,v), \end{aligned} \tag{4}$$

where u and v are the parameters of screw surface, t is the time within one revolution of the workpiece, p is the parameter of screw and ω_0 is the angular velocity of the hob.

During one revolution of the workpiece the tool generates the tooth space F_1. F_2, ... F_{k+1} denote from the second to (k+1)-th tooth spaces which are cut during the second to (k+1)-th revolution of the workpiece. *s* is the feed of hob during one revolution of the workpiece.

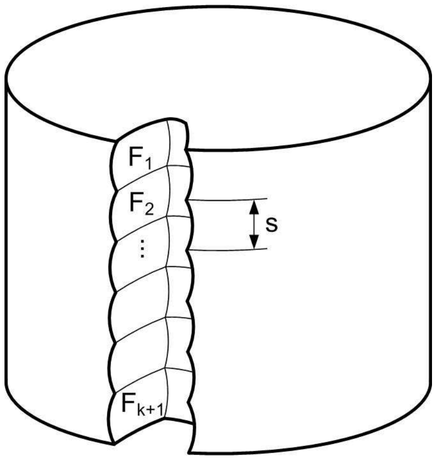

Figure 4. Real tooth surfaces of a cylindrical spur gear

Let T be the time during one rotation of the workpiece. When the surface F_{k+1} is cut the position of the origin O_0 along the axis z is

$$z = -v_s\left(t + kT\right) \tag{5}$$

where v_s is the velocity of feed. The workpiece turns the angle $\omega(t + kT)$, which corresponds to the angle $(\omega t + 2k\pi)$. For cutting the surface F_{k+1} the equation system has the following form:

$$\begin{aligned} x_0 &= x_0(u,v), \\ y_0 &= y_0(u,v) + p\omega_0(t + kT), \\ z_0 &= z_0(u,v). \end{aligned} \tag{6}$$

Transform the surface-series given by equations (6) into the coordinate system xyz:

$$\begin{bmatrix} x \\ y \\ z \\ 1 \end{bmatrix} = M \begin{bmatrix} x_0 \\ y_0 \\ z_0 \\ 1 \end{bmatrix}. \tag{7}$$

The transfer matrix M is as follows:

$$M = \begin{bmatrix} \cos\omega t & \sin\Sigma\sin\omega t & -\cos\Sigma\sin\omega t & a\cos\omega t \\ -\sin\omega t & \sin\Sigma\cos\omega t & -\cos\Sigma\cos\omega t & -a\sin\omega t \\ 0 & \cos\Sigma & \sin\Sigma & -v_s\left(t + kT\right) \\ 0 & 0 & 0 & 1 \end{bmatrix}. \tag{8}$$

An arbitrary surface F_n can be determined by solving Eq. (7) when $k = n - 1$ is substituted and at the same time relationship is produced between the parameters *u*, *v*, *t*. One possible way to determine the relation between parameters when the determinant *D* becomes zero:

$$D = \begin{bmatrix} \frac{\partial x}{\partial u} & \frac{\partial x}{\partial v} & \frac{\partial x}{\partial t} \\ \frac{\partial y}{\partial u} & \frac{\partial y}{\partial v} & \frac{\partial y}{\partial t} \\ \frac{\partial z}{\partial u} & \frac{\partial z}{\partial v} & \frac{\partial z}{\partial t} \end{bmatrix} = 0\,. \tag{9}$$

Expressions (7) and (9) together define any surface element F_n of the tooth surface.

Examined case of hobbing concerns to the production of cylindrical gears. The presented formulas will valid for the manufacture of crowned teeth by the following conditions:

– in addition to the axial feed velocity v_s should be considered a radial velocity v_r,

– this motion occurs continuous changing in centre distance.

The proportion of radial and axial velocities is expressed by the following equation based on the prescribed path of tool

$$\frac{v_r}{v_s} = \frac{B}{\sqrt{A^2 - B^2}}\,. \tag{10}$$

$B = b/2$ belongs to the position of tool $z = 0$ and the relationship $B = z + \frac{b}{2}$ is valid where *b* is the face width of the gear. The change of centre distance is described by Eq. (3). Substituting the relation between *B* and *z*

$$a(z) = \sqrt{A^2 - \left(z + \frac{b}{2}\right)^2} - R + r_1 \tag{11}$$

is obtained. It describes the change of centre distance, while the cutter passes along a prescribed path and the temporary position of the tool is determined by the coordinate *z*. All these indicate that the mathematical model for cylindrical gears is suitable to describe the crowned teeth, if the changing of centre distance is considered in the last column of transform matrix (8). Substituting (5) into (11) the changing of centre distance as a function of the time is:

$$a(t) = \sqrt{A^2 - \left[\frac{b}{2} - v_s\left(t + kT\right)\right]^2} - R + r_1\,. \tag{12}$$

This relationship should be taken into account in calculating the matrix *M*.

4. Equations of the crowned tooth surfaces

Based on the above-mentioned description, it is found that the resulted tooth surface depend on several parameters. Thus it is influenced by the size of the hob (r_0) and the feed. In fact, it is also true for hobbing of cylindrical gears, that one gear produced by different hob or different feed has several tooth surfaces. The cylindrical gears with involute tooth surfaces are idealized surfaces.

The idealized tooth surface for crowned gearing will be derived so that involute tooth surfaces having variable profile shifting in parallel transverse planes are assumed.

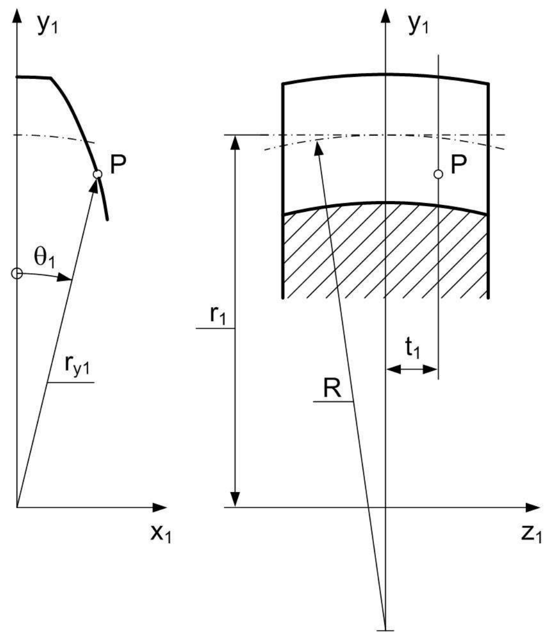

Figure 5. Crowned tooth surface

Equations of the tooth surface are:

$$\left.\begin{aligned} x_1 &= r_{y1}\sin\theta_1, \\ y_1 &= r_{y1}\cos\theta_1, \\ z_1 &= t_1. \end{aligned}\right\} \tag{13}$$

where r_{y1} is the arbitrary radius along the tooth profile, and θ_1 is the tooth angle. To calculate it the following expression is used:

$$\theta_1 = \frac{s}{2r_1} + inv\alpha - inv\alpha_{y1} \tag{14}$$

where s is the tooth thickness along the pitch cylinder, r_1 is the pitch radius, α is the standard pressure angle, α_{y1} is the pressure angle at radius r_{y1}. α_{y1} can be determined by the following equation:

$$\cos\alpha_{y1} = \frac{r_{b1}}{r_{y1}} . \tag{15}$$

Here r_{b1} is the radius of base circle. In Eq. (14) the *inv* means the involute function, which is interpreted as inv $\alpha = \tan\alpha - \alpha$.

The tooth thickness along the pitch cylinder is

$$s = s_0 - 2(R - \sqrt{R^2 - z_1^2})\tan\alpha , \tag{16}$$

where s_0 is the tooth thickness in the plane $z_1 = 0$.

All these indicate that θ_1 depend on the radius r_{y1} and the coordinate $z_1 = t_1$, i.e. in Eq. (13)

$$x_1 = x_1(t_1, r_{y1})$$

and

$$y_1 = y_1(t_1, r_{y1}). \tag{17}$$

5. Manufacture methods for internal gears

Manufacture methods of the internal gears may be classified into two categories, which are the forming and generating procedures. The forming processes include the form milling and broaching.

The form milling is realized by hobbing machine using form milling head and finger type or disk type milling cutter. The teeth are formed one by one without generating motion. Form milling may be used economically for machining the gears which have large diameter and high module. Disk type cutters having carbide bit realize appropriate productivity. The disadvantage of the procedure to be less accurate than the generating methods and large ring gears can be manufactured only. The tip diameter of gear should be many times as large as the milling head. Form milling is not suitable for preparation of helical teeth.

The broaching is the most productive method for manufacture of internal gears, but also the most expensive as well. In consideration of the prime and foundation costs of broaching machines and the high price of the broach, the broaching should only be used economically in quantity production. To produce helical teeth using special machine is possible, but the fabrication and sharpening of tool and the guiding of tool along helical path are very difficult tasks.

The generating processes are the gear shaping, gear skiving and gear hobbing.

The gear shaping was the first generating process which is suitable to produce internal gears too. This procedure is still the best known and most widely used method.

Since the gear shaping has low productivity due to intermittent operation, several attempts have been made to develop efficient production methods. Such methods were the gear skiving and gear hobbing for internal teeth generation.

The gear skiving was created as a special blend of the gear shaping and hobbing. The cutter comes from gear shaping while the movements come from gear hobbing. The productivity of gear skiving is similar to the gear hobbing of external gear teeth. It can be mentioned as an advantage that the helix angle may be set between wide limits, compared to other procedures that are either unsuitable for the manufacture of helical teeth, or just defined helix angle values can be produced. The special tool holder ("flying cutter") did not provide sufficient rigidity, therefore the gear skiving did not come in general use.

Gear hobbing for internal gears can be done on conventional hobbing machine using special tool clamping device. In the course of production barrel-shape hob is used. The spread of procedure was obstructed by the cost of complicated hob geometry, the convenient solution to a rigid tool holder and the size limit, which arises from the fact that the tool holder device must have fit to the internal ring.

Henceforward we consider the gear shaping because it is the only generating process using the manufacture of internal gear, which is widely used, reliable, and has adequate precision.

6. Gear shaping

The gear shaper and shaper cutter were developed and patented by Fellows in 1897. The position of workpiece and cutter and the characteristic movements of gear shaping are illustrated in *Figure 6*.

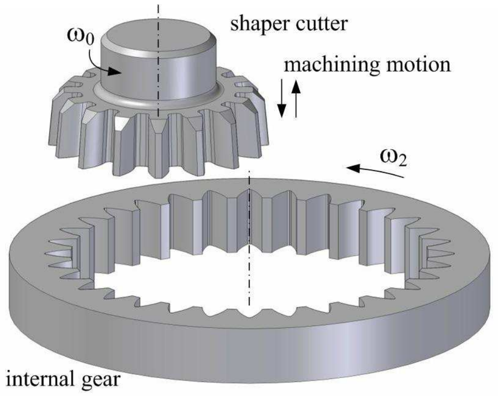

Figure 6. Gear shaping of an internal gear

Axes of workpiece and cutter are parallel to each other. The generation is produced by the harmonized rotation between the cutter and gear blank. The relationship between the angular velocities can be expressed as the gear ratio:

$$\frac{\omega_0}{\omega_2} = \frac{z_2}{z_0} = u \ . \qquad (18)$$

The cutting motion is a vertical (at certain types of machine is horizontal) reciprocating movement of the cutting tool. In the machining process there are two type of feed in radial and tangential direction. The radial feed is realized by cam mechanism or threaded spindle. The tangential feed is the rotation in mm referred to one stroke and measured on the pitch circle of cutter. During cutting neither cutting tool nor workpiece does not rotate. The generating movement that is a slight rotation is carried out during the return motion of cutter.

By gear shaping spur and helical gears can be generated too. Spur gears are produced by straight-toothed tool and helical gears are manufactured by helical shaper cutter. Since the gear couplings contain spur internal gear, hereafter deal with straight teeth only.

7. Equations of the tooth surfaces for internal gear

Theoretical tooth surfaces of the internal gears are involute cylinders. *Figure 7.* shows the tooth profile and the parameters of tooth surface.

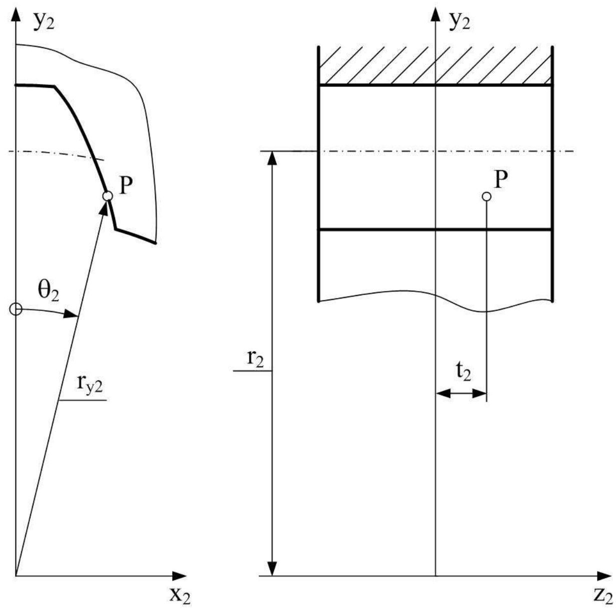

Figure 7. Tooth surface of internal gear

Equations of the tooth surface are:

$$\left.\begin{aligned} x_2 &= r_{y2}\sin\theta_2, \\ y_2 &= r_{y2}\cos\theta_2, \\ z_2 &= t_2. \end{aligned}\right\} \qquad (19)$$

Where r_{y2} is the arbitrary radius along the tooth profile, and θ_2 is the angle of tooth space. To calculate this angle the following expression is used:

$$\theta_2 = \frac{e}{2r_2} + inv\alpha - inv\alpha_{y2} \qquad (20)$$

where e is the tooth width of space along the pitch circle, r_2 is the pitch radius, α is the standard pressure angle, and α_{y2} is the pressure angle at radius r_{y2}. It can be determined by the following equation:

$$\cos\alpha_{y2} = \frac{r_{b2}}{r_{y2}}. \tag{21}$$

Here r_{b2} is the radius of base circle. In Eq. (20) the *inv* is the involute function, which is interpreted as inv α = tan $\alpha - \alpha$.

The tooth surface is described by two independent parameters r_{y2} and t_2:

$$\left.\begin{aligned} x_2 &= x_2(r_{y2}),\\ y_2 &= y_2(r_{y2}),\\ z_2 &= z_2(t_2). \end{aligned}\right\} \tag{22}$$

Acknowledgements

"This research was carried out as part of the TAMOP-4.2.1.B-10/2/KONV-2010-0001 project with support by the European Union, co-financed by the European Social Fund."

REFERENCES

[1] F. L. Litvin: *A fogasakerék-kapcsolás elmélete.* Műszaki Könyvkiadó, Budapest, 1972.
[2] F. L. Litvin–N. N. Krylov–M. L. Erikhov: *Generation of tooth surfaces by two-parameter enveloping*. Mechanism and Machine Theory, 10, 1975, 365–373. p.
[3] K. Mitome: *Table sliding taper hobbing of conical gear using cylindrical hob*. Transactions of the ASME, 103, 1981, 446–451. p.
[4] J. Szente: *Fogazott elempárok tervezéséhez kapcsolódó vizsgálatok.* A Miskolci Egyetem doktori (PhD) tézisfüzetei, Miskolc, 1997.
[5] J. Szente: *Egyenes fogú belső fogazatú hengeres kerekek, fogaskerék-bolygóművek.* Gépelemek. (Szerk.: P. Szendrő). Mezőgazda Kiadó, 2007, 564–569. p.
[6] J. Szente: *Belső fogazatú fogaskerekek fogazószerszámainak megválasztása*. Egyetemi doktori értekezés, Miskolc, 1984.

Design of Machines and Structures, Vol. 2, No. 1 (2012), pp. 83–93.

THREE DIMENSIONAL SOLUTION SPACE IN DESIGN METHODOLOGY

ÁGNES TAKÁCS
University of Miskolc, Department of Machine and Product Design
3515 Miskolc-Egyetemváros
takacs.agnes@uni-miskolc.hu

Theoretical basis of a method will be introduced in this paper. With the combination of the tools of design methodology this method can be used with great profit during the generation process of the optimal product variant, besides it also takes care for costumers' requirements.

1. Criticising traditional design methodology

A significant disadvantage of existing methods is that their adaptability to computers is limited. Traditional methods suggest several possibilities for the sequential steps realising the given logical step that implies their multiple character. Firstly a fix sequential design method has to be created instead of traditional methods, though utilizing their positive features.

Keeping physical principles in view is the second great disadvantage of traditional methods. It is disadvantageous because the constructor may limit the solution possibilities in a very early phase of the design process. This way he may unwittingly eliminate solutions that could be really valuable in the period of selection, because they are novel or absolutely new concepts. This way the second task is to generate the solution variants, without paying any attention to physical principles.

The third –and maybe the greatest– deficiency of existing methods is that they do not even try to generate all the possible solutions that could be made on the basis of the given functions, because they pay attention to the human capacity and not to the capacity of computers. So it can happen that some –or significantly a great number of – principally correct and absolutely new solutions escape the designer's eyes. That is why the most important task is to make it possible to generate and handle all the solutions that can be generated on the basis of the given functions.

2. Computer Aided methodological Concept Building (CACB)

Analysing other technologies integrated into CAD systems –so the CAxx technologies [2] – in connection with the whole design process it can be defined that aiding of the design process by computer was developed counter direction to the advancement of it (*Figure 1*.). Computer technologies appear first time in the documentation period of the design process that can be taken as the last phase of it, while the computer aid of conceptual design –that can be taken as the basis of the design – is not yet solved even today. Designers have to keep their eyes on the consumer's criteria as well, although these criteria can eliminate some originally new solutions. This way in this paper a method is suggested that combined with the tool system of the design methodology can be used with a great benefit in the period of conceptual design that is during the working out of the basis of the optimal product variant, and it also pays attention for the consumer's criteria.

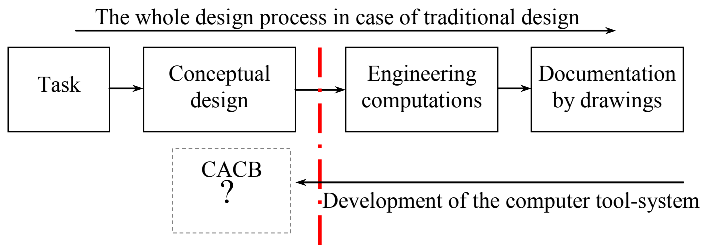

Figure 1. CACB (Computer Aided methodological Concept Building), suggestion for expanding the application of computer tool-system

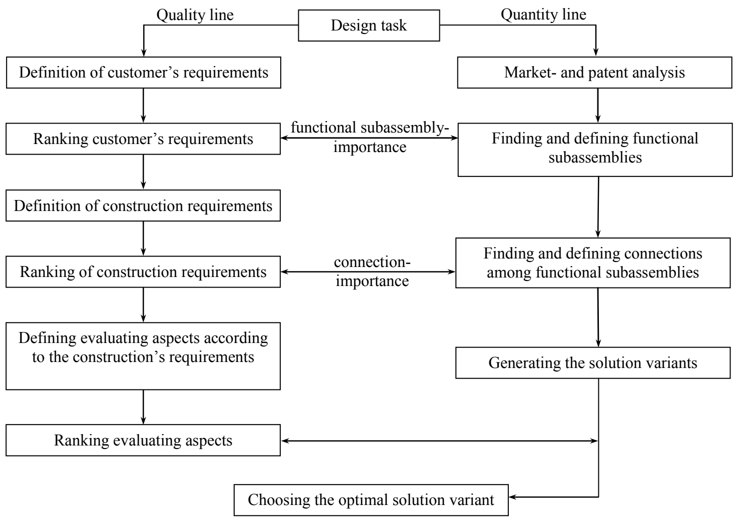

Figure 2. Logical steps of the suggested computer aided concept building

Methods that are suitable for computer application and are developed on the basis of the advantages of the traditional design methods – that are not directed by any computer application – should be created in order to get the conceptual design phase computer aided, and to find the optimal concept for the given design task. Logical steps of the suggested Computer Aided methodological Concept Building (or CACB) is shown in *Figure 2*. Before elaborating the design task it should be analysed. The tools for that are the market research and the analysis of patented solutions. In parallel with this customer's requirements should be found and defined. These requirements should be evaluated and ranked with the designer's eyes, because these requirements are the basis of the evaluation at the end of the concept building method. All the possible functional subassemblies should be defined during the market research and the analysis of patented solutions. Product structures or solution variants can be generated from these subassemblies. These variants should be evaluated by the designer. The optimal solution that is the result of the concept building is the one that fulfilled all the evaluation criteria.

2.1. Customers' requirements

Customers' requirements and claims established to the product are usually ready for the designer at the beginning of the design process in a shape of a claim-list [1]. According to this list criteria can be collected and ranked through the designer's eyes. The basis of this ranking is the fuzzy logic, but it also applies the couple comparison suggested by the traditional design methodology.

Ranking the criteria can be described by the equation (1) that also can be determined by equation (2) that is the **K** criteria matrix. Criteria should be compared in couples. It should be analysed if the criteria in the columns of the matrix are more important than those can be find in the rows of the matrix. The k_{ij} elements of the matrix according to (1) and (2) can get the value 0 and 1. The lower triangular of the matrix is the complement of the upper triangular.

$$\begin{array}{c|ccccc|c} & K_1 & K_2 & K_3 & \dots & K_n & \Sigma \\ \hline K_1 & 0 & k_{12} & k_{13} & \dots & k_{1n} & k_{1f} \\ K_2 & k_{21} & 0 & k_{23} & \dots & k_{2n} & k_{2f} \\ K_3 & k_{31} & k_{32} & 0 & \dots & k_{3n} & k_{3f} \\ \dots & \dots & \dots & \dots & 0 & \dots & \dots \\ K_n & k_{n1} & k_{n2} & k_{n3} & \dots & 0 & k_{nf} \end{array} \tag{1}$$

$$K := (k_{ij})_{n\times n} \tag{2}$$

$$1 - k_{ij} = k_{ji} \tag{3}$$

Important features of the criteria matrix are:

– the major diagonal of the criteria matrix can contain only zeros,
– if the elements above the major diagonal is summarised their pairs under the major diagonal, the result is always 1 (3).

According to that it is also enough to have the elements above the major diagonal; the value of the elements under the major diagonal can be calculated. So the number of the elements that is enough to determine a similar square matrix can be described by a mathematical row according to (4).

$$\begin{aligned} z = n\cdot(n-1) - [(n-1)\cdot(n-1)] + [(n-2)\cdot(n-2)] - \dots \\ \dots + [(n-i)\cdot(n-i)] - \dots + \dots[(n-n)\cdot(n-n)] \end{aligned} \tag{4}$$

Summarising row-by-row the results of the criteria comparison according to equation (5) effects the importance of the criteria. So a (6) $\underline{k_f}$ criteria importance vector arises that should be considered when defining criteria.

$$k_{if} = \sum_{j=1}^{n} k_{ij} \tag{5}$$

$$\underline{k_f} = \lfloor k_{1f} \quad k_{2f} \quad k_{3f} \quad \dots \quad k_{nf} \rfloor \tag{6}$$

2.2. Generating solution variants

Functional subassemblies that are important during the generation of new solution variants and can be found in the known solutions should be disclosed by the patent and market analysis. Sometimes new functional subassemblies should be determined by intuition. Generating variants can be realised in several way – e.g.: according to binary logic or random generation. When the designer would like to perform a preliminary selection with analysing the functional subassemblies ranking according to equation (1) and (2) should be repeated with the functional subassemblies:

$$\begin{array}{c|c|c} & \begin{matrix} F_1 & F_2 & F_3 & \cdots & F_n \end{matrix} & \Sigma \\ \begin{matrix} F_1 \\ F_2 \\ F_3 \\ \cdots \\ F_n \end{matrix} & \begin{bmatrix} 0 & f_{12} & f_{13} & \cdots & f_{1n} \\ f_{21} & 0 & f_{23} & \cdots & f_{2n} \\ f_{31} & f_{32} & 0 & \cdots & f_{3n} \\ \cdots & \cdots & \cdots & 0 & \cdots \\ f_{n1} & f_{n2} & f_{n3} & \cdots & 0 \end{bmatrix} & \begin{matrix} f_{1f} \\ f_{2f} \\ f_{3f} \\ \cdots \\ f_{nf} \end{matrix} \end{array} \tag{7}$$

$$F := \left(f_{ij}\right)_{n\times n} \tag{8}$$

$$1 - f_{ij} = f_{ji} \tag{9}$$

Summarising the values in each row of the matrix it eventuates the importance of the functional subassemblies (10). This can be described by the (11) importance vector of the functional subassemblies.

$$f_{if} = \sum_{j=1}^{n} f_{ij} \tag{10}$$

$$\underline{f_f} = \lfloor f_{1f} \quad f_{2f} \quad f_{3f} \quad \cdots \quad f_{nf} \rfloor \tag{11}$$

Than the rank of each functional subassembly should be given on an open interval, between 0 and 1, so each of them has a fuzzy value.

After this the designer also determines the solution level with a value between 0 and 1. Determining the solution level means that we should withdraw those subassemblies that has a smaller rank than a given value from the set of those functional subassemblies that are building up solutions. This way the designer eliminates several solution-possibilities, but those functional subassemblies that are the most valuable in technical meaning assist generating significant solutions. The value of the solution level is the closer to zero, the more functional subassembly constitutes the generated solution. So giving a value to each solution level is not showing the quality of the solutions that can be generated, but results a quantity selection. This selection can be shortening the period of the generating. Raising the value of the solution level the complexity of the product can be decreased, so the costs of the product can be also decreased. But this way it is not sure that the most important costumers' criteria will be fulfilled.

Than the connections between functional subassemblies constituting variants should be defined, so it should be controlled which functional subassembly can be connected to which one. According to this the **C** connection matrix (12), (13) can be determined.

$$\begin{array}{c} \\ C_1 \\ C_2 \\ C_3 \\ \ldots \\ C_n \end{array}\begin{array}{c} \begin{array}{ccccc} \mathrm{C_1} & \mathrm{C_2} & \mathrm{C_3} & \ldots & \mathrm{C_n} \end{array} \\ \begin{bmatrix} 0 & c_{12} & c_{13} & \ldots & c_{1n} \\ c_{21} & 0 & c_{23} & \ldots & c_{2n} \\ c_{31} & c_{32} & 0 & \ldots & c_{3n} \\ \ldots & \ldots & \ldots & 0 & \ldots \\ c_{n1} & c_{n2} & c_{n3} & \ldots & 0 \end{bmatrix} \end{array} \tag{12}$$

$$C := \left(c_{ij}\right)_{n \times n} \tag{13}$$

The components of the matrix can be 0, 1 and x letters. These characters describe if there is connection or not between the given functional subassemblies in the structure. If the connection is defined by x, than during the generation the program has the right to make a decision whether the connection takes part in the structure or not. This way during the generation each solution has another connection matrix, so each solution can be defined by an **S** structure matrix (14), (15), that has absolutely binary structure, consisting only zeros and ones.

$$\begin{array}{c} \\ S_1 \\ S_2 \\ S_3 \\ \ldots \\ S_n \end{array}\begin{array}{c} \begin{array}{ccccc} \mathrm{S_1} & \mathrm{S_2} & \mathrm{S_3} & \ldots & \mathrm{S_n} \end{array} \\ \begin{bmatrix} 0 & s_{12} & s_{13} & \ldots & s_{1n} \\ s_{21} & 0 & s_{23} & \ldots & s_{2n} \\ s_{31} & s_{32} & 0 & \ldots & s_{3n} \\ \ldots & \ldots & \ldots & 0 & \ldots \\ s_{n1} & s_{n2} & s_{n3} & \ldots & 0 \end{bmatrix} \end{array} \tag{14}$$

$$S := \left(s_{ij}\right)_{n \times n} \tag{15}$$

Each structure can be characterised by a structure graph as well. These graphs define the connections among the different functional subassemblies of solution variants. Nodes of the graphs mean the functional subassemblies; the edges of the graphs mean the connections among the functional subassemblies. Structures can also be defined by structure equations that describe the edges of the structure graphs, or those connections that are writing down the structure of each solution variant. Synthesis of a structure equation is very simple: it contains the connections between functional subassemblies denoted by 1 in the structure matrix. For example:

$$F_1 - F_2, F_1 - F_i, F_j - F_i, F_j - F_n \,. \tag{16}$$

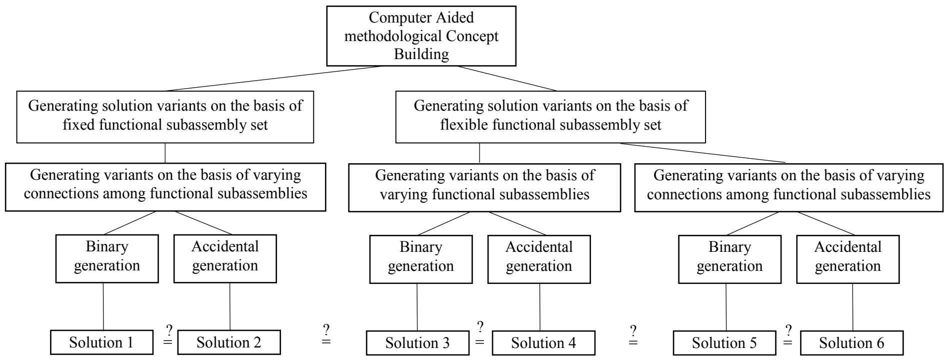

Figure 3. Generating solution variants

Generating variants can be realised basically in two different ways as it is shown in *Figure 3.;* on the basis of the fixed functional subassembly set, or the flexible functional subassembly set. There are cases when giving the importance of the functional subassemblies can be eliminated. In this case the set of functional subassemblies is not changing, so the generating happens according to the fixed functional subassembly set. When the set of functional subassemblies is decreased by giving the importance of functional subassemblies and determining the solution level, the size of the functional subassembly set changes, so the generating happens according to the flexible functional subassembly set.

Exploring the optimal field of use and analysing the efficiency of the mentioned methods needs more examination. In case of some products – *e.g.: rear-view mirror of a car–* by the definition of a low solution level all of the functional subassemblies can take part in the product structure, but at a higher solution level only those functional subassemblies are missing that has not effect on the basic operation of the product. In case of these products the hardness of the solution level does not influence the operation. But there are those kinds of products as well – *e.g.: solutions variants deriving from the connection of different kinds of planetary gears–*, where all the functional subassemblies are necessary to generate operable solutions. That is the reason for the generating solution variants according to varying connections between the functional subassemblies can be called total combination, because if the connections between the functional subassemblies are preliminary not defined, all the possible solutions can be generated by binary generation. It is not sure that according to the theory of random numbers all the possible solutions can be generated.

The method worked out basically deals with two different theories: solution variants generated by varying the functional subassemblies and solution variants generated by varying the connections among the functional subassemblies. The research shows two mathematical solutions for both theories: the binary logics, and the generation of random numbers. As it is shown in Figure 3., the different generation theories can show different results. These methods do not eliminate the possibility that the results can fall in with each other.

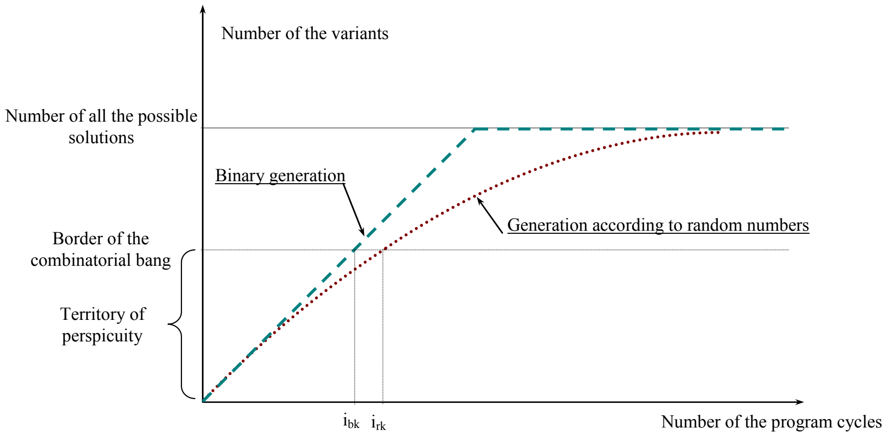

Figure 4. The maximum number of solution variants according to the binary logics and the theory of random numbers

There is no need for defining the connections between the functional subassemblies in case of generation according to random numbers, because than the main point is that the computer randomly determines solutions from all the possibilities. These solutions should be examined by a strict value analysis, if they are operable solutions. According to binary generation each functional subassembly can be connected to each of them so it is sure that all the possible solution variants can be created. But the user of the program can also fix connections, than the generation is resulted less solution. Generating according to different theories can bring different solutions. Efficiency-analysis of the methods needs more examinations.

Figure 4. shows the expectable number of solutions generated according to binary generation and the theory of random numbers depending on the number of the generating cycles, besides the computer assistance of the suggested methods. As it can be seen on the figure all the possible solution variants can be created by binary generation even besides finite cycle number. The curve of the generating according to the theory of random numbers only fitting the horizontal line of all the possible solutions in case of endless cycle number. Depending on the input data of solution generating it can happen that the border of the combinatorial bang realises at a lower number of solutions, than the number of all the possible solutions. In that case the set of solutions will be inhomogeneous, because of the lack of those solutions that were generated after reaching the border of the combinatorial bang. So if it happens it is better to use the generation according to the theory of random numbers, because solutions generated up to the borders of the combinatorial bang are from the full set of the generation that is why the set of the solutions will be homogeneous. Generating the same number of solutions i_{rk} is always higher than i_{bk}, so in the case of the generation according to the theory of random numbers more program cycle is needed than according to binary generation.

2.3. Evaluating step

In the evaluating step the generated solutions should be evaluated. During this process the **E** value matrix (17) and (18) can be created. This matrix ranks the evaluating aspects according to the consumers' criteria. Summarising row-by-row the result of the comparison of the evaluating aspects it eventuates the importance of the evaluating aspect (20). This can be described by the (21) importance vector of the evaluating aspects.

$$E := \left(e_{ij}\right)_{n\times n} \tag{17}$$

$$\begin{array}{c|c|c} & \begin{matrix} E_1 & E_2 & E_3 & \dots & E_n \end{matrix} & \Sigma \\ \begin{matrix} E_1 \\ E_2 \\ E_3 \\ \dots \\ E_n \end{matrix} & \begin{bmatrix} 0 & e_{12} & e_{13} & \dots & e_{1n} \\ e_{21} & 0 & e_{23} & \dots & e_{2n} \\ e_{31} & e_{32} & 0 & \dots & e_{3n} \\ \dots & \dots & \dots & 0 & \dots \\ e_{n1} & e_{n2} & e_{n3} & \dots & 0 \end{bmatrix} & \begin{matrix} e_{1f} \\ e_{2f} \\ e_{3f} \\ \dots \\ e_{nf} \end{matrix} \end{array} \tag{18}$$

$$1 - e_{ij} = e_{ji} \tag{19}$$

$$e_{if} = \sum_{j=1}^{n} e_{ij} \tag{20}$$

$$\underline{e_f} = \left[e_{1f} \quad e_{2f} \quad e_{3f} \quad \dots \quad e_{nf}\right] \tag{21}$$

The ranked evaluating aspects should be characterised by a weighting factor. After that using the weighted product characters method a table according to *Table 1*. should be defined. Each variants should be evaluated with points between 1 and 5 (***the worst is 1–means*** p_{min}***, the best is 5- means*** p_{max}), than should be multiplied with the given weighting factor. Than the weighted values should be summarised in each row, so the rank of the evaluated solutions denoted by $\underline{q}$ vector is resulted. This vector can be found in the last column of the table. The q_i element of the $\underline{q}$ vector that has the highest value gives the optimal solution (22).

Table 1.

The method of weighted product characters

	A_1	A_2	A_3	…	A_m	Σ	$\underline{q}$
V_1	$p_{min}\div p_{max}$	$p_{min}\div p_{max}$	$p_{min}\div p_{max}$		$p_{min}\div p_{max}$		q_1
wV_1	w_1V_1	w_2V_1	w_3V_1		w_nV_1	ΣwV_1	
V_2	$p_{min}\div p_{max}$	$p_{min}\div p_{max}$	$p_{min}\div p_{max}$		$p_{min}\div p_{max}$		q_2
wV_2	w_1V_2	w_2V_2	w_3V_2		w_nV_2	ΣwV_2	
V_3	$p_{min}\div p_{max}$	$p_{min}\div p_{max}$	$p_{min}\div p_{max}$		$p_{min}\div p_{max}$		q_3
wV_3	w_1V_3	w_2V_3	w_3V_3		w_nV_3	ΣwV_3	
…							
V_n	$p_{min}\div p_{max}$	$p_{min}\div p_{max}$	$p_{min}\div p_{max}$		$p_{min}\div p_{max}$		q_n
wV_n	w_1V_n	w_2V_n	w_3V_n		w_nV_n	ΣwV_n	

$$V_{opt} = \max \underline{q} \tag{22}$$

3. Representing the fuzzy solution-family in three-dimensional space

The fuzzy solution-family consists of those solutions that were correct solutions of the generating according to the flexible subassembly set. In Descartes coordinate-system the space determined by the V elements of the solution-family, the F functional subassemblies used during the generation and the importance of the functional subassemblies is the Ω fuzzy solution space (*Figure 5.*). The Ω fuzzy solution space can be described by a **B** product complexity matrix and an $\underline{f}_f$ functional subassembly importance vector.

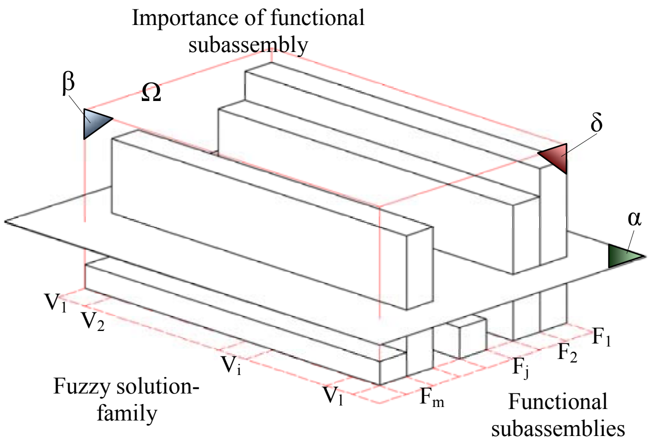

Figure 5. The importance of functional subassemblies, the complexity of solutions

$$B := (b_{ij})_{n\times m} \tag{23}$$

$$\begin{array}{c} \\ V_1 \\ V_2 \\ V_3 \\ \dots \\ V_n \end{array} \begin{array}{c} \begin{array}{ccccc} F_1 & F_2 & F_3 & \dots & F_m \end{array} \\ \begin{bmatrix} b_{11} & b_{12} & b_{13} & \dots & b_{1m} \\ b_{21} & b_{22} & b_{23} & \dots & b_{2m} \\ b_{31} & b_{32} & b_{33} & \dots & b_{3m} \\ \dots & \dots & \dots & \dots & \dots \\ b_{n1} & b_{n2} & b_{n3} & \dots & b_{nm} \end{bmatrix} \end{array} \tag{24}$$

The Ω solution space can be sectioned by 3 excellence planes. Either of the planes parallel with the plane determined by the solutions and the functional subassemblies are the α fuzzy product complexity planes. It shows which functional subassemblies take part in a solution at different level of the importance of functional subassemblies. Those functional subassemblies that has a higher importance than the α product complexity level, takes part in the solutions. Moving the plane in vertical direction the complexity of products can be controlled. Different (α) levels of product complexity can be featured by the product complexity matrix.

The Ω solution space sectioned by a plane that is perpendicular to the axis of solutions the β fuzzy functional subassembly importance plane arisen. This plane shows how important the functional subassemblies that are building up the solutions in certain solutions. The Ω solution space sectioned by the β plane shows a "*prismatic*" nature, because it shows the same frame in case of each solution. Differences between the solutions come from the different connections between the functional subassemblies written by the **S** structure matrixes. The β plane of the functional subassembly importance can be characterised by the (11) $\underline{f}_f$ functional subassembly importance vector.

The Ω solution space sectioned by a plane that is perpendicular to the axis of functional subassemblies the δ fuzzy functional subassembly incidence plane is offered. It shows whether the certain functional subassemblies are in the set of those elements that are building up the fuzzy solution family and if it is so, how important they are. The δ plane can be featured by any element of the $\underline{f}_f$ functional subassembly importance vector according to (11).

The relationship of the introduced planes can be defined according to the followings:

- The intersections defined by the planes α and β determine, which functional subassemblies are building up a given solution of the solution-family.
- The intersection can be defined by a vector that has a value-range of 0 and 1.
- Intersections determined by the planes that are parallel with α–δ planes show the importance of those functional subassemblies that are the members of the solutions in a solution-family. The intersection-line is a certain element of the $\underline{f}_f$ functional subassembly importance vector according to (11).
- Intersections determined by the planes that are parallel with β–δ planes show the incidence of those functional subassemblies that are the members of the solutions in a solution-family at a certain level of importance, so at the level of α solution level. The intersection-line can be described by a vector with each element the same: 0 or 1.

The point of intersections determined by the above introduced three planes (*fuzzy product complexity plane, fuzzy functional subassembly importance plane and fuzzy functional subassembly incidence plane*) is the importance point of a functional subassembly, as it defines the importance of the given functional subassembly. The Ω solution space has a constant vertical size, and its maximum value is 1. But the size of the Ω solution space can be modified in the direction of V and F that can be influenced by the following factors:

- Modifying the fuzzy product complexity level the number of the functional subassemblies taking part in the solution generation can be influenced. This has an effect on the number of the solution variants.
- The number of the solution variants also depends on the values of the connection matrix.

4. Adaptability of the suggested methods for computer

It must be noticed that the introduced methods generating solution variant are able to operate effectively only then, when the application of a computer is solved. These methods make a suggestion for how to generate the more possible solution built up from the functional subassemblies, determined at beginning of the process. It is only the binary method of generating variants on the basis of varying connections among functional subassemblies capable for introducing all the possible solution variants. It was interpreted that in case of a big amount of variable connections it is better to use the method of accidental generation, because this way an overall view of the whole solution-space is given. Binary generation is eligible to use, when the number of all the possible solution probably not overruns the Territory of perspicuity. As a summary it can be established that the introduced methods show a possibility for an algorithm of the design methodology, beat the human limits, shorten the design period, proving the probable quality of the technical plan.

Acknowledgement

"This research was carried out as part of the TAMOP-4.2.1.B-10/2/KONV-2010-0001 project with support by the European Union, co-financed by the European Social Fund."

REFERENCES

[1] E. R. Deciu–E. Ostrosi–M. Ferney–M. Gheorghe: *Configurable product design using multiple fuzzy models.* Journal of Engineering Design, Vol. 16., No. 2., Taylor and Francis, 2005.

[2] I. Horváth–I. Juhász: *Számítógéppel segített gépészeti tervezés*. Műszaki Könyvkiadó, Budapest, 1996.

REVIEWING COMMITTEE

University of Miskolc, Department of Research Management and International Relations
Responsible for publication: Prof. Dr. Mihály Dobróka prorector
Miskolc-Egyetemváros
Editor: Dr. Ágnes Takács
Published by the Miskolc University Press under leadership of Erzsébet Burmeister
Responsible for duplication: Erzsébet Pásztor, works manager
Number of copies printed: 50
Put to the Press on June, 2012
Number of permission: 237